2017•2018

Faculteit Industriële ingenieurswetenschappen

master in de industriële wetenschappen: verpakkingstechnologie

Masterthesis

Creating multilayered polymer nanocomposites using a static mixer

PROMOTOR :

Prof. dr. ir. Naveen REDDY

Prof. dr. ir. Mieke BUNTINX

Giel Jansen

Scriptie ingediend tot het behalen van de graad van master in de industriële wetenschappen: verpakkingstechnologie

Universiteit Hasselt | Campus Diepenbeek | Agoralaan Gebouw D | BE-3590 Diepenbeek

Universiteit Hasselt | Campus Hasselt | Martelarenlaan 42 | BE-3500 Hasselt

2017•2018

Faculteit Industriële ingenieurswetenschappen

master in de industriële wetenschappen: verpakkingstechnologie

Masterthesis

Creating multilayered polymer nanocomposites using a static mixer

PROMOTOR :

Prof. dr. ir. Naveen REDDY

Prof. dr. ir. Mieke BUNTINX

Giel Jansen

Scriptie ingediend tot het behalen van de graad van master in de industriële wetenschappen: verpakkingstechnologie

UHASSELT KU LEUVEN

Acknowledgements

To conclude my education in industrial engineering packaging technology at the University of Hasselt, I now present the results of my research during my internship in the research center Packaging Center Imo-Imomec in Diepenbeek.
During this period, I investigated the production of multilayer polymer nanocomposites. In this reference work you can read how this was done, which methods and techniques were used and the results of the research.

By my mentor, Prof. dr. ir. Naveen REDDY, I was encouraged and supported to carry out these investigations. However, the content of this project has been researched on a very limited scale worldwide, so there is no effective frame of reference for comparing the results. This means that the project is quite unique and to me this accelerates it to a higher level and greater challenge to obtain a final result.

I would like to thank my mentor Prof. dr. ir. Naveen Reddy for this challenge and the confidence that he placed in me to entrust this project to me. During this period he has always supported me with advice and assistance in finding solutions for all kinds of problems that arose during the research and in the preparation of the research methodologies.

I would also like to thank prof. dr. ir. Mieke Buntinx for the follow-up and interest she showed in the subject of this project. Thanks to her support, I have been able to realize this reference work.

At the start of the project I worked with Maria Carolina Lins de Albuquerque Nonô, a Brazilian exchange student. Her own vision and working method contributed to the start-up phase of the project. I would also like to thank her for the support and practical help with the construction of the first test setups.

In the research center Packaging Center Imo-Imomec, where I worked with several colleagues during the internship, I also learned to work together with various colleagues in addition to the scientific field. Because of this I also evolved on a personal level. That is why I would like to give a word of thanks for their support, help and understanding during my internship. I am aware that they have also contributed to the space and comfort that I received during this period in order to arrive at the results that I can present to you today in my reference work. I thank them for their help and their willingness to assist me to carry out the research tests and obtain the results. In particular, I am also indebted to Ida, who always provided me with the necessary materials and made her lab available.

Outside the permanent team with whom I worked in the research center, I could count for help and support from others. Several times I was able to use their services for embedding and analyzing samples. From this co-operation I learned a lot. I want to thank Jan D'Haen and Christel Willems for their contribution.

I also want to thank my entire network of friends for their support. Their experiences, their feedback and feedforward have also contributed to my persistence in my studies and my internship, so that I can ultimately write this final piece. They stimulated me, but also regularly gave other signals, so that I experienced my entire education as a learning process in which choices had to be made, in which I have certainly not only grown as an engineer, but also as a person!

Finally, I thank my family, my father, mother and sister for their support, understanding and unlimited patience. During my entire education they were my best supporters. At times when it was difficult, they have taken care of me, again and again. Their unconditional support has always strengthened me and is one of the most important pillars in the realization of this thesis.

Thanks to all of you for all the opportunities that are offered to me.

Table of contents

List of figures

List of Graphs

List of tables

Glossary

Aggregate	Stacking particles on top of each other.
Biaxial	In two directions
cm	Centimeter
Delaminate	Separation of particles that lie on top of each other.
e.g.	Exampli gratia
g	Grams
MMT	Montmorillonite
mN	Milli Newton
Multilayer	A composition of several layers
n	The preferred orientation
N_2	Nitrogen gas
Nanocomposite	A solid multiphase material with a nanoscale structure.
Nanoparticles	Particles that are less than 100 nm in size [1].
O_2	Oxygen gas
p	A nanoplates normal
p180	A sanding belt with an average particles diameter of 78 μm.
Pa	Pascal
PEO	Polyethylene oxide
PP	Polypropylene
PS	Polystyrene
R^2	The correlation coefficient
RH	Relative Humidity
S	Order parameter
S	Striation thickness
SEM	Scanning Electron Microscope
Static mixer	A highly-engineered motionless mixing device that for continuous blending of fluids.
wt%	Weight percentage
θ	The angle between the direction of the preferred orientation and the nanoplates normal unit vectors.
μm	Micrometer
η	Dynamic viscosity
$\dot{\gamma}$	Shear rate

Abstract

In the industry, it is important to pack products adequately and protect them against external influences. For this, multilayer foils are commonly used. These foils are widely produced using extruders which require high temperatures and energy consumption. Static mixers could offer the solution to produce multilayers at lower costs. This master's thesis aims to create particle filled multilayer polymer foils using static mixers.

Based on experimental tests with different materials such as children's modeling clay, PEO, MMT, Epofix and PS, the flow behavior of the test materials in the static mixer is analyzed and optimized. The main focus was on the flowability of the test materials and its impact on the formation of multilayer structures using static mixer.

Test results show that multilayer foils can be produced using a static mixer. In this thesis it is found that viscosity and shear resistance have an influence on the production of multilayer foils. On one hand, if the viscosity is too low, the test materials mixes with each other destroying the multilayer structure and additionally the output sheet will collapse. On the other hand, a too high viscosity will require high force to push the material into the static mixer and this high force destroys the static mixer. The shear resistance near the walls of the static mixer causes non-uniform layers at the outer edge of the nanocomposite. Thus controlling viscosity and shear resistance of the test material within the static mixer will lead to uniform multilayer nanocomposites.

Abstract in Dutch

Voedingsproducten moeten adequaat worden verpakt en beschermd tegen externe invloeden. De industrie gebruikt hiervoor voornamelijk meerlaagse folies. Deze worden op grote schaal geproduceerd met extruders die hoge temperaturen en hoog energieverbruiken vereisten. Static mixers kunnen de oplossing bieden om meerdere lagen te produceren bij lagere kosten. Deze masterproef heeft als doel het creëren van met deeltjes gevulde meerlaagse polymeer folies met static mixers.

Door experimentele testen met verschillende materialen zoals kinderklei, PEO, MMT, Epofix en PS, wordt het vloeigedrag van de materialen in de static mixer geanalyseerd en geoptimaliseerd. De nadruk lag vooral op de stroombaarheid van de materialen en de impact ervan op de vorming van meerlaagse structuren met static mixers.

Testresultaten tonen aan dat met static mixers meerlaagse folies geproduceerd kunnen worden. In deze thesis is gebleken dat viscositeit en schuifweerstand invloed hebben op de productie van deze folies. Wanneer de viscositeit te laag is, mengen de materialen en vernietigen de meerlaagse structuur. Bovendien zal de output laag samenklappen. Daarnaast zal te hoge viscositeit hogere kracht vereisen om het materiaal in de static mixer te duwen en wordt de mixer vernietigd. De schuifweerstand nabij de wanden van de static mixer veroorzaakt niet-uniforme lagen aan de buitenrand van de nanocomposiet. Het regelen van de viscositeit en afschuifweerstand van het materiaal in de static mixer zal leiden tot uniforme meerlaagse nanocomposieten.

1 Introduction

The introductory chapter of this thesis is dedicated to the research question and design. This chapter outlines the situation and problem statement of the thesis, as well as the objectives of this research.

1.1 Situating and Problem statement

The Packaging Technology Center is an independent research institute whose activities are aimed at supporting companies of different industrial sectors with packaging problems. They help and offer services to companies to resolve issues with their packaging. These problems can be extended across different research areas from material characteristics (e.g., gas permeability) to transport simulation of packaging [2]. In addition to the direct services to companies the Packaging Technology Center works, in collaboration with companies, on projects [2].

The research group of the Packaging Technology Center is part of the Institute of Materials Research (Imo-Imomec) of the Hasselt University. They are active in both applied and fundamental research [2]. The fundamental research projects are aimed at optimizing the properties of (bio)plastics to enhance their applicability as packaging material [2]. In addition to other functions such as storing, informing, transporting, etc., protecting the packed product is one of the most important functions of the package [3]. Therefore, different materials are used or integrated into the multilayer packaging materials. The choice of the materials will be determined by the requirements of the packed product. These (barrier) materials protect the packed product from external influences such as dust, organic liquids, vapors and gases, but also contribute to maintaining the product's quality through preservation to the internal environment.

An important property of a packaging material is its permeability to gases [4]. The quality of the preserved packed product is often determined by the permeability of the packaging material to gases. For example, oxygen gas (O_2) can permeate through many packaging materials. It is known that in food products aerobic bacterial or fungal growth develops when they come into contact with oxygen leading to oxidation reactions. Because of this, the quality of the food products decreases, and finally the shelf life declines [4].

In the industry, it is very important to pack products adequately and to protect the product against various influences. Many of these influences are determined by the permeability of the packaging material. A very commonly used packaging material is plastic foil. They are used in different types of sectors to pack and protect products. In each sector, plastic foils must meet different requirements to protect the product optimally. Some of these requirements can be met by using different polymer layers. When the desired requirements of a foil can't be reached, the foil must be optimized so the requirements will be reached. In order to change the properties of a foil, particles can be added to the film's structure. The addition of nanoparticles in the structure of the film improves or deteriorates the properties. Within this master's thesis, the focus is towards creating unique particle filled multilayer polymer foils.

Currently foils are widely produced using extruders which require high temperatures leading to high energy consumption and high costs [5]. A process that could reduce these factors would be beneficial in many areas, including environment, production costs, etc. To overcome the above high energy process this thesis focuses on creating particle filled multilayers polymer foils using static mixers. In this thesis, we specifically concentrate on the challenges related to the construction and optimization of static mixer that can produce 16 and 64 layer foils with and without particles.

1.2 Objectives

The main objective of the project is to develop and create a laboratory scale static mixer. For this purpose, an existing static mixer that is normally used for uniform mixing of polymers (to create blends) will be modified to create an unmixed polymer-multilayers. The main question is whether it is possible to develop a static mixer that can effectively make multilayer polymer composites. If this is possible and successful, larger multilayer polymer sheets can be produced that in the future can be an effective barrier material for gases.

The main objective, is divided into 4 sub-objectives as follows,

- To build static mixers that can create 16 layers. For this an initial proof of concept with 16 layers will be created using children's modeling clay.

- To produce uniform, alternate multilayered polymer nanocomposites consisting of polyethylene oxide (PEO) solution and montmorillonite clay particles (MMT) suspension. Here water will be used as suspending medium.

- To use polymer resin filled with microbeads to create multilayers where the resin solidifies with time. This we expect will help to visualize the micro-bead embedded layers using scanning electron microscope.

- To create polymer resin made with 64 alternating layers of pure resin and resin with MMT.

2 Literature study

2.1 Permeability theory

Permeability is theoretically defined as the verification of permeate transmission of gas or vapor through a resistance material. In a material that has no damage such as holes or cracks, a gas and water vapor will pass through a film or coating by an activated diffusion (Figure 1). When a permeate comes into contact with a resistance material it will diffuse through the resistance material. This diffusion is driven by a concentration gradient. This means that the permeate from the side of the matrix with the highest concentration will diffuse to the side of the matrix with the lowest concentration. This diffusion is done in 3 steps (Figure 1) [6].
First the permeate will be absorbed by the matrix of the resistance material. Because the solubility of gases differs, dissolving the gases in the matrix will influence the diffusion of the gases. When the resistance material is crystalline and thus contains polymer crystallites, it will not be possible for the penetrating molecules to be absorbed by the polymer matrix. This is because polymer crystallites are impenetrable. This is why molecules in semi-crystalline polymers diffuse through the amorphous part of the polymer [6].
The second step in the diffusion process is the diffuse through the matrix itself. The penetrating molecules will find their way through the matrix. Depending on the length and the tortuosity of this job, it will take more or less time for the molecules to pass the matrix. Diffusion is also influenced by a number of other factors such as the polarity, shape and size of the penetrating molecules, the degree of crosslinks, crystallinity and the chain-segmental movement of the polymer matrix [6].
When the permeate is on the other side of the matrix, it will evaporate back on the surface. This third and final step is called desorption [6].

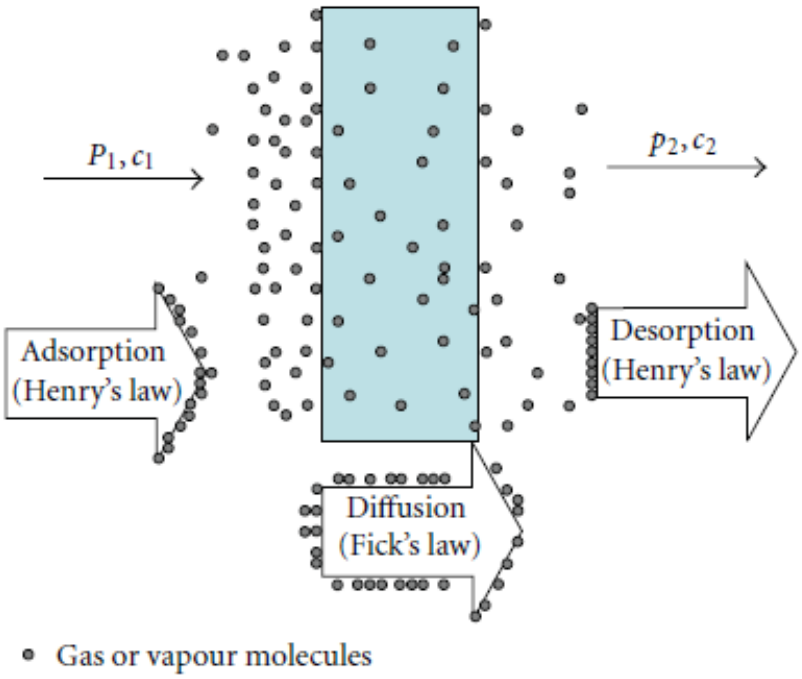

Figure 1: General mechanism of gas or vapor permeability through a plastic film [6]

2.2 Improvement of the gas permeability

An important property of packaging materials is its permeability towards gases. This has a major impact on the quality retention of the packaged products. For example, when oxygen gas passes through a package and makes contact with the packaged product, bacterial or fungal growth can occur. This growth will reduce the quality of the product and ultimately also reduce the shelf life [7].

Gas barrier properties of packaging materials can be optimized by means of nanoparticles. These particles are added to the matrix of a polymer whereby polymer nanocomposites are obtained. The key to obtaining polymer nanocomposites with excellent permeability is to maximize the aspect ratio of the nanoparticles by orienting the surface of each nanoparticle in a direction perpendicular to the direction of the gas diffusion path and by improving the interfacial adhesion between the nanoparticles and the polymer [8]. When dilute amounts of nanoparticles (particularly clay platelets) are added in a polymer matrix, the processability and transparency of a plastic made from this polymer will not be significantly affected. But the mechanical and gas permeability properties of the polymeric nanocomposites will be considerably increased. For example, when large amounts of clay platelets are added, the dispersion of the particles in the polymer matrix will be more difficult. This is because of the less controlled structure that occurs which can cause an accumulation of the clay platelets (aggregation). This results in increased opacity and reduced mechanical and gas permeability properties [9].

There are several factors that influence the gas barrier properties of polymer nanocomposites, such as the relative orientation of nanoparticles in a polymer matrix, the aggregation state, the concentration and the length of the nanoparticles. All of the above factors influence the tortuosity and path length of the penetrated molecules to move from one side to the other in a matrix. Increasing the path length for the gas molecules that diffuse through the polymer matrix will result in an improved gas permeability property [10].

2.2.1 The effect of the concentration and the length of the nanoparticles

By increasing the length of the nanoparticles, the penetrating molecules will have to follow a longer path to move through the polymer matrix. This also takes more time before the penetrating molecules have traversed through the matrix. This results in a lower gas permeability and thus an improvement of the gas barrier of the polymer.

The concentration or number of nanoparticles in a polymer matrix is also an important factor. The higher the concentration (the more nanoparticles are added to the plastic), the more bends there will be in the path that the penetrating molecules have to travel. A more tortuous path means that it will take more time for the penetrating molecules to cross the matrix. As a result, the permeability of the material will be lower.

2.2.2 The effect of nanoparticle orientation on gas barrier property

There are three different orientations that nanoparticles can take when they are added in a polymer matrix. These orientations can be related to the orientation of the nanoparticles defined by the order parameter S [10]. Following equation defined the order parameter S [10].

$$S = \frac{1}{2} \cdot (3 \cdot cos^2\theta - 1)$$

In this equation, θ is the angle between the direction of the preferred orientation (n) and the nanoplates normal (p) unit vectors as shown in Figure 2 [10]. This angle can vary between a range from 0 to π radians.

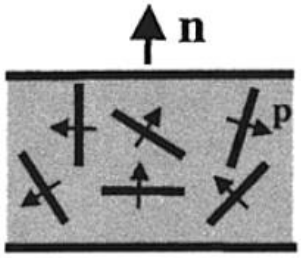

Figure 2: The preferred orientation (n) of nanoplates normals (p) with respect to the film [10]

A first possible orientation is parallel to the direction of the gas flow (Figure 3.a) [10]. In this situation, the orientation of the nanoparticles is related to an order parameter that is equal to -1/2. The value of this order parameter corresponds to an angle θ of $\frac{\pi}{2}$ radians. With this orientation, there will be a lot of space in the plastic matrix, allowing the penetrating molecules to take the least tortuous and shortest path through the polymer matrix [10]. This results in a high gas permeability.

A second option represents an arbitrary orientation of the nanoparticles relative to the gas flow (Figure 3.b) [10]. Here the order parameter is zero and there will be nanoparticles that are oriented randomly to the plane of the film. This means that the angle between the direction of the preferred orientation (n) and the nanoplates normal (p) unit vectors vary between 0 an π radians [10]. As a result, the gas barrier will be better than in a situation with an order parameter of -1/2 and worse than in a situation with an order parameter of 1.

In the third option, the nanoparticles lie in a direction perpendicular to the gas flow (Figure 3.c) [10]. This position of the nanoparticles is related to an order parameter equal to 1 and a θ of zero radians. With an order parameter of 1, it will be difficult for the penetrating molecules to pass through the matrix. The nanoparticles will be oriented parallel to the film, and the penetrating molecules will be forced to follow a much longer and a more tortuous path to pass through the matrix [10].

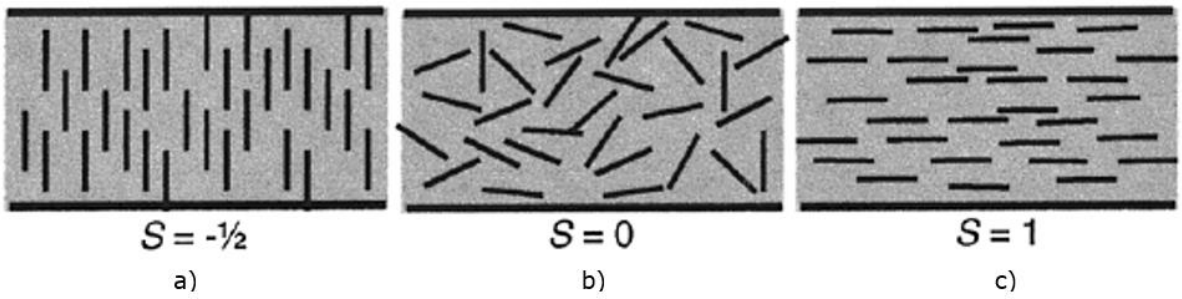

Figure 3: Possible orientations of nanoparticles with respect to gas flow direction, a) parallel, b) random and c) perpendicular [10]

2.2.3 The effect of aggregation and delamination

Nanoparticles can, in addition to having different orientations, also be stacked on top of each other in a polymer matrix [10]. When nanoparticles are stacked on top of each other (aggregated), intercalation is discussed (Figure 4). Intercalation will reduce the tortuosity of the path resulting in an easier path to pass the polymer matrix. This will increase the gas permeability and the opacity of the polymer [10]. When nanoparticles are stacked on top of

each other, it is also possible to separate them (to delaminate). When nanoparticles are delaminated, this is called 'exfoliation' (Figure 4). Exfoliation will spread the nanoparticles in the polymer matrix. This results in more bends (more tortuous) and a more difficult path for the nanoparticles to pass through the polymer matrix, which will reduce the gas permeability [10].

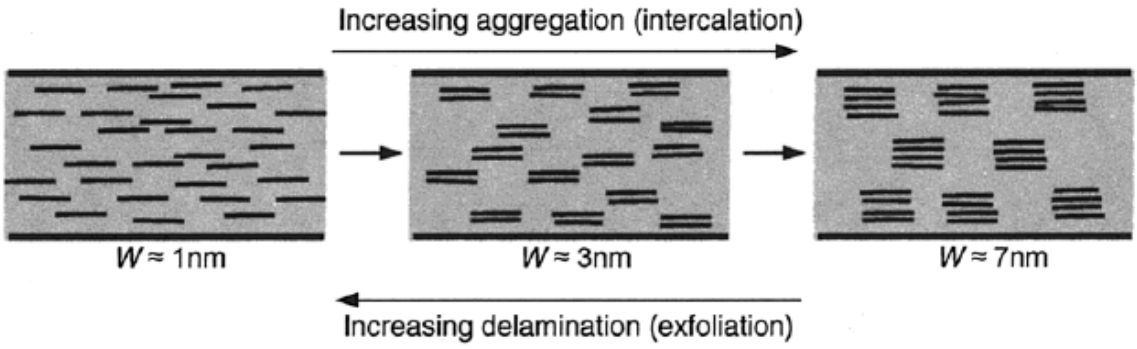

Figure 4: Intercalation and exfoliation principle [10]

2.3 Mixing process

When substances are mixed in a space such as a pipe with a single-phase flow, the mixture can either behave like a laminar flow or a turbulent flow. Using the Reynolds number, it can be determined whether the flow is laminar or turbulent [11]. The Reynolds number is a measure of the ratio between the inertial forces and the viscous forces. When the Reynolds number of a flow is lower than 2300, the flow in the pipe is considered laminar [11]. The transition from a laminar to a turbulent flow is difficult to determine precisely. As a result, a 'transition' is defined between which the change from a laminar to a turbulent flow takes place [11]. This 'transition' takes place between the Reynolds number 2300 and 3200. Above a Reynolds number of 3200 a flow is considered turbulent [11].

The first static mixers were designed to achieve good mixing of a laminar flow in a round tube [12]. In order to obtain this good mixing, motionless inserts such as corrugated plates or blades were placed in static mixers that caused changes in the liquid lines [12]. In addition to motionless inserts, inserts with helical elements, hols, channels and oblique blades were also placed in static mixers that provided stretching of the fluid and local accelerations [12]. These inserts split the incoming liquid into layers and then combine the layers in a new order. These mixing actions ensured mixing by means of convection instead of diffusion [12]. This is called distributive mixing. To quantify distributive mixing use is made of the striation thickness (S) [12]. This is the distance between stripes of contrasting color in a fluid. As can be seen in Figure 5 shall the striation thickness decrease when shear of the fluid occur perpendicular to the initial striations. Because of this the interfacial area between the black and white fluids increase [12].

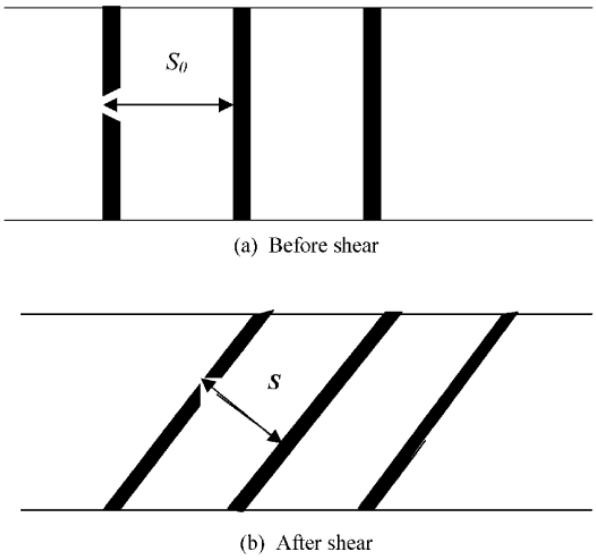

Figure 5: The response of the striation shear when simple shear performs. (a) initial configuration; (b) after simple shear [12]

Static mixers also can be used to mix solid–liquid systems [12]. They are used to disperse the solid particles into a liquid. They are also being able to break aggregates that are bound with van der Waals interactions [12]. Dispersing solid materials in fluids is difficult and a complex operation that is why only laminar flow systems are discussed. The first step for a dry solid material is solid wetting. This step depends on the chemical and physical properties of the mixture and the initial dispersion of the particles [12]. Many powders that are produced in industries have characteristic dimensions below 1 mm. Colloidal forces predominate when solid particles or drops or liquid drops have dimensions lower than 1 mm [12]. Colloidal forces can cause irreversible agglomeration [12]. This will happen due to linkages by strong forces. The agglomerates can form less stable and larger structures. These structures will be form by flocculation due to Van der Walls attractions [12]. Flocculates can be broken by shear forces.
Two different mechanisms can reduce the size of agglomerates. These are erosion and breakage. The mechanism breakage requires high shear stresses and produce daughter particles that are a lot smaller than the initial flocculates [12]. Erosion decreases the particle dimensions but the daughter particles tend to flocculate [12]. Figure 6 shows the different mechanisms. There are a lot of theoretical and empirical models but there is not a general manner to predict a suspensions viscosity [12]. Generally, it can be safely assumed that suspensions are Newtonian fluids at low shear rates. They also exhibit shear-thinning behavior and contain a Newtonian-plateau at high shear rates [12].

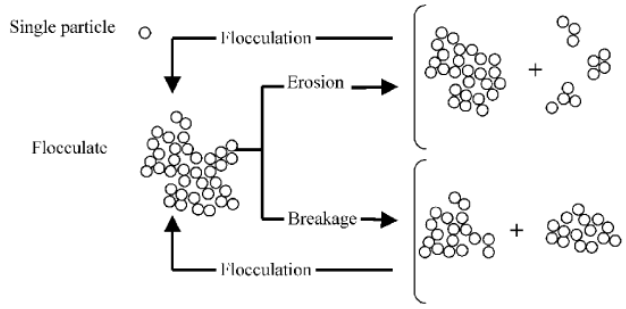

Figure 6: Schematic conception of the mechanisms breakage, erosion and flocculation for liquid-solid systems [12]

2.4 Working principle of static mixers.

Static mixers, also known as motionless mixers [12], are currently used to mix substance tot blends. To achieve these blends, they use the most efficient mixing process, namely the application of the baker's transformation [13]. In this transformation the substance will be stretched, cut and stacked back together [13]. This will be done in the same manner as a baker folds and rolls his dough. Based on the baker transformation, static mixers can produce multilayered structures. Figure 7 shows the different stages of the baker's transformation. All these stages will be performed in the first mixing element of the static mixer. In section a, the two materials (a white and a grey one), that are injected in the static mixer, are separated from each other by a wall. In the next section, the two materials are stacked together and thereafter cut into two parts by a wall. In section c to f, the materials will be stretched and eventually stacked together [13]. After section a to f has been passed, a flow of 4 layers is obtained.

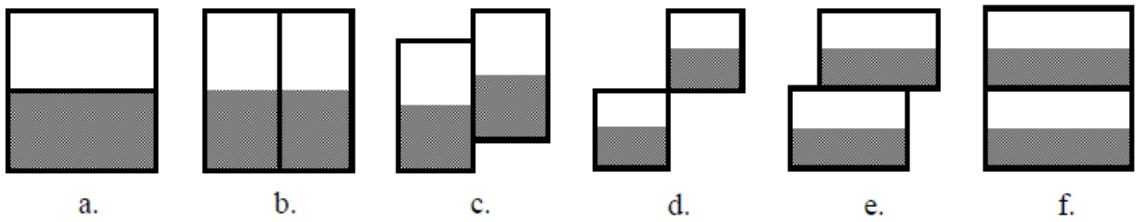

Figure 7: The different cross sections of a static mixers first mixing element [13]

when multiple mixing elements are added to the static mixer, outputs with multiple layers can be obtained. For each mixing element that is added to the structure of the static mixer the number of resulting layer can be doubled. The output will have a final number of layer that is equal to $m \cdot 2^n$ [13]. In this equation, m is the number of layers that are injected in the static mixer and n is the number of mixing elements that are used in the static mixer [13].

The velocity and the volume flux are two important factors by the creation of multiple layers. These two factors are related to each other. When the velocity of the layers is constant and equal than the volume flux of the layers will also be equal [13]. But when the velocity of the materials is not constant, then the cross section surfaces of the created layers will not be equally because the volume flux of the different layers in the mixer are not equally [13].

2.5 Methods for preparing nanocomposites

Polymer nanocomposites are produced by dispersing fillers in a polymer matrix [8]. Generally, polymer / clay nanocomposites can be formed with clay or organoclay. There are three ways to disperse the fillers and form nanocomposites namely in situ polymerization (Figure 8), solution intercalation (Figure 9) and melt intercalation (Figure 10) [8].

2.5.1 In situ polymerization

In in-situ polymerization techniques (Figure 8), delaminated clay platelets are produced in a polymer / clay nanocomposite by means of polymerization reactions [8]. Before the polymerization, the used clay is soaked in a liquid monomer or monomer solution. These monomers will settle in the clay structure and cause the clay to swell. Thereafter the polymerization will be initiated with the aid of radiation, heat, pre-integrated initiators or catalysts. As a result the monomers in the clay structure will form polymer chains and will ensure an exfoliation of the clay platelets [8].

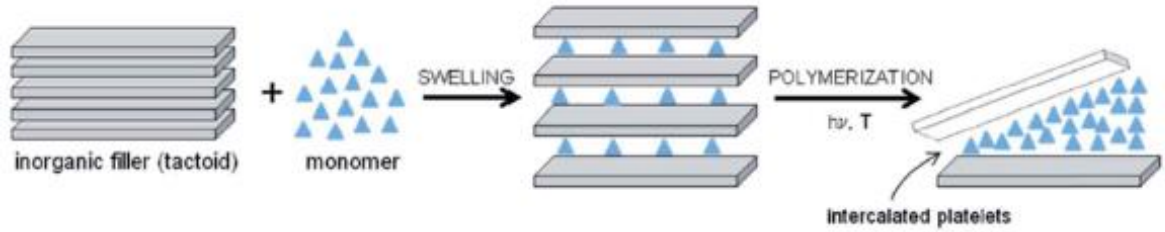

Figure 8: Process mechanism of in situ polymerization [8]

2.5.2 Solution intercalation

In solution intercalation (Figure 9), the layered clays are dissolved in a solvent. As a result, the clay layers will be separated from each other into individual clay plates [8]. The used polymer is also dissolved in the same solvent. The solvent must be chosen such that the used polymer is soluble in the solvent [8]. The 2 suspensions are mixed together, so that the polymer is absorbed between the clay platelets. Subsequently, the solvent from the clay polymer complex is eliminated by evaporation. Eventually a structure of clay sheets and polymers is obtained [8].

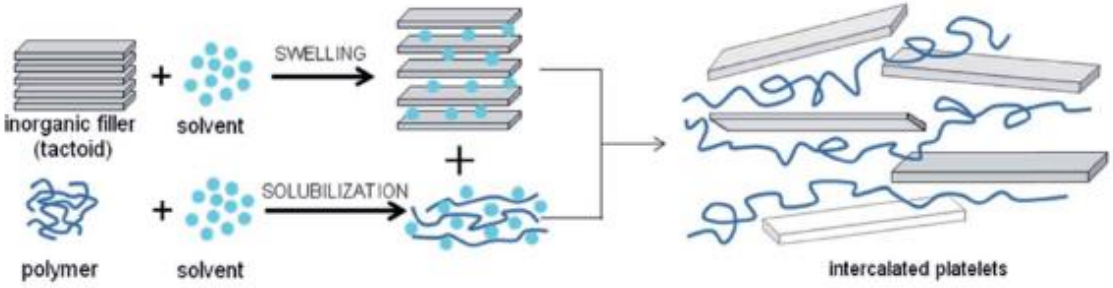

Figure 9: Process mechanism of solution intercalation [8]

2.5.3 Melt intercalation

In melt intercalation (Figure 10), the polymer and the layered clay are mixed together and heated to the processing temperature of the polymer [8]. During mixing, tensions will occur between the clay platelets. Because of this, large stacks of clay platelets (tactoids) will be split into smaller tactoids. When there is affinity between the polymer chains and the layered clay surfaces, the polymer will settle between the clay platelets causing exfoliation and individual platelets to be formed [8]. If there is no affinity between the layered clay and the polymer, this can be remedied by adding surfactant (active substances) to the suspension [8].

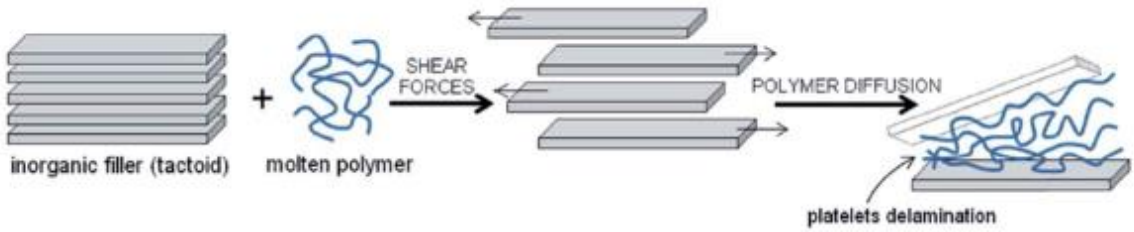

Figure 10: Process mechanism of melt intercalation [8]

3 Material and Methods

One of the most important challenges is creating uniform alternating layers of material. To check whether the existing static mixer (Figure 12) does work, namely to create multilayers, pretests were performed.

3.1 Constructing the static mixer setup

Prior to the execution of a pretest, the static mixer setup must be constructed. Needles will be glued to the static mixer (which act as input point for fluid to flow into the static mixer) in such a way that the test material does not leak. The needles are fastened to two syringes by means of two plastic tubes. To glue the needles to static mixer, 2-component glue is used (Figure 11). When the components of each bottle make contact with each other, a chemical reaction will occur that causes the glue to harden.
Finally, the 5 individual plates of the static mixer are stacked together and attached to each other by screws. The technical drawings of the static mixer have been added to the appendix (appendix A).

Figure 11: 2-component glue

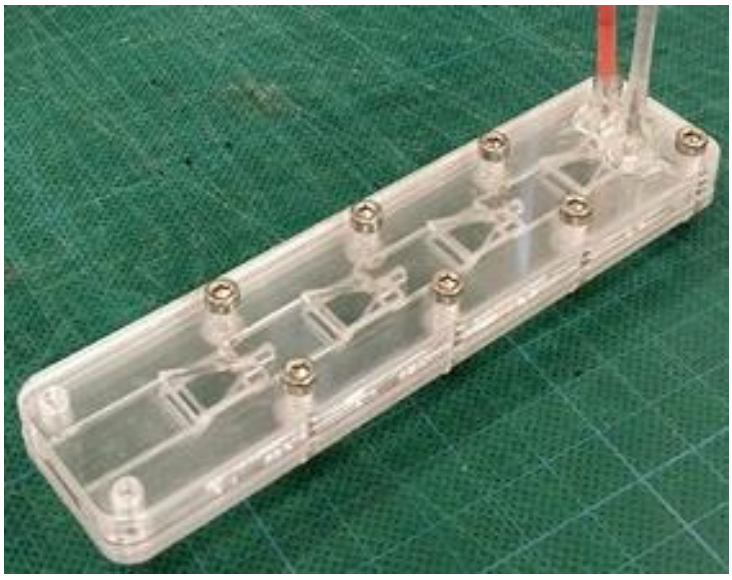

Figure 12: Lab scale static mixer

3.2 Pretests

The test materials for the pretests are two mixtures of differently colored children's modeling clay and water. These mixtures are made less viscous by adding water in order to have the correct viscosity to be pushed through the static mixer. Initially, these tests were performed manually, meaning that the syringes are manually operated. In the next step the syringes were operated mechanically using a universal testing machine (MTS 10/M). The pretest are used to check whether the static mixer creates colored alternating layers.

3.3 Development of a tripod

To carry out tests with a machine, a tripod was developed to ensure that the different components of the setup are fixed and stable. For example, the syringes must be fixed to a stationary object to allow the test solution to be pushed gradually through the static mixer by means of a machine. These tripod will be developed with a computer program named

‘Autodesk Inventor‘ (Figure 13). The technical drawings of the tripod have been added to the appendix (appendix E).

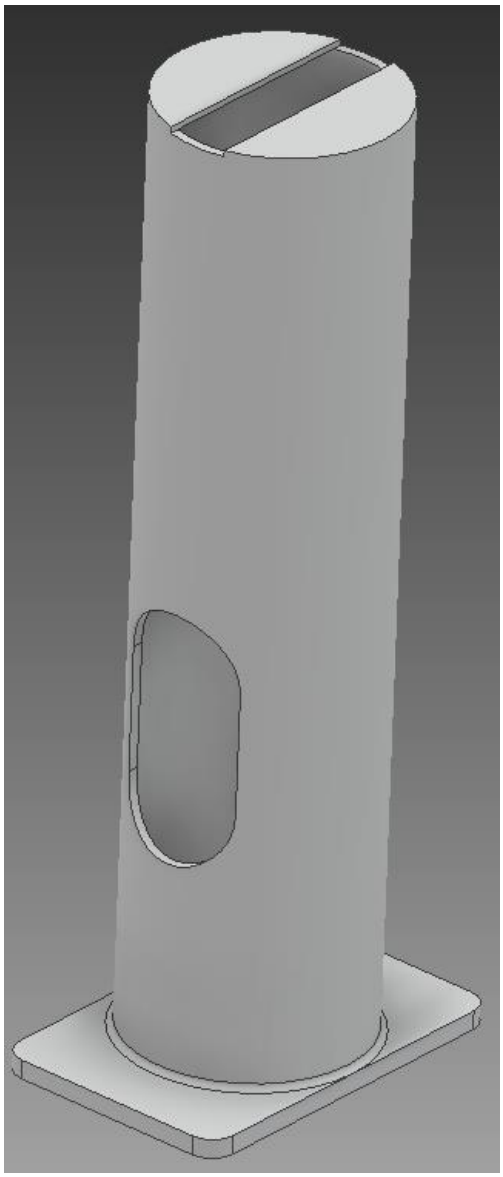

Figure 13: The tripod to fix the syringes while testing

3.4 Modifying the static mixer

After the ‘children’s modeling clay-pretests’ are completed, the existing static mixer was modified by scaling it up and the new test set up was constructed. By scaling up the static mixer, the produced film will be sufficiently large to do permeability tests. This scaling was done with the drawing program Autodesk Inventor. The static mixer was scaled that the resulting multilayer polymer composite achieves a width of at least 3,5 cm. The scaled static mixer will be built using Plexiglas by laser cutting and assembling the sheets.

3.5 Prepare and test PEO and (PEO+MMT) -mixtures

The materials to perform tests, are polymer solutions of polyethylene oxide (PEO) and montmorillonite (MMT) clay nanoparticles. To start, literature data will be used to determine

the correct concentration of PEO and MMT. Then four different solutions are made, a PEO-solution and PEO solutions with 1, 5 and 10 wt% MMT nanoparticles respectively.
To carry out tests with PEO and MMT, the solutions of these substances must have the correct viscosity. So they can be pushed through the tubes, needles and static mixer without any problem. At a right viscosity, the output will form a film and will not collapse. This viscosity is obtained by allowing the solutions to dry in the air and to heat them in the oven. As a result, water from the solutions will evaporate and the solution will thicken to the correct viscosity. After obtaining the correct viscosity of the PEO and MMT solution and the MMT solution, the solutions can be used for testing. These tests are carried out using the tensile machine and with the upscaled static mixer. The outputs of the tests, the solid nanocomposites sheets, will be prepared by removing the water initially through letting them dry at room temperature. Then the nanocomposites will be putted in an oven to completely remove all the water and achieve a film.

Based on the polymer solutions, various tests will be performed using the modified static mixer. In a first test, same polymer solutions are injected into the static mixer's inputs. After this test, trials are performed in which a PEO solution is injected into one input of the static mixer and a PEO solution with MMT nanoparticles is injected into the other input. In these tests, the nanoparticle weight percent (wt%) will change between 1%, 5% and 10%. The outputs of these processes will be collected and will be investigated for permeability and the uniformity of the different layers. The uniformity of the layers will be investigated with an optical microscope in the Packaging Technology Center and a scanning electron microscope in IMO.

3.6 Prepare and test Epofix mixtures

In addition to the polymer mixtures, Epofix mixtures are also used to perform tests. These mixtures will be prepared with Epofix resin and Epofix hardener. At these mixtures polystyrene (PS) particles with different dimensions and MMT particles will be added. Different mixtures are made, Epofix mixtures with 80 and 20 μm diameter PS particles, 20 μm diameter PS and MMT particles and finally an Epofix mixture with 6 μm diameter PS and MMT particles. These mixtures will be used to perform tests mechanically with the tensile machine.

3.7 Expanding the static mixer

Finally, the static mixer will be expanded with additional compartments so that more alternating layers will be formed. The expansion will be developed with a computer program named 'Autodesk Inventor'. The expanded static mixer will be built using Plexiglas by laser cutting and assembling the sheets. This expansion will result in an output consisting of 64 alternating layers. This static mixer will be tested with children's modeling clay and Epofix mixtures as test materials.

4 Results and discussion

4.2 Pretests

In order to determine the actual operation of the static mixer, pretests were carried out. Suspensions of different types of children's modeling clay and water were used as test material.

4.2.1 Red and white children's modeling clay

The first pretest was carried out manually with red and white children's modeling clay materials (Figure 14). During this test the suspension went smoothly through the tubes into the static mixer. Once the suspensions were in the static mixer halfway, the suspensions came out along the side of the static mixer (Figure 15).

Figure 14: Children's modeling clay

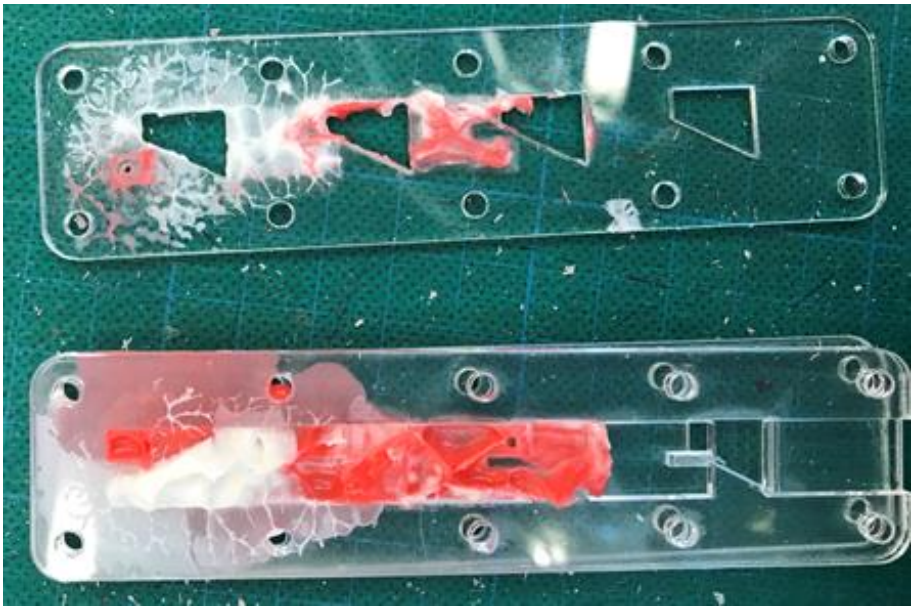

Figure 15: Disassembled static mixer after the clay came out along the side of the static mixer

This phenomenon is probably due to high viscosity. Because of the high viscosity, the pressure in the static mixer becomes too high even at small flow rates and the suspensions leave the static mixer the easiest way (the side of the static mixer). A lower viscosity might give less pressure in the static mixer. Another possible factor that influences this phenomenon is the number of

screws used to bolt the 5 static mixer sheets together. The static mixer was screwed tight with 6 screws instead of 10 whereby the plates of the static mixer were not pressed enough on each other.

4.2.2 Orange and red children's modeling clay

In a second pretest experiment, orange and red children's modeling clay were used as test material. This test resulted in an output. The output was cut into pieces with a knife so the different layers of the output could be observed under the optical microscope. By using a knife, the different layers, when cutting the output, were pushed together so that the layers could not be seen under the microscope. This was because the knife was too thick. To avoid this, a sharp, thin razor blade was used to cut the output. Figure 16 shows the microscopic image of the output.

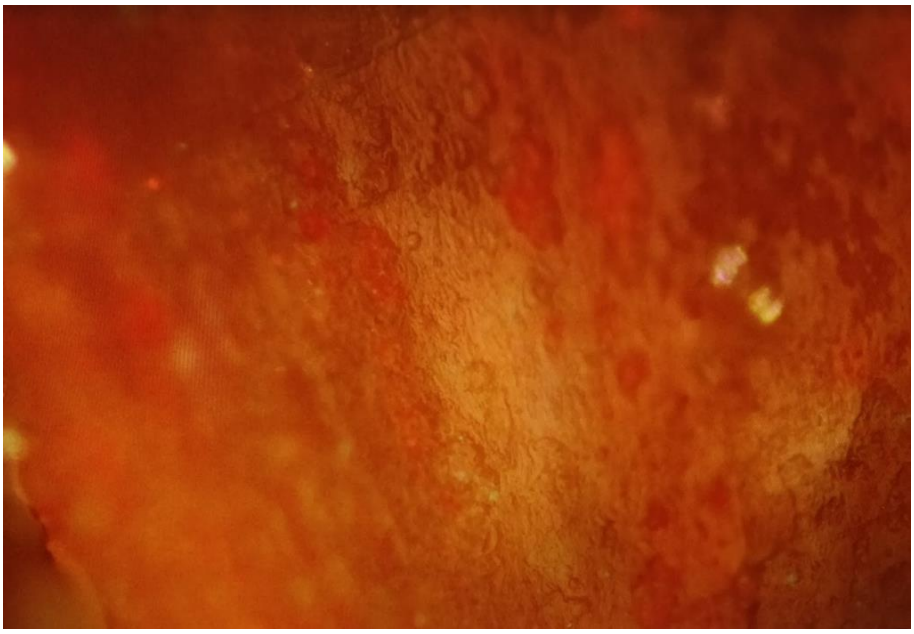

Figure 16: Microscopic view of the output with yellow/red ‘children’s modeling clay’

In Figure 16, the layers are not clear. This is because of the contrast between the colors yellow and red is not sufficient. The colors yellow and red are too close together in the color spectrum (red has a wavelength between 620 and 780 nm and yellow has a wavelength between 570 and 585 nm) [14].

4.2.3 Orange and blue children's modeling clay

The third manual pretest was carried out with orange and blue children's modeling clay as test material. The obtained output was cut into pieces with a sharp, thin razor blade so the output could be viewed under the optical microscope. Figure 17 and Figure 18 show the microscopic image of the output.

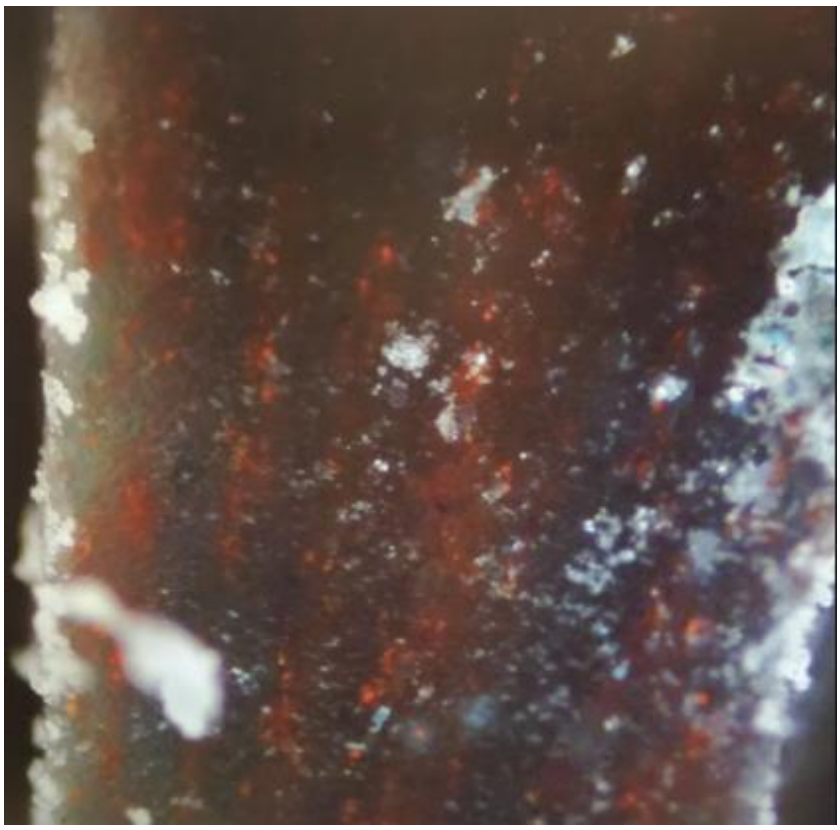

Figure 17: Microscopic view of the output with blue/orange children's modeling clay

Figure 18: Microscopic view of the output with blue/orange children's modeling clay

In Figure 17 and Figure 18, the layers of the different clay-mixtures are slightly visible. Some blue and orange layers aren’t that clear. A possible explanation for this phenomenon may be due to the non-uniform pressure applied to the syringes of the static mixer. As the test was carried out manually, the pressure exerted on the syringes to make the solutions move through the static mixer at different rate. As a result, the solutions will not arrive simultaneously in the static mixer and the solutions will not be pushed simultaneously through the static mixer at the same speed. The end product was still not optimal as the children's modeling clay was flexible and 'soft' which resulted in a soggy dry layer.

4.2.4 Modeling clay

Because the children's modeling clay was still flexible and 'soft' after drying, it was difficult to cut without damaging the various layers on the output. Therefore another clay was used to carry out similar tests. Here modeling clay of the brand Darwi has been used (Figure 19). This clay becomes completely hard on drying, making it easier to cut into pieces for viewing under the microscope. In this test two clay mixtures were used, namely a white clay mixture and a purple clay mixture that was obtained by adding ink (from writing pen) to the white clay mixture. The test is carried out manually.
The obtained output is cut into pieces with a sharp, thin razor blade so that they can be viewed under the optical microscope. Figure 20 shows the microscopic image of the output.

Figure 19: Modeling clay [15]

Figure 20: Microscopic view of output of manual test with Darwi-clay mixtures

Figure 20 shows the internal structure of the output. On this figure, only some non-uniform layers can be observed. A possible explanation for this is because the two clay mixtures mix together. That will happen when the mixtures aren't injected simultaneously or the mixtures have a too low viscosity.

4.2.5 Green and white airy clay

In the next test an airy white and green clay has been used (Figure 21 and Figure 22). This test is carried out manually. This clay was easy to handle, and therefore made it possible to push the clay easy in the tubes and the static mixer, without the addition of water. But, after testing it turned out to be the opposite. This test hasn't obtained an output because the clay contains lot of air which when pushed into the static mixer at high pressure causes the clay to compress and air to be ejected from the sides. The resulted compressed clay became hard and it was difficult to push the clay manually through the small needles and tubes.

Figure 21: Green airy clay

Figure 22: White airy clay

Finally, water was added to the clay so a clay mixture with a lower viscosity was obtained. Test was carried out manually with these clay mixtures. This output was dried and cut into pieces with a razor blade. Figure 23 shows the microscopic image of the output.

Figure 23: Microscopic view of manually created output with white and green airy clay mixtures

Figure 23 shows the inner structure of the output. The inner structure isn't layered but there are some white and green areas. A possible explanation for this structure can be due to uneven pressure (as the sample was pushed with the hands) in the syringes. There are also a lot of air bubbles in the structure. This is because the clay originally contains a lot of air. Because of these bubbles, the inner structure of the output not clearly visible.

4.2.6 Mechanical tests

To do the tests more accurate and mechanically a tripod is developed (Figure 24). With this tripod, the syringes can be fixed and the tests can be done by a tensile machine (MTS 10/M) (Figure 25). This tripod is built using steel pipe which is welded close to one side with a small plate. This plate serves for the stability of the tripod. The other side of the pipe is also closed but contained a slit. This slit has a width that has the same size as the diameter of the syringes. In this slit the syringes are fixed. In the hull of the pipe, a hole has been made. Through this hole the tubes of the static mixer can be connected with the syringes. To press the syringes simultaneously, a small steel plate will be used (Figure 26). This plate will be attached on the plungers of the syringes. The tensile machine can then press on the plate and the pressure can be evenly distributed over the 2 plungers.

Figure 24: The tripod for the mechanical tests

Figure 25: Tensile machine

Figure 26: Metal plate of the top of the setup

With the tripod, tests could be carried out with the tensile machine and a constant pressure can be applied. First, a test was performed with the white and green airy clay mixtures. The clay mixtures were too liquid because without pressing on the syringes the mixtures went through the tubes as a result of the gravity. The tensile machine pushed the plunger into the syringe barrel with a speed of 10 mm/minute. The mixtures went smooth but not simultaneously through the static mixer because one mixture went already further in the tubes (caused by gravity) than the other mixture. This wasn't a big problem because at the first few millimeters of the clay output the clay mixtures didn't come at the same time in the static mixer causing not a layered structure. The other parts of the output came at the same time in the static mixer so these parts will have a layered structure. The output was collected but due to the low viscosity of the clay mixtures the layered structure collapsed. This output was dried and analyzed under a microscope (Figure 27).

In Figure 27, it can be seen that there are different colors in the inner structure of the output but there are not multilayers. Possible reason for this phenomenon can be due to the low viscosity of the clay mixtures. Because of this the mixtures started to mix and no layered structure could be formed. Also can be seen that there are air bubbles in the structure. This is because the clay originally contains a lot of air which could not be removed.

Figure 27: Output of the test using the tensile machine and the airy clay mixtures

After this test, a test was performed with the ‘Darwi’ white and purple clay mixtures using the tensile machine. The tensile machine compressed the syringes with a speed of 10 mm/minute and an output was obtained. This output was dried and analyzed under the microscope (Figure 28 and Figure 29). Figure 28 and Figure 29 shows the inner structure of the clay output. These figures show clearly that there are multilayers layers. These layers are not uniform as the shear rate with the static mixer is not constant. The layers close to the walls of the static mixer gets sheared more than the inner layers and because of this the layers close to the wall become thinner. Additionally, the bottom layers get compressed during drying due to the weight of the top layers.

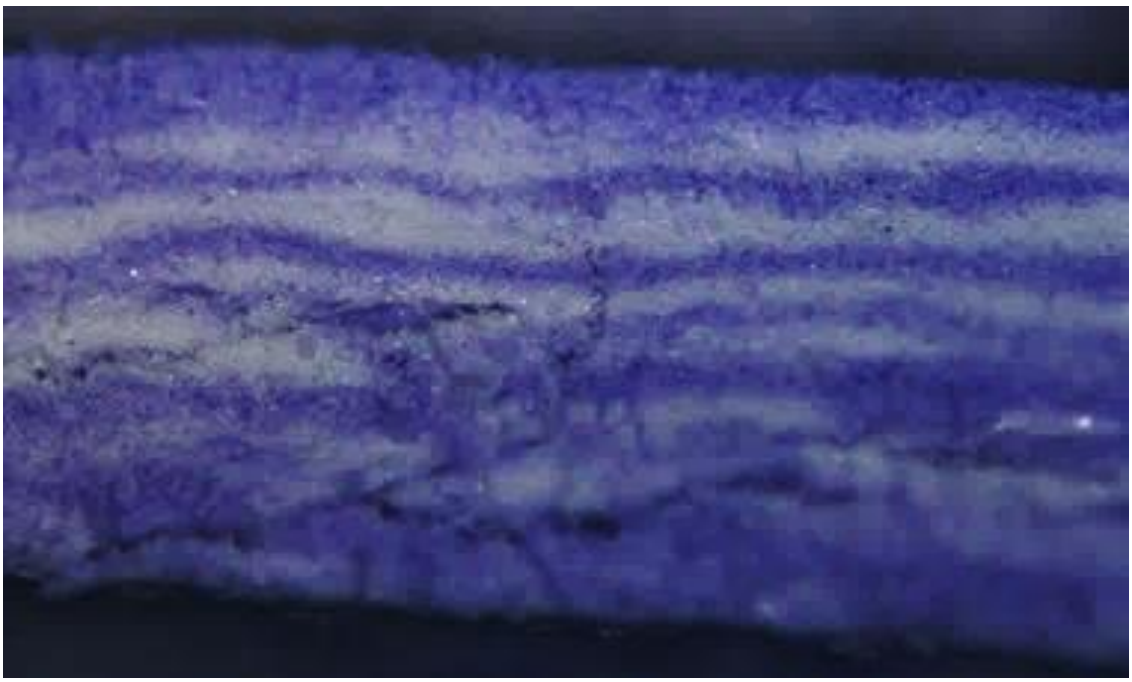

Figure 28: Output of the test with the tensile machine and the Darwi clay mixtures

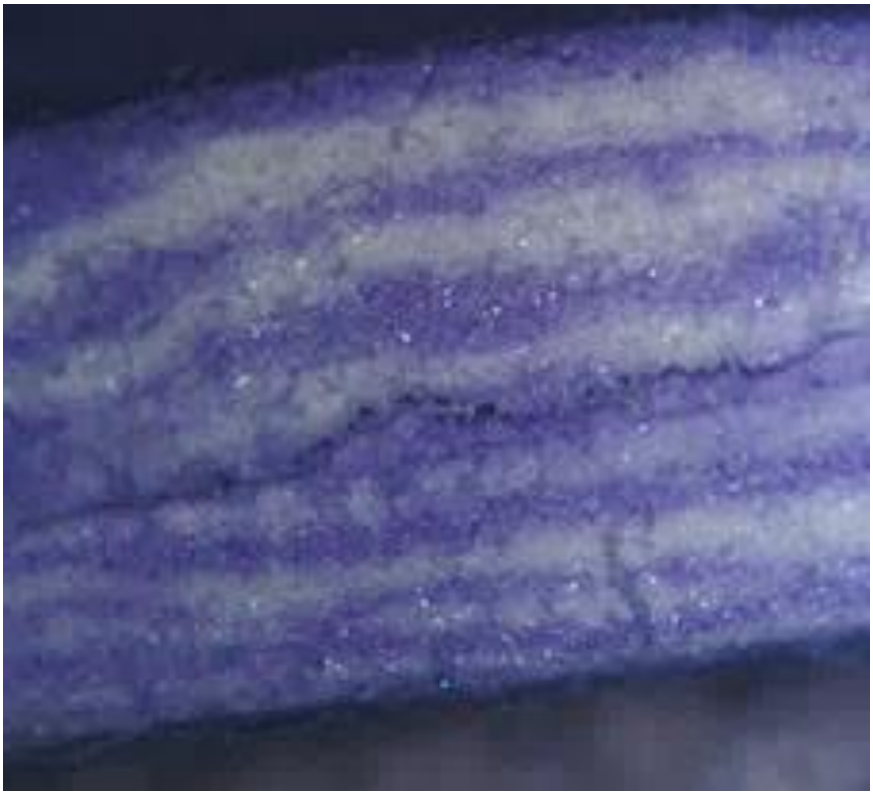

Figure 29: Output of the test with the tensile machine and the Darwi clay mixtures

From the results of the pretests it can be concluded that the static mixer does create different multilayers.

4.3 Upscaled modified static mixer

From the pretests it was possible to deduce that the static mixer creates multilayers. In the next step the static mixer width was increased to obtain wider multilayer output that is suitable for

testing permeability using commercial equipment (for example Mocon). For this reason, the width of the static mixer was increased from 1 cm to 3.5 cm.

4.3.1 First version

Figure 30 and Figure 31 show the design of 2 plates of the first version of the modified static mixer. In the first version, the static mixer has the same length as the static mixer used for pretest but the width is 3.5 times wider. The width of the output is increased to 3.5 cm because this is the minimum diameter for samples that are tested for gas permeability on the Mocon.

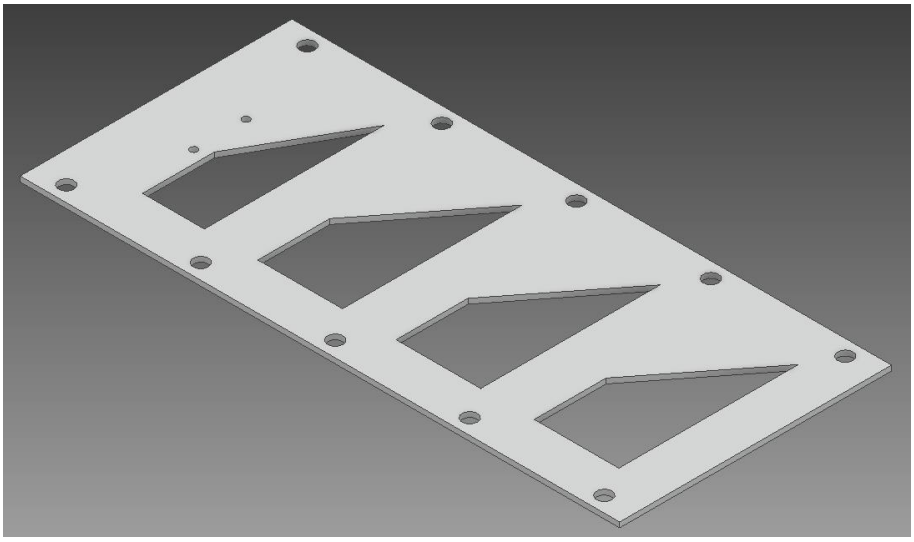

Figure 30: One of the 5 plates of the first version of the modified static mixer where the sample gets biaxial stretched

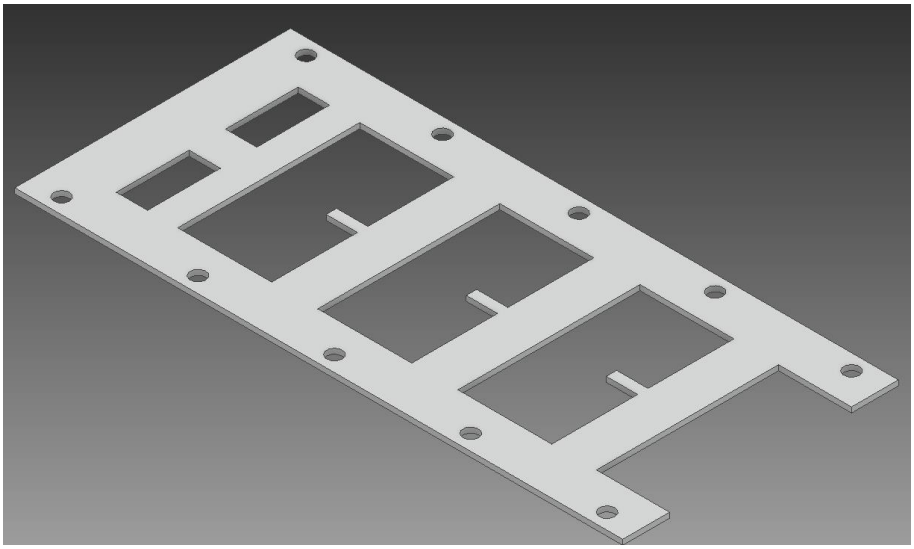

Figure 31: One of the 5 plates of the first version of the modified static mixer where the sample gets stacked and then cut

The test results from this static mixer did not give good result. This is because the design of the static mixer has only been enlarged in width, so the test material in the compartments of the plate of Figure 30 does not reach the extreme corners of the compartments. The formed layers do not get the time to stretch. As a result, the width of 3.5 cm with uniform multilayers was not obtained. The technical drawings of the static mixer have been added to the appendix (appendix B).

4.3.2 Second version

Because the first design did not provide uniform multilayers, the static mixer was further developed into a second design. In this version both the width and the length of the static mixer was increased. The output of this design has the same width (3.5 cm) similar to the first version but here we increase the length to 319.87 mm such that the layers have time to spread through the static mixer. The technical drawings of the static mixer have been added to the appendix (appendix C).
Figure 32 and Figure 33 show the design of 2 plates of the second version of the modified static mixer.

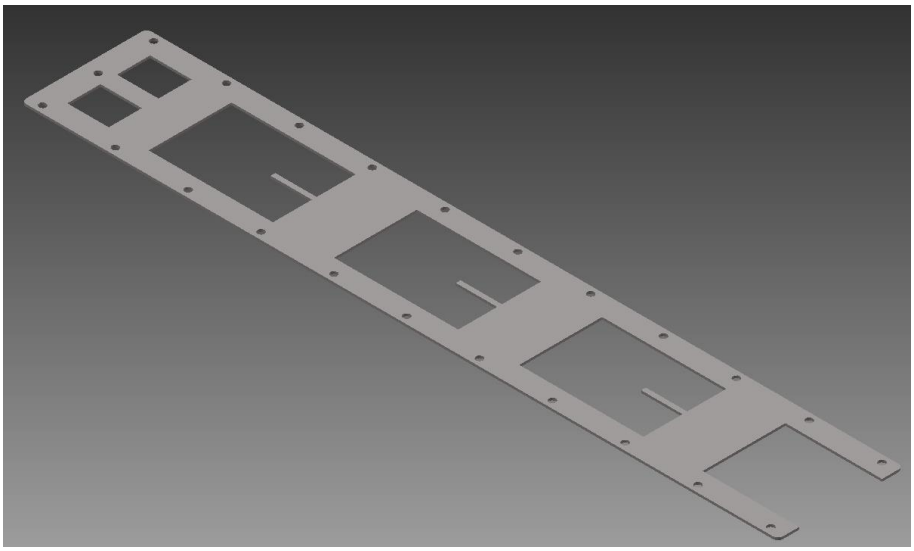

Figure 32: One of the 5 plates of the second version of the modified static mixer where the sample gets stacked and then cut

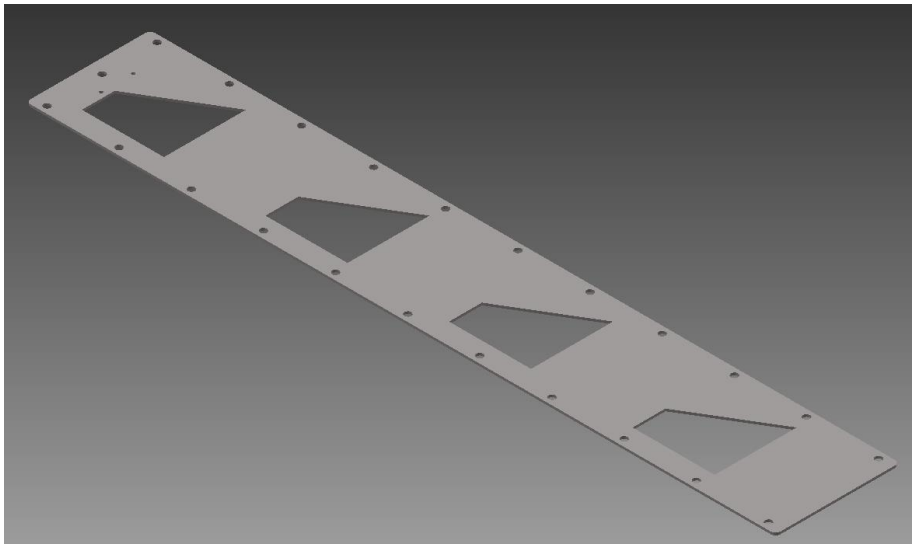

Figure 33: One of the 5 plates of the second version of the modified static mixer where the sample gets biaxial stretched

The design has been tested using the tensile machine with the purple and white modeling clay mixtures as test material. Because the static mixer is enlarged, more test material will be needed to completely fill the static mixer. Therefore, larger syringes are used during the test. The plunger of the syringes has a larger surface so when is pushed at a same speed as using a small syringe with a small plunger, the pressure in the needle and tubes becomes too large. As a result

of this high pressure, defects occurred during the test, such as leaks on the glued areas or bursting of the tubes. As a result, the plunger was pushed into the syringes at a lower speed of 1 mm/min instead of 10 mm/min.

Figure 34, Figure 35 and Figure 36 show the result of the test with the second version of the modified static mixer. These figures show that the clay mixtures leave the static mixer along the side. The failure of the test can be due to various reasons. A first reason is the fact that the compartment where the white clay mixture enters the static mixer overlaps with the next compartment of the purple clay mixture (see red circle Figure 36). As a result, white clay mixture ends up with the purple clay mixture. Because of this, these mixtures mix and no layers was formed (see red circle Figure 35). A second reason is the fact that the pressure that holds the different plates together is too small, mainly in the middle of the plates, so the clay no longer moves through the compartments of the static mixer but moves in between the plates (Figure 34). This does not result in a layered structure. The reason why the pressure on the plates is too low is probably due to the width of the static mixer. The larger the width, the smaller the force (which the screws exert to hold the plates together) in the middle between the screws.

Figure 34: Result of a failed test carried out with the second version of the static mixer

Figure 35: Result of a failed test carried out with the second version of the static mixer

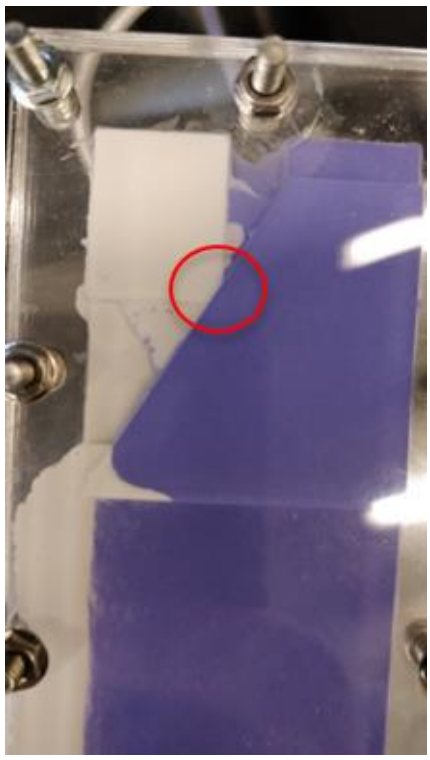

Figure 36: Result of a failed test carried out with the second version of the static mixer

After testing with the 2nd version of the modified static mixer, tests were performed with the existing small static mixer to obtain the target 'produce uniform, alternate multilayered polymer nanocomposites‘.

4.4 Tests with PEO and (PEO+MMT)-mixtures

4.4.1 Preparing the test solutions

After the pretests, tests were carried out with the actual test materials, namely solutions with polymers and nanoparticles. Before they could be used those solutions had to be prepared. For the polymer solutions, polyethylene oxide (PEO) is used. The polymer with nanoparticles solution is made with the components PEO and montmorillonite nanoparticles (MMT).

4.4.2 PEO-solution

The concentration of the PEO solution to be obtained was set at 5 wt% in advance. Thus ± 5 grams (exactly 5.16 g) of PEO was dissolved in 100 ml of deionized water. The deionized water is brought to a temperature of 60 ° C by using a heated stirring plate with sensor (Figure 37). To obtain a good distribution of the added heat a rod-shaped magnet is added. This will rotate around its axis and mix the solution. When the required temperature is reached, small amounts of PEO powder are added to the heated deionized water. When large quantities of PEO powder are added, they can start to stick together, resulting in larger particles. These larger particles dissolve less easily than small particles so the dissolution will take longer. The addition of the PEO particles is done at a higher temperature than the ambient temperature so the particles will disperse more rapidly in the solvent. To maintain a 100 ml solution, deionized water is added during stirring.

Figure 37: Setup for preparing the PEO-solution

4.4.3 (PEO + MMT) -suspension

It was decided to prepare a suspension of PEO and MMT with a ratio of 1/1. This means that the same amount of PEO as MMT particles must be added to the suspension. To make the MMT nanoparticles suspension, ± 5 grams (5.25 grams exactly) is added in a beaker with 75 ml or deionized water. The bottle is closed with parafilm and is shaken very hard so that all the clay particles dissolve in the water. Then 25 ml deionized water is added in the beaker so a 100 ml solution is obtained. The beaker with the solution is putted on a heated stirring plate with a temperature sensor (Figure 38). In the beaker a rod-shaped magnet is added. These will turn around his axis to ensure good mixing. The temperature sensor measures the temperature of the solution. When the solution is mixing, small amounts of PEO were added in the solution. Small amounts will be added because big amounts will result in clots and these are more difficult to dissolve. To dissolve the PEO faster, the solution is heated until 80 °C. Because of this, evaporation of the water of the solution will occur. To obtain a 100 ml solution at the end water was added to the beaker. In total 4.75 grams of the total 5.25 grams PEO is added in the solution. The resulting suspension has a ratio of PEO and MMT that is nearly equal to one.

Figure 38: Setup for preparing the (PEO+MMT) -suspension

4.4.4 Getting the right viscosity

After the PEO solution and the (PEO + MMT) -suspension have been prepared, it is opted to achieve the correct viscosity of these mixtures. The correct viscosity is achieved by allowing water to evaporate from the mixtures. This can be done either on the atmospheric air or with the help of an oven.
Graph 1 shows the evaporation of the PEO and (PEO + MMT) -mixtures to the atmospheric air. The average ambient temperature and relative humidity were 23.4 ° C and 49.8% respectively. From Graph 1 it can be deduced that the loss in weight of both mixtures as a result of evaporation of water decreases linearly with time. After being exposed to the atmosphere for 240 hours, about 15 g of water was evaporated from the (PEO + MMT) solution. Only ± 12 grams of water evaporated from the PEO solution in 240 hours. Since, after being exposed to the atmosphere for 240 hours, the correct viscosity had still not been reached and the evaporation of water from the mixtures into the atmosphere was a slow process, the mixtures were put in an oven.

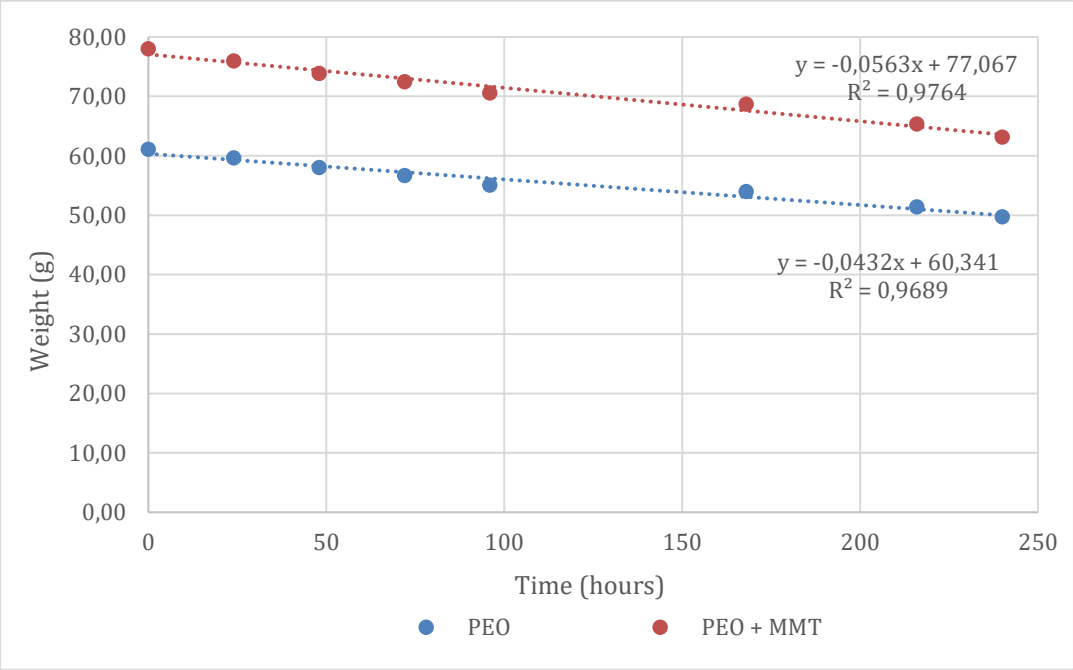

Graph 1: Evaporation of PEO and (PEO+MMT)-mixture in the air at 23.4°C and 49.8%

Graph 2 shows the evaporation of the PEO solution in the oven. The oven had a temperature of 50 ° C. A higher temperature than 50 ° C was not taken since the melting temperature of PEO is between 59 and 64 ° C [16]. From Graph 2 can be observed that the loss in weight of the solution due to evaporation of water decreases linearly with time. After being exposed to 50 ° C in the oven for 315 minutes, about 7 g of water was evaporated from the PEO solution. In the graph it can be seen that 2 values for the weight of the solution occur around a time of 75 minutes. This is because after 75 minutes the solution was removed from the oven and exposed to the air. This was done to prevent the solution from being left in the oven for a full night and thereby the solution would be completely dehydrated. After the solution finally sat for 315 minutes in the oven, it was visually determined that the correct viscosity was achieved

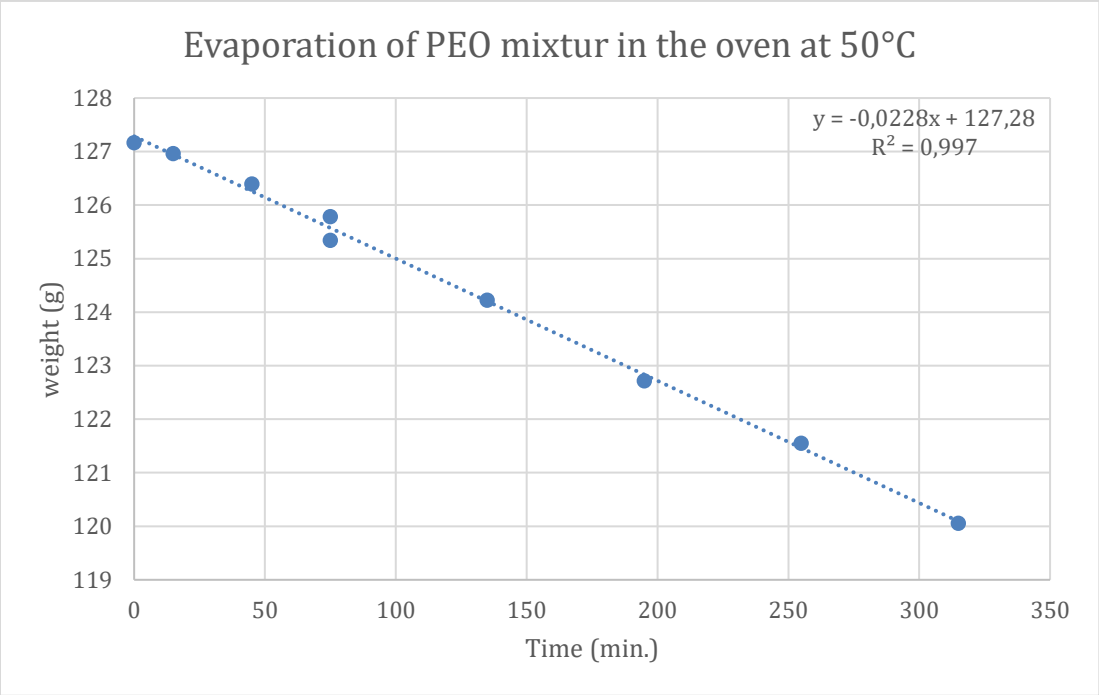

Graph 2: Evaporation of PEO-mixture in the oven at 50°C

Graph 3 shows the evaporation of the (PEO + MMT) -suspension in the oven. The oven had a temperature of 50 ° C. A higher temperature than 50 ° C was not taken since the melting temperature of PEO is between 59 and 64 ° C [16]. From Graph 3 can be observed that the loss in weight of the suspension due to evaporation of water decreases linearly with time. After being exposed to 50 ° C in the oven for 190 minutes, about 5 g of water was evaporated from the (PEO + MMT) -suspension. In the graph can be seen that 2 values for the weight of the suspension occur around a time interval of 70 minutes. This is because after 70 minutes the suspension was removed from the oven and exposed to the air. This was done to prevent the suspension from being left in the oven for a full night and thus the solution would be completely dehydrated. After the solution finally sat 190 minutes in the oven, it was visually determined that the correct viscosity was achieved.

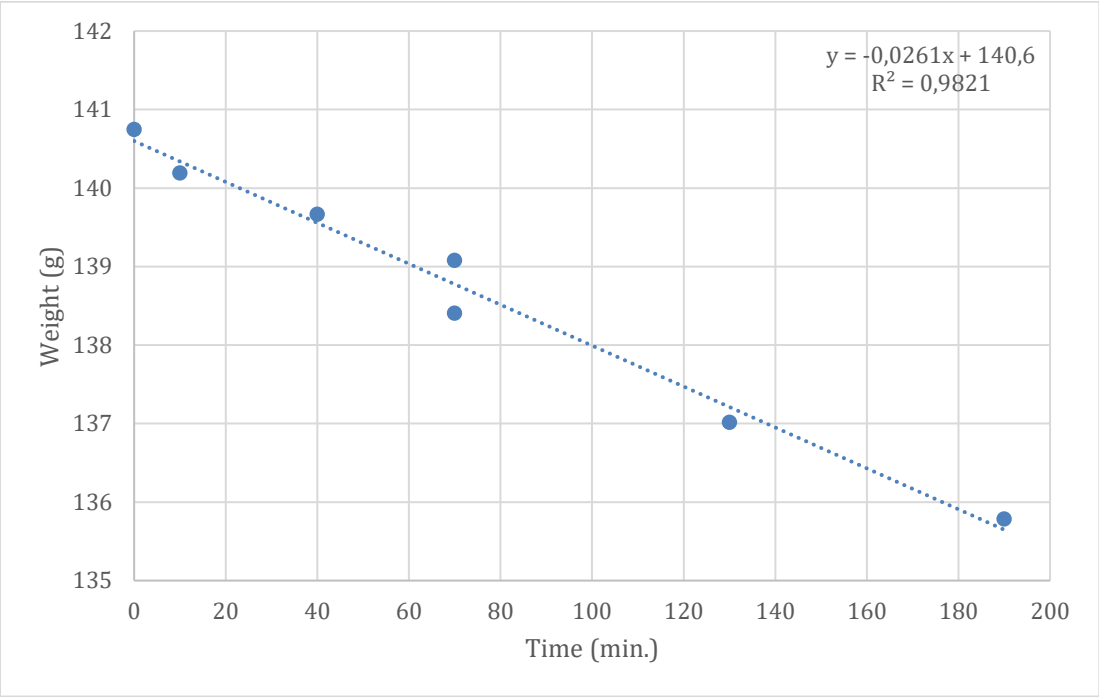

Graph 3: Evaporation of (PEO+MMT) -mixture in the oven at 50°C

After the correct viscosity of the PEO and (PEO + MMT) -mixtures was visually determined, the exact viscosity of these mixtures was measured with a rheometer. Graph 4 and Graph 5 show the viscosity according to the shear rate of the two mixtures.

From both graphs it also can be observed that the viscosity of both mixtures decreases as the shear rate increases. This phenomenon is called shear thinning [17]. This behavior is typical for a suspension. Shear thinning is caused by the disentanglement of polymer chains and the disassembly of agglomerates during the flow of the mixtures [18] [19]. The polymer chains of the mixtures are intertwined at rest and have an arbitrary orientation. When the mixtures are set in motion, the polymer chains will disentangle and assume the same orientation. As a result of this, the viscosity will decrease [19]. The agglomerates will also disintegrate and will form individual particulates that aligns similar to a biking team to reduce air drag. As a result the viscosity will also drop [18].

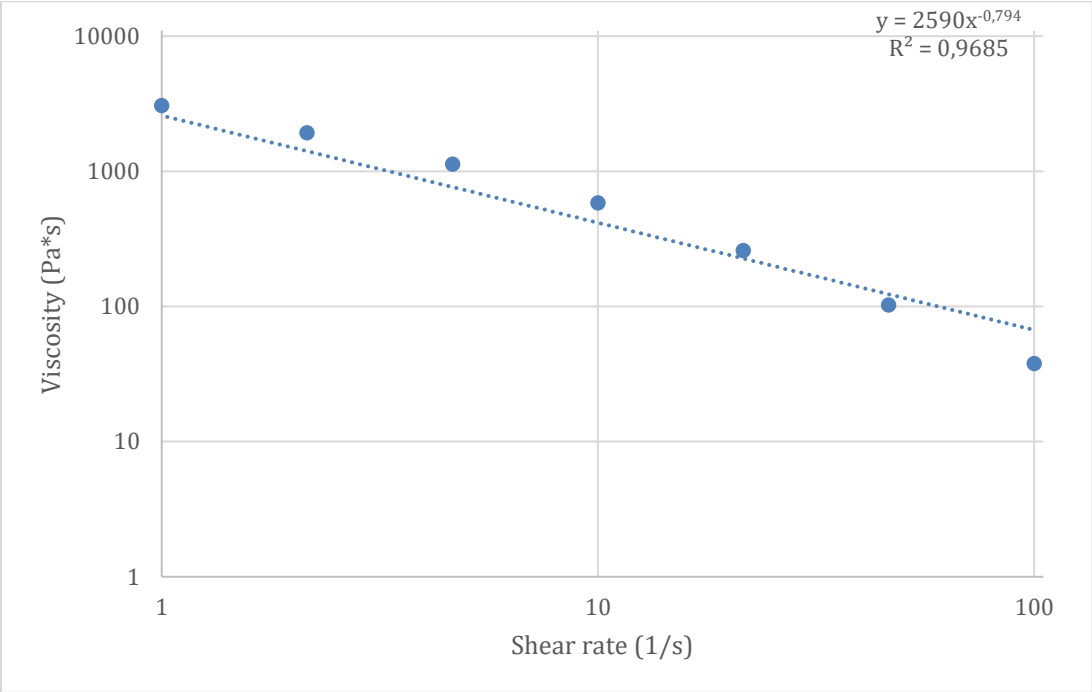

Graph 4: Viscosity measurement of the PEO-solution

When both graphs are compared, it can be observed that the viscosity of the PEO solution is initially higher than the viscosity of the (PEO + MMT) -suspension. This difference can be due to the concatenation of the PEO particles. In the PEO solution the PEO particles can interact better than in the (PEO + MMT)-suspension. In the (PEO + MMT)-suspension, the MMT particles will ensure that the PEO particles can react less well with each other and resulting in fewer chains that interlock. As a result the viscosity of the suspension will be lower.

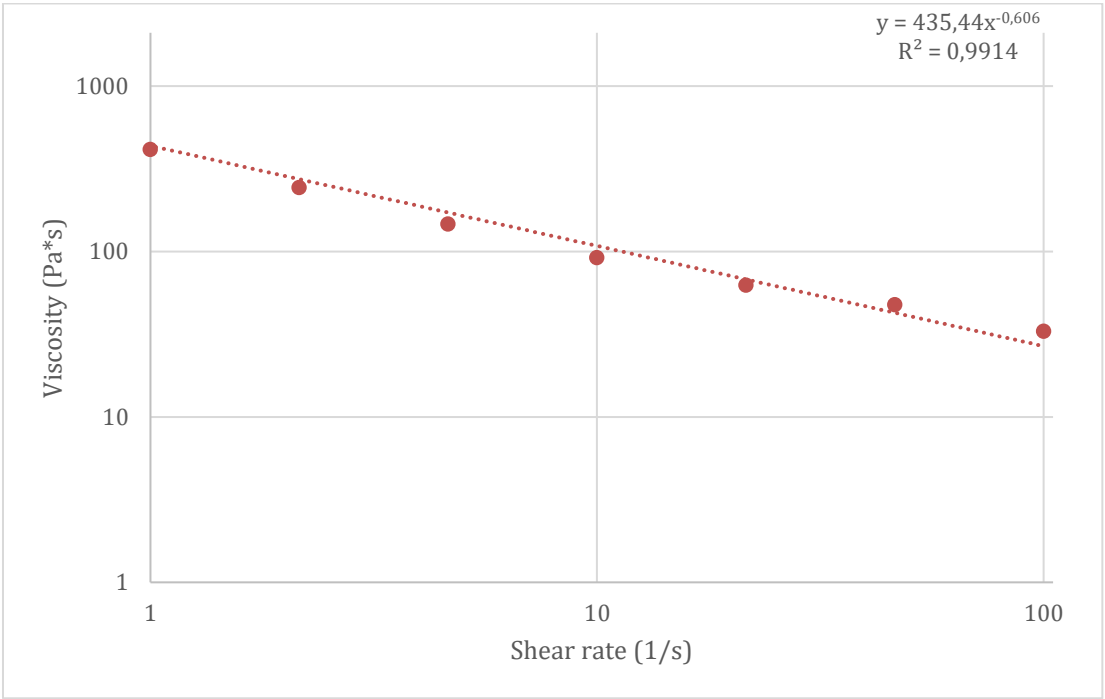

Graph 5: Viscosity measurement of the (PEO+MMT)-mixture

Using Graph 4 and Graph 5, the correct viscosity can be determined for the PEO-solution and the (PEO + MMT) suspension when pushed through the tubes. For this the shear rate must first be determined. This can be calculated using the formula below [20]:

$$\dot{\gamma} = \frac{\theta}{d/2} = \frac{0.5mm/min.}{\frac{1mm}{2}} = \frac{\frac{0.5\ mm}{60\ sec.}}{\frac{1\ mm}{2}} = \frac{1}{60} = 0.0166\ sec^{-1}$$

In this formula, $\dot{\gamma}$ represents the shear rate, Θ the rate at which the fluid is forced through the tube, and d represents the inner diameter of the tube [20].
When this shear rate is entered in the equations of Graph 4 and Graph 5, the viscosity is determined for these mixtures:

- PEO-solution:

$$\eta = \dot{\gamma} = 2590 \cdot x^{-0.794}$$
$$= 2590 \cdot 0.0166^{-0.794}$$
$$= 67147.45\ Pa \cdot s$$

- (PEO+MMT)-mixture:

$$\eta = \dot{\gamma} = 435.44 \cdot x^{-0.606}$$
$$= 435.44 \cdot 0.0166^{-0.606}$$
$$= 5218.47\ Pa \cdot s$$

The calculated viscosities of the PEO and (PEO + MMT) suspensions are very different. This can be due to the forces between the particles of the mixtures. The PEO-suspension only consists of PEO particles that will concatenate together. At the (PEO + MMT) suspension, the MMT particles will disrupt the concatenations of the PEO particles. This will make it easier to break the forces between the PEO particles than when only PEO particles are present in the suspension. This results in a lower viscosity.

4.4.5 Gas permeability

To find out the practical value of the gas permeability of the mixtures, various substrates such as a beaker, paper, a cutlery folder, a watch glass and a plastic petri dish were used with PEO solution and (PEO + MMT)-suspension and cured in the oven.
The cutlery folder is probably made of polystyrene (PS) and the Petri dish is probably made of polypropylene (PP). By adding the mixtures on the beakers, paper and watch glasses the mixtures remained fixed on their place when they were spread over the surface. But by adding on the cutlery folder and the plastic Petri dishes, the mixtures creep back together into a drop. A possible reason for this phenomenon can be related to the surface energy of the substrates. Table 1 shows the solid surface energy of PP, PS, glass and PEO at 20°C. The surface energy of PEO is larger than that of PP or PS. As a result, the intermolecular forces of the PEO-solution will increase the attractiveness of the substrate [21]. Which means that the PEO solution wants to have a contact surface with the substrate (PP and PS) as small as possible. As a result, the solution curls up into a drop and the entire surface will not be covered with the solution (Figure 39).
The surface energy of the substrate glass is higher than those of the PEO solution. Because of this, the attraction forces of the substrate are larger than the intermolecular forces of the solution. As a result, the solution will not form a drop but spread over the surface of the substrate.

Table 1: Solid surface energy of some substrates and PEO at 20 °C [22] [23]

Materials	Solid surface energy (mN/m)
Polystyrene (PS)	40.7
Polypropylene (PP)	30.1
Glass	> 200
Polyethylene oxide (PEO)	42.9

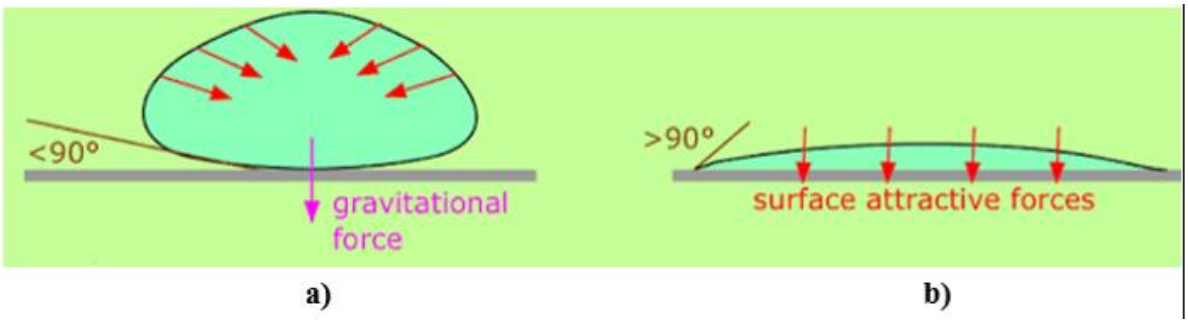

Figure 39: a) the surface energy of the solution is bigger than the surface energy of the substrate; b) the surface energy of the substrate is bigger than the surface energy of the solution [19]

The substrates with mixtures placed into the oven at a temperature of 50 °-C were the plastic Petri dishes, the beakers and the paper. These were placed in the oven so that they would dry out completely. As all the water evaporates from the mixtures, the mixtures solidify and a film is obtained. These films could be tested for gas permeability on the Mocon measuring device. The maximum thickness of the samples for the permeability tests is 2 mm. The thickness of the films that would be obtained with the cutlery folder and the watch glasses would be thicker than 2 mm. So these films could not be tested on the Mocon. Therefore, the solutions on these substrates were not cured in the oven.

When the solutions have become hard in the oven, they are analyzed just by looking with the naked eye (Figure 40, Figure 41, Figure 43 and Figure 44) and under the optical microscope (Figure 42 and Figure 45).
Figure 40 and Figure 41 show PEO-solutions on different substrates. Figure 40 shows a paper soaked with PEO-solution that is dried in the oven. On the figure can be seen that there are folds in the paper. These folds ensure that certain areas of the paper are thicker than others. This will result in a wrong permeability value because at these places the gas molecules have to diffuse a longer distance through the material. Figure 41 shows the petri dish with dried PEO-solution. On this figure can be seen that there are no air bubbles in the structure and that there are two different areas, a white one and a transparent one. A possible explanation for this phenomenon can be that one area has less solution than the other and thus is less thick. Figure 42 shows the microscopic view of the PEO-solution. On this figure can be seen that there are no internal air bubbles.

Figure 40: Paper soaked with PEO-solution and dried in the oven

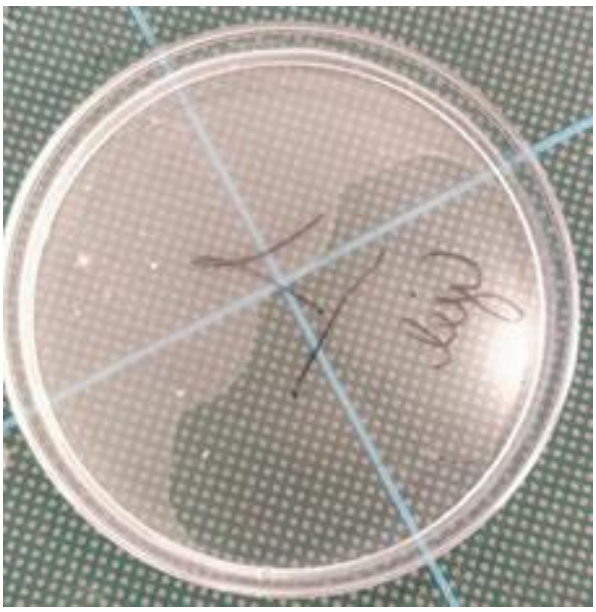

Figure 41: Petri dish with dried PEO-solution

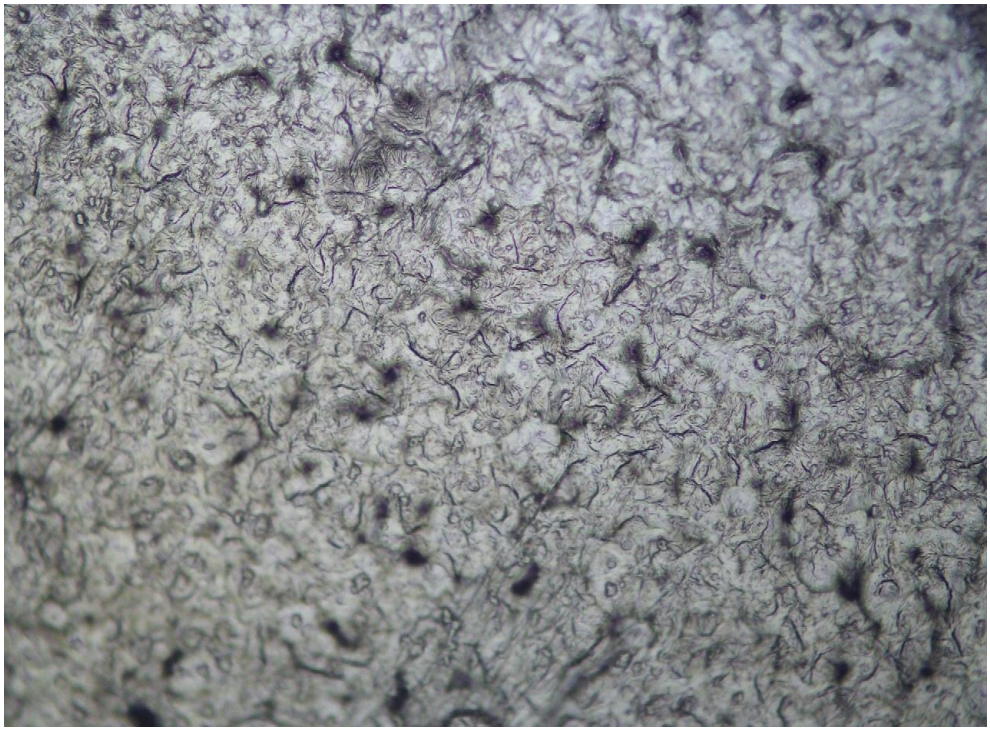

Figure 42: Microscopic view of PEO-solution with a magnification of 20X

Figure 43 and Figure 44 show (PEO+MMT)-mixtures on different substrates like a plastic Petri dish and a beaker. On these figures can be seen that there are air bubbles in the structure. Also the MMT-particles are clearly viewed.

Figure *45* shows the microscopic view of the (PEO+MMT)-suspension. On this figure it can be seen that there are holes in the structure. These holes are snapped air bubbles. These holes and air bubbles will be a problem when permeability tests are carried out. At the places where the air bubbles snapped will the thickness be less than on other places. This will result in a wrong

permeability value because at these places the gas molecules have to diffuse a shorter distance through the material.

Figure 43: Petri dish with dried (PEO+MMT)-suspension

Figure 44: Beaker with dried (PEO+MMT)-suspension

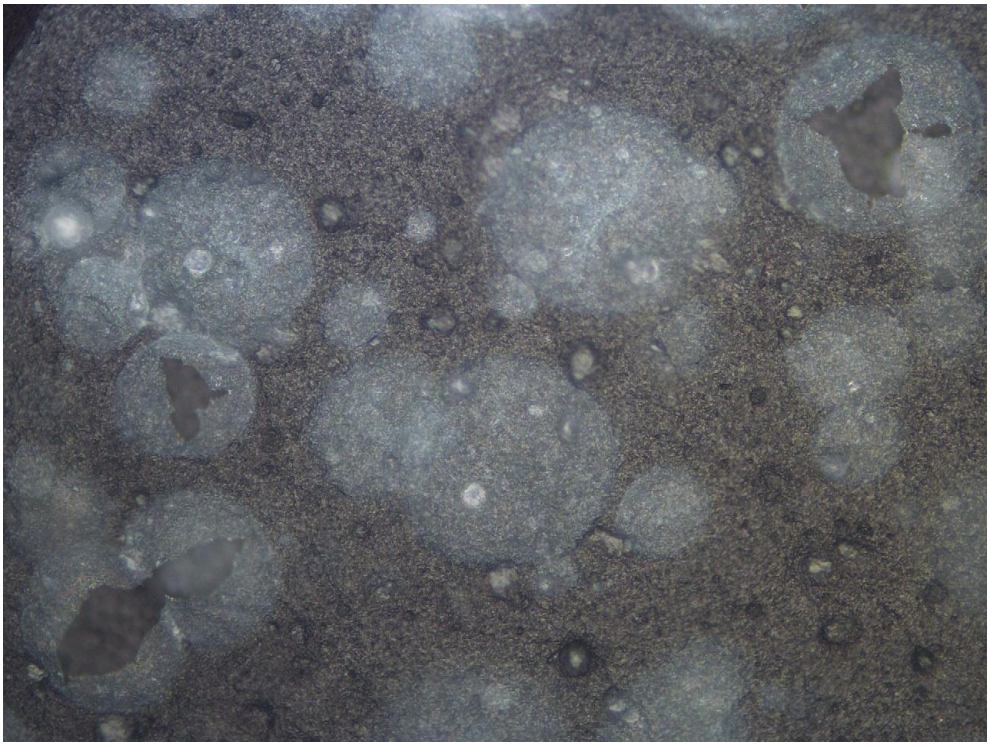

Figure 45: Microscopic view of (PEO+MMT) -suspension with a magnification of 20X

The film consisting of PEO-solution from the petri dish (Figure 41) can be used for gas permeability tests. Before the film is tested for gas permeability, the thickness of the film was measured using the MTS MI20 micrometer. The thickness of a film is measured because it has an influence on the gas permeability of a film. The thicker the film, the longer it takes for a gas to pass through the film. On the PEO-film, 10 thickness measurements are carried out on 10

different locations (Figure 46). The average of these thickness values is determined and showed in Table 2.

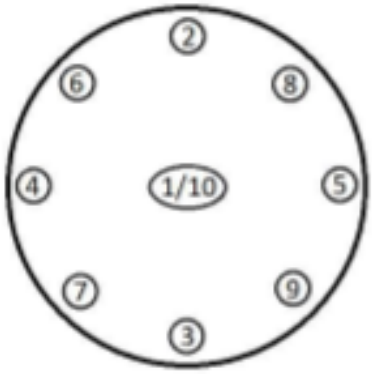

Figure 46: Locations where the sample thickness is measured [24]

Table 2: Thickness measurements of the PEO-film

Measurements	Thickness of the PEO-film (mm)
1	0.0700
2	0.0744
3	0.0653
4	0.0622
5	0.0643
6	0.0699
7	0.0611
8	0.0696
9	0.0619
10	0.0703
Average thickness	0.0669 mm

After the average thickness of the film has been determined, the film is provided with a mask so that no leaks can occur during the test (Figure 47). Then the film can be tested for oxygen permeability using the Mocon Oxtran Model 2/21 ML measuring device (Figure 48). The conditions in which the test was carried out were at 23 °-C and 0% RH. 100% oxygen gas (O_2) is injected on one side of the film and 100% nitrogen gas (N_2) on the other side of the film. The output of this test resulted in a 'fail'. This means that the permeability of the sample was too high to measure for the measuring device. A possible reason may be that the thickness of the film was too small. This means that the sample did not resist diffusion, as a result of which the O_2 could easily diffuse through the film. Another possible explanation may be that during the gluing of the film on the mask some areas are not glued. As a result of this openings are formed along the sample. So through these openings O_2 can easily pass through the film. This result may also be due to a too high natural gas permeability of PEO.

Figure 47: The PEO-film glued in a mask

Figure 48: Mocon Oxtran Model 2/21 ML

A 2nd oxygen permeability test was performed on the PEO film under the same conditions, namely 23 ° C and 0% RH. Only the percentage of O_2 is reduced to 21%. The percentage N_2 remains the same. The output of this test also resulted in a 'fail'. The permeability was too high for the Mocon to measure. Possible explanations for this result may be due to the thickness of the film, any leaks in the mask or a too high natural gas permeability of PEO.

4.4.6 Tests in the static mixer

Using the existing small static mixer, the prepared PEO solution and (PEO + MMT)-suspension, tests were performed on the tensile machine.
A first test was performed using only the (PEO + MMT) -suspension. In this test, the syringes were pushed at a speed of 0.5 mm/min so that the mixtures slowly passed through the tubes and needles into the static mixer. Figure 49 and Figure 50 show the microscopic view of the output of the test. On these figures different layers can be observed. In contrast to the layers obtained in (Figure 28 and Figure 29), these layers are straight. Above these layers there is an area where no layers can be observed. In this area, the mixtures are probably mixed together, resulting in a 'turbulent' flow of the mixtures.

Figure 49: Microscopic view with a magnification of 5X of an output using (PEO+MMT) -suspension as test material

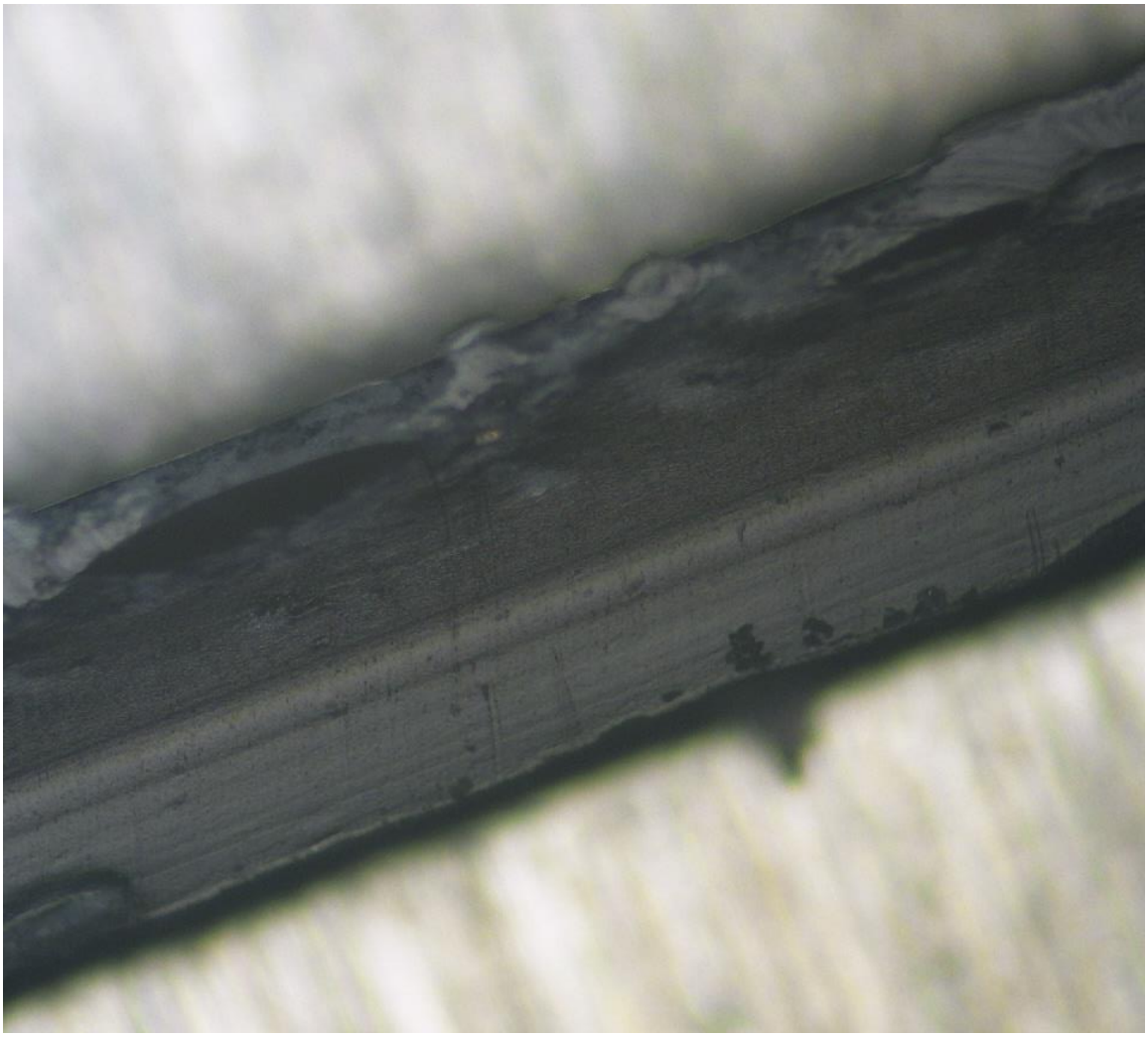

Figure 50: Microscopic view with a magnification of 5X of an output using (PEO+MMT) -suspension as test material

As a second test, both the PEO solution and the (PEO + MMT)-suspension were used as test material. In this test, the syringes were pushed at a speed of 1 mm/min so that the mixtures slowly passed through the tubes and needles into the static mixer. During this test the glued area leaked. Due to this, test material came out of the tube (Figure 51). Because of this leak, the test was stopped and no output was obtained. A possible reason for this incident may be a blockage of particles. As a result, the pressure in the tube can become too large and the glued zones can eventually start to leak under the high pressure.

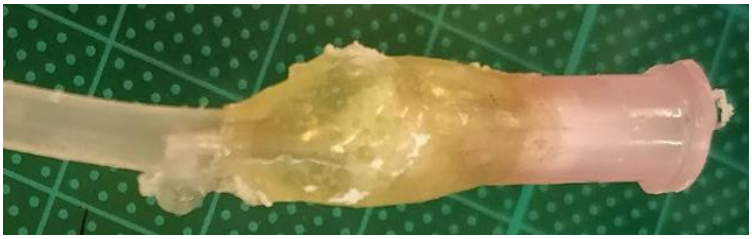

Figure 51: a leak in the glued zone

After the repair of the leak, another test was carried out with the same test materials. During this test a tube burst, so the test could not be continued and no output was obtained. A possible reason for this event could be damage to the inside of the tube. When the needles are placed in

the tubes, the tubes will be damaged inside. This is because the outer diameter of the needles is 1.2 mm while the inner diameter of the tubes is equal to 1.00 mm. As a result, a part of the inside of the tube is scraped away, making the tube thinner and therefore weaker. This damage is prevented in further tests by rounding the ends of the needles. This is achieved by sanding the needles against a fine sanding belt until the sharp edge of the needle has been removed (Figure 52).

Figure 52: Sanding needles to eliminate the sharp edges

After the needles were flattened and a new setup was made, the test was repeated with the PEO solution and the (PEO + MMT)-suspension. In this test, the syringes were pushed at a speed of 1 mm/min so that the mixtures slowly passed through the tubes and needles into the static mixer. During the test there were no defects and an output was obtained. Because the output collapsed when it came out of the static mixer, the remainder of the output was held in the static mixer to harden. After a few days it could be observed that the output had hardened but that it had no closed but crumbled, dried-out structure (Figure 53). Figure 53 shows that the output in the static mixer contains large gaps in its structure. The possible reason for this phenomenon may be due to the evaporation of the water from the mixtures. The water of the mixtures left the output by evaporation. Because the static mixer is a dense construction, the water has made its way through the output and caused large gaps in the structure.

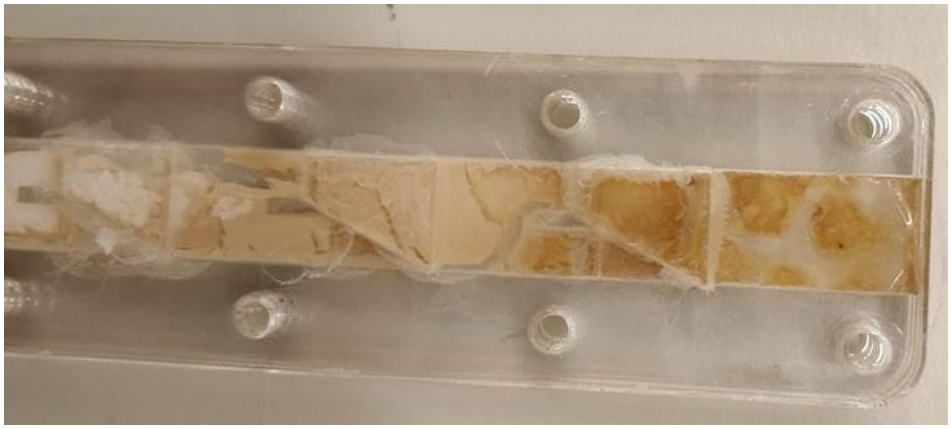

Figure 53: Crumbled, dried out structure of an output with PEO and PEO+MMT as test materials

4.5 Epofix mixtures with PS and MMT particles

Because of the phenomenon from Figure 53 the thesis has worked further with other materials: polystyrene, epoxy resin and epoxy resin hardener. Epofix resin is a cold-curing resin consisting of 2 liquid epoxy components [25]. Epofix hardener or Triethylenetetramine [26] is a substance that will make the Epofix resin hard [27] .

4.5.1 Preparing the test solutions

Before tests can be carried out with these materials, pretests must first be carried out to determine how the materials behave in the static mixer. These tests were performed using the existing small static mixer. With each pretest, the suspensions must be prepared a short time before the experiment. This is because Epofix hardener is added in the suspensions. This substance ensures that the suspension will become hard and no longer usable within ± 30 minutes [25]. As a result, this suspension cannot be prepared in advance. The mixture will be totally cured after a drying time of ± 8 hour [25].

4.5.2 Pretests

At the first pretest 2 suspensions were made using Epofix resin, Epofix hardener and PS particles. Both suspensions were prepared by mixing 5 ml Epofix resin with 1 ml Epofix hardener and the amount of one teaspoon of PS particles. PS particles with a diameter of 80 μm were added to one suspension, while PS particles with a diameter of 20 μm were added to the other suspension. During this pretest the tensile machine pushed on the syringes at a speed of 0.5 mm/min. During the pretest, the suspension with 20 μm particles went into the static mixer while the suspension with 80 μm particles came into the tube and got stuck here causing the tube to swell and eventually burst. A possible reason for this event may be due to agglomeration of the PS particles. By means of agglomeration a large PS particle can be formed, causing the tube or the input needle of the static mixer to become clogged and the tube bursting due to the high pressure in the tube. A second possible reason may be that the mixture had already become partially hardened. As a result, the mixture could also get stuck in the tube so that the pressure can rise high. A third possible explanation can be found with a too high viscosity of the suspensions. Due to a high viscosity, it is difficult for the suspension to flow from one part of the test setup to the other part (e.g., from the syringe to the needle, from the tube to the needle). As a result, high pressures can also be created in the tubes.

A second pretest was carried out using 2 suspensions prepared with Epofix resin, Epofix hardener and PS particles. Both suspensions were prepared by mixing 5 ml of Epofix resin with 1 ml Epofix hardener and the amount of one teaspoon of PS particles. PS particles with a diameter of 20 μm were added to one suspension, while PS particles with a diameter of 6 μm were added to the other suspension. During this pretest the tensile machine pushed on the syringes at a speed of 0.5 mm/min. During the pretest, the suspension with 6 μm particles went into the static mixer while the suspension with 20 μm particles came into the tube and got stuck here causing the tube to swell. A possible reason for this event may be due to agglomeration of the PS particles. By means of agglomeration, a large PS particle can be formed, causing the tube or the input needle of the static mixer to become clogged and the tube swelling up due to the high pressure in the tube. A second possible reason may be that the mixture had already become partially hardened. As a result, the mixture could also get stuck in the tube so that the pressure can rise high. A third possible explanation can be found with a too high viscosity of the suspensions. Due to a high viscosity, it is difficult for the suspension to flow from one part of the test setup to the other part (e.g., from the syringe to the needle, from the tube to the needle). As a result, high pressures can also be created in the tubes.

Subsequently, a third pretest was performed using 2 suspensions prepared with Epofix resin, Epofix hardener and PS particles. Both suspensions were prepared by mixing 5 ml of Epofix resin with 0.5 ml Epofix hardener and the amount of half a teaspoon of PS particles. The amount

of epoxy hardener and the amount of PS particles are halved so that the suspensions would harden less rapidly and the viscosity of the suspensions would be lower. As a result, the suspensions will flow more easily through the different parts of the setup. PS particles with a diameter of 20 μm were added to one suspension, while PS particles with a diameter of 6 μm were added to the other suspension. During this pre-test tesnsile machine pushed on the syringes at a speed of 0.5 mm/min. During the pretest, the suspension with 6 μm PS particles was faster in the static mixer than the suspension with 20 μm PS particles. This phenomenon is probably due to the size of the PS particles of the suspensions. The 20 μm PS particles experience more resistance during the flow than the 6 μm PS particles, causing the suspension of the 20 μm PS particles to move more slowly. The obtained output was kept in the static mixer for curing. This is done because the output collapses when it comes out of the static mixer. Because the added amount of Epofix hardener and PS particles has been reduced, the suspensions could flow more easily through the arrangement.

4.5.3 Tests

Knowing that the suspensions flow more easily through the setup when halving the amount of PS particles and Epofix hardener, further tests were carried out with these amounts. In the following tests, suspensions are prepared with 5 ml Epofix resin, 0.5 ml Epofix hardener and PS particles were used. The size of the PS particles was varied between different tests.

4.5.3.1 80/20 μm PS particles

A first test was carried out using 2 suspensions prepared with Epofix resin, Epofix hardener and PS particles. In one suspension, an amount of 1.45 g of PS particles having a diameter of 80 μm was added while in the other suspension an amount of 1.45 g of PS particles with a diameter of 20 μm was added. In this test the tensile machine pushed the syringes at a speed of 0.5 mm/min. During the pretest, the suspension with 20 μm PS particles was faster in the static mixer than the suspension with 80 μm PS particles. This phenomenon is probably due to the size of the PS particles of the suspensions. The 80 μm PS particles experience more resistance during the flow than the 20 μm PS particles, causing the suspension of the 80 μm PS particles to move more slowly. The obtained output was kept in the static mixer for curing. This is done because the output collapses when it comes out of the static mixer.

After the output was cured in the static mixer, the static mixer was cut at into the last compartment. The cut pieces were embedded in epoxy resin and polished to smooth the rough surface of the samples (Figure 54). By polishing the samples no dirt will adhere to the surface of the samples [28]. Finally, a carbon layer was applied to the embedded samples. This layer will ensure that the samples are not loaded when they are fired with electrons under the Scanning Electron Microscope (SEM).

Figure 54: An embedded and polished static mixer sample

Figure 55 and Figure 56 show a microscopic view obtained with the SEM of the output. Figure 55 shows the full thickness of the output while on Figure 56 the particles can be observed individually. On the figures the difference between the 2 types of particles is difficult to see. These can only be distinguished from each other on the basis of size. This is because in both mixtures particles of the same material were used, so there is little to no contrast between these particles on the figures. On Figure 55 can be seen that no layers have been formed but that the suspensions are mixed together. This may be due to the fact that the suspension with 20 µm particles was earlier in the static mixer than the suspension with 80 µm particles. The suspension with 20 µm particles partially filled the compartment of the suspension with 80 µm particles. As a result, the suspension with 80 µm particles can take particles of the suspension with 20 µm particles with them during the flow. This probably results in the mixing of the suspensions. Another factor that probably has an influence is the shear resistance of the mixtures against the walls of the static mixer. Due to this shear resistance, the suspension against the walls will move more slowly than the middle part of the suspension that does not make contact with the walls of the static mixer.

As a result, part of the suspensions will remain, which will eventually also result in the mixing of the suspensions.
Figure 56 is the enlarged image of the red rectangle in Figure 55. In Figure 56 it can be seen that agglomeration occurs at the PS particles, since certain particles on the figure are larger than the actual size of the particles. As a result of agglomeration, the particles cluster in the suspension. This phenomenon will also have an influence on the flow of the suspensions and thus also on the formation of the layers.

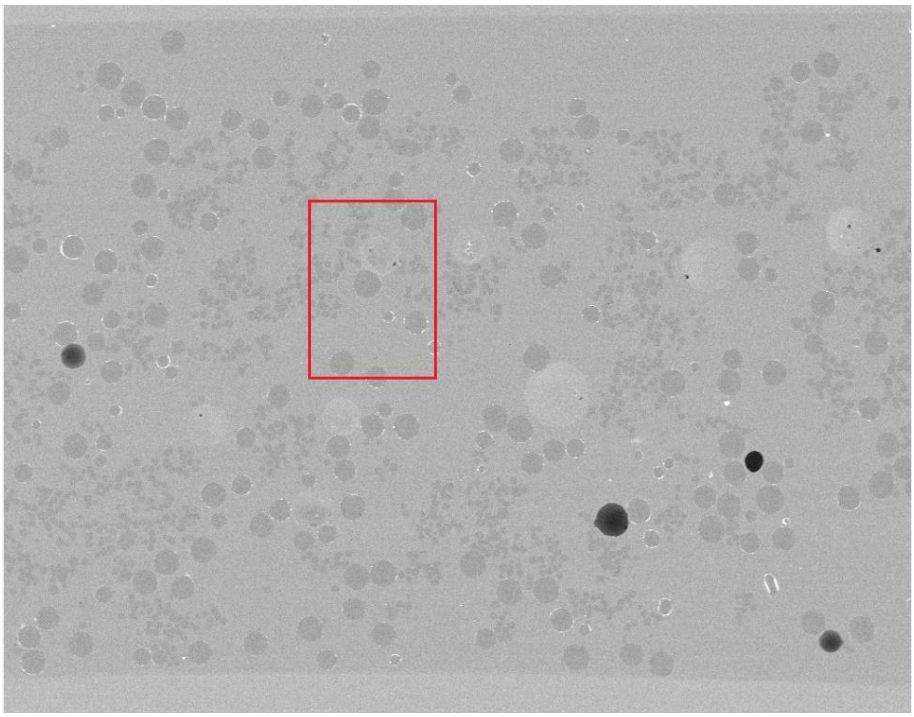

Figure 55: Microscopic SEM view (magnification of 100X) of an output of a sample made with 80 and 20 µm particles suspensions

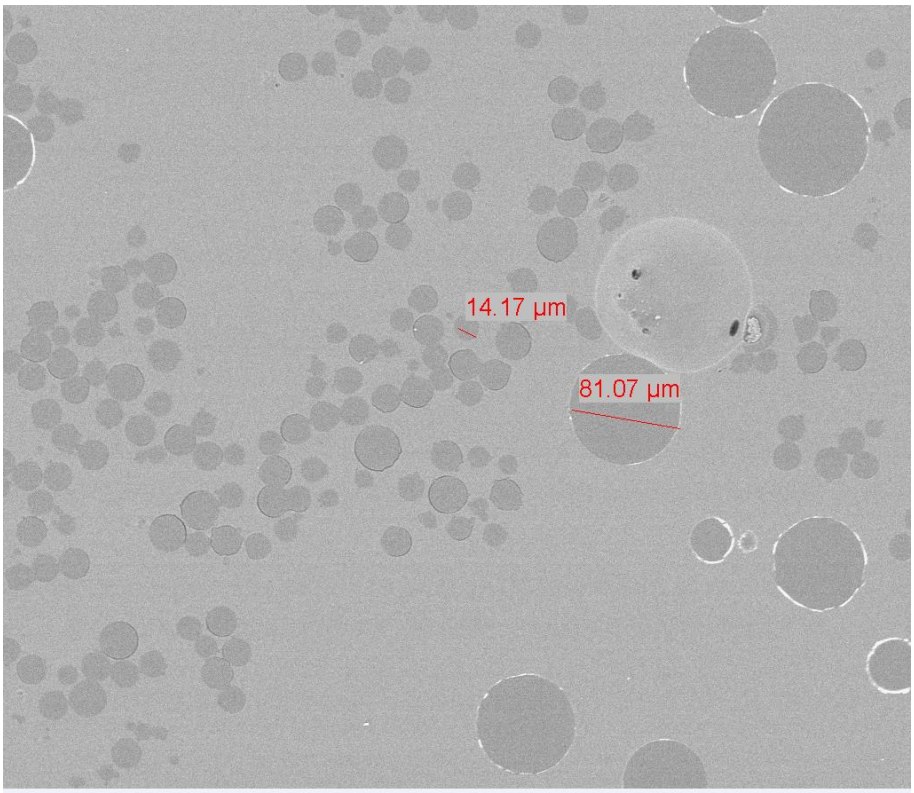

Figure 56: Microscopic SEM view (magnification of 400X) of an output of a sample made with 80 and 20 µm particles suspensions

4.5.3.2 20 µm PS particles and MMT particles

A second test was performed using 2 suspensions prepared with Epofix resin, Epofix hardener, PS particles and MMT particles. In one suspension, an amount of 1.56 g of PS particles having a diameter of 20 µm was added while in the other suspension an amount of 1.56 g of MMT particles was added. In this test the tensile machine pushed on the syringes at a speed of 0.5 mm/min. During the performance of the test, the suspension with MMT particles was earlier in the static mixer than the suspension with 20 µm PS particles. This phenomenon is probably due to the difference in size of the particles of the suspensions. The 20 µm PS particles experience more resistance during the flow than the MMT particles, causing the suspension of the 20 µm PS particles to move more slowly. The obtained output was kept in the static mixer for curing. This is done because the output collapses when it comes out of the static mixer.

After the output was cured in the static mixer, the static mixer was cut at the last compartment. The cut pieces were embedded in epoxy resin and polished. Finally, a carbon layer was applied to the embedded samples. This layer will ensure that the samples are not loaded when they are bombed with electrons under the Scanning Electron Microscope (SEM). Figure 57 and Figure 58 how a microscopic view obtained with the SEM of the output. Figure 57 shows the full thickness of the output while on Figure 58 the particles can be observed individually. On the photos the difference between the 2 types of particles is easy to see because of the difference in contrast. The brighter particles are the MMT particles and the darker particles are the PS particles. On Figure 57 can be seen that no layers are formed but that the suspensions are mixed together. This may be due to the fact that the suspension with MMT particles was earlier in the static mixer than the suspension with 20 µm particles. The suspension with MMT particles partially filled the compartment of the suspension with 20 µm particles.

As a result, the suspension with 20 µm particles can take particles of the suspension with MMT particles with them during the flow. This probably results in the mixing of the suspensions. Another factor that probably also plays a role is the shear resistance of the mixtures against the walls of the static mixer. Due to this shear resistance, the suspension against the walls will move more slowly than the middle part of the suspension that does not make contact with the walls of the static mixer. As a result, part of the suspensions will remain, which will eventually also result in the mixing of the suspensions.

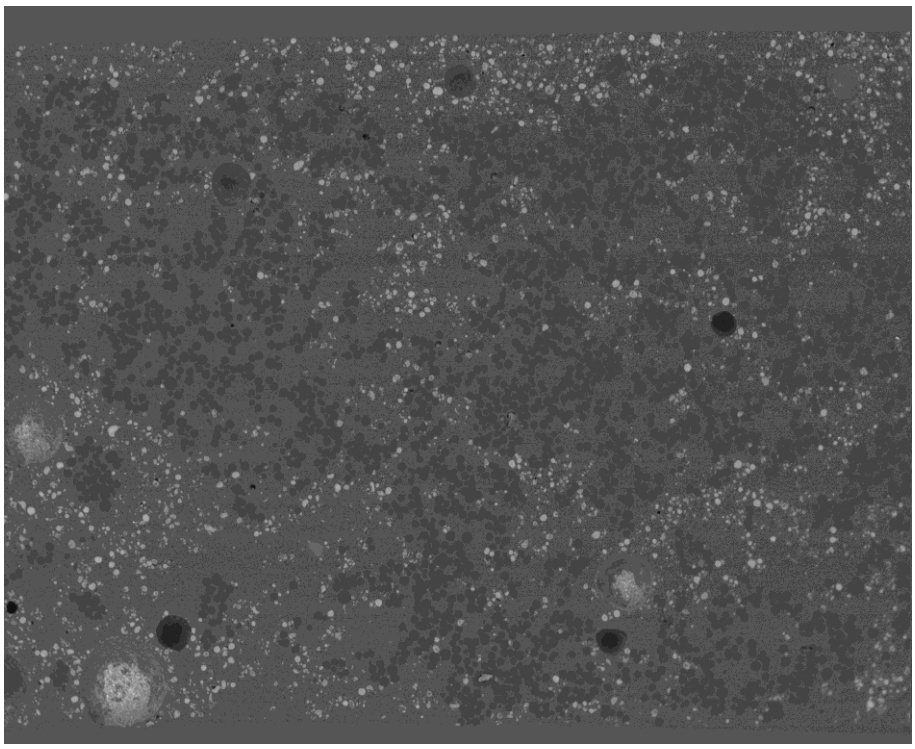

Figure 57: Microscopic SEM view (magnification of 88X) of an output of a sample made with 20 µm particles suspension and MMT suspension

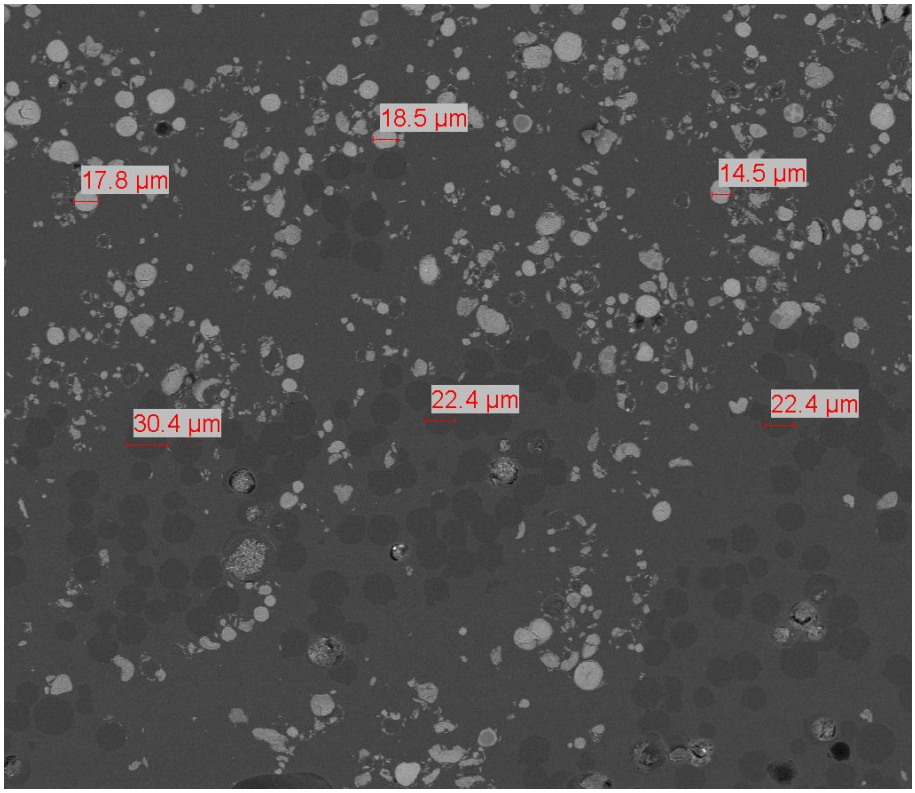

Figure 58: Microscopic SEM view (magnification of 400X) of an output of a sample made with 20 µm particles suspension and MMT suspension

4.5.3.3 6 µm PS particles and MMT particles

Subsequently, a third test was carried out using 2 suspensions prepared with Epofix resin, Epofix hardener, PS particles and MMT particles. In one suspension, an amount of 1.27 g of PS particles having a diameter of 6 µm was added, while an amount of 1.28 g of MMT particles was added to the other suspension. In this test the tensile machine pushed on the syringes at a speed of 0.5 mm/min. During the performance of the test, the suspension containing MMT particles and the suspension with 20 µm PS particles were injected simultaneously into the static mixer. This will be due to the fact that the dimensions of the particles are small enough. So they can easily flow through the different parts of the setup. The obtained output was kept in the static mixer for curing. This is done because the output collapses when it comes out of the static mixer

After the output was cured in the static mixer, the static mixer was cut at the last compartment. The cut pieces were embedded in epoxy resin and polished. Finally, a carbon layer was applied to the embedded samples. This layer will ensure that the samples are not loaded when they are bombed with electrons under the Scanning Electron Microscope (SEM). Figure 59, Figure 60 and Figure 61 show a microscopic view obtained with the SEM of the output. Figure 59 and Figure 60 show the full thickness of the output while on Figure 61 the particles can be observed individually. On the figures the difference between the 2 types of particles is easy to see because of the difference in contrast. The brighter particles are the MMT particles and the darker particles are the PS particles. On Figure 59 and Figure 60 it can be seen that layers have been formed finally. This may be due to the fact that the suspensions were injected into the static mixer at the same time, so no mixing could occur. On Figure 59 and Figure 60 can be observed that no uniform layers are formed. This may be due to the shear resistance that occurs against the wall of the static mixer in both mixtures.

Due to this shear resistance, the suspension against the walls will move more slowly than middle part of the suspension that does not make contact with the walls of the static mixer. As a result, part of the suspensions will remain, which will ultimately result in non-uniform layers.

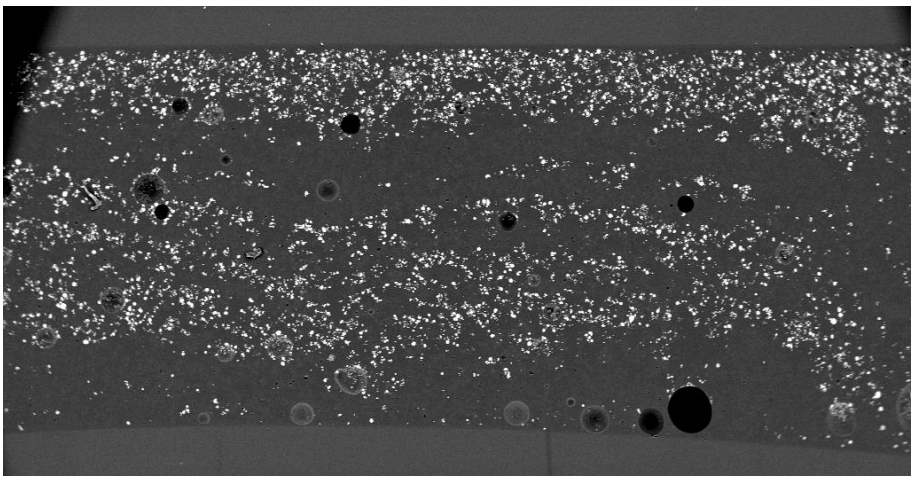

Figure 59:Microscopic SEM view (magnification of 57X) of an output of a sample made with 6 µm particles suspension and MMT suspension

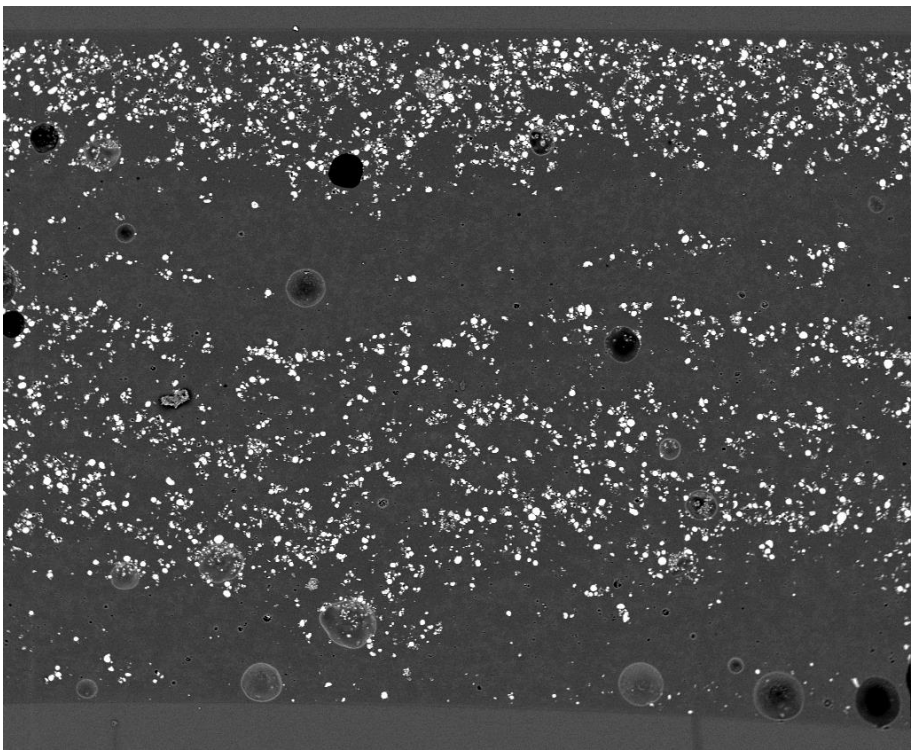

Figure 60: Microscopic SEM view (magnification of 100X) of an output of a sample made with 6 µm particles suspension and MMT suspension

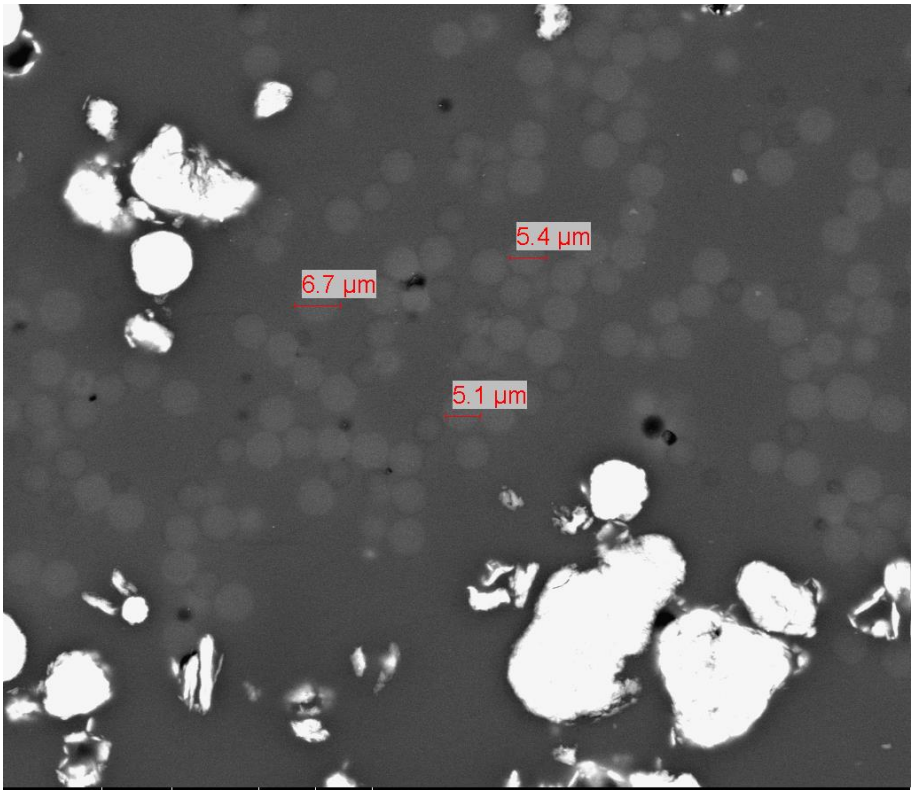

Figure 61: Microscopic SEM view (magnification of 2000X) of an output of a sample made with 6 µm particles suspension and MMT suspension

4.6 Static mixer with output of 64 layers

The lab scale static mixer has been extended so that the final output contains 64 alternating layers. In the design of the lab scale static mixer, two compartments have been added to the plate that stack the test materials on each other and then cut them in two (see red circles Figure 62). In addition, 2 extra compartments have been added to the plate that stretches the test materials biaxial (see red circles Figure 63). By means of these extra compartments, an output of 64 layers will be obtained instead of an output of 16 layers, which produces the lab scale static mixer. The width of the static mixer remains unchanged, but the length of the static mixer will increase 168.89 mm. This means that the output will retain a width of 1 cm. The technical drawings of the static mixer have been added to the appendix (appendix D).

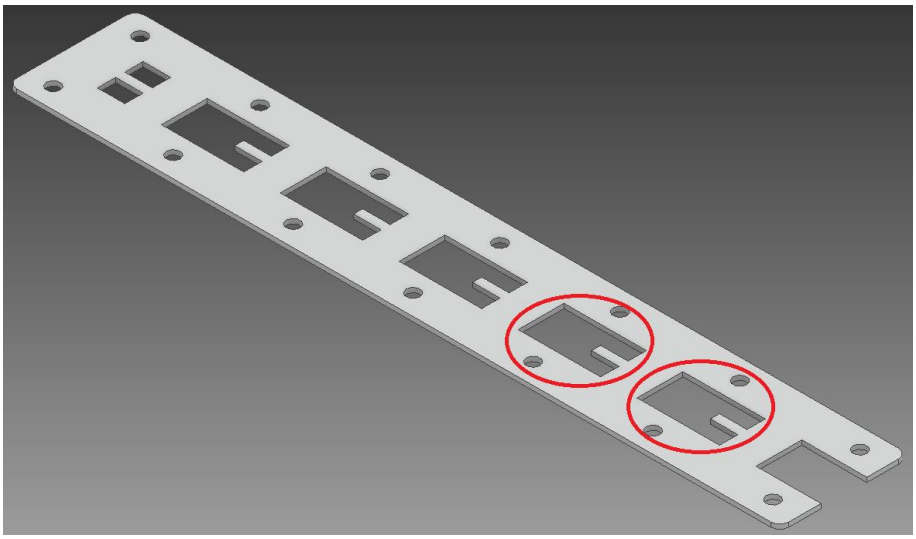

Figure 62: One of the 5 plates of the extended static mixer where the sample gets stacked and then cut

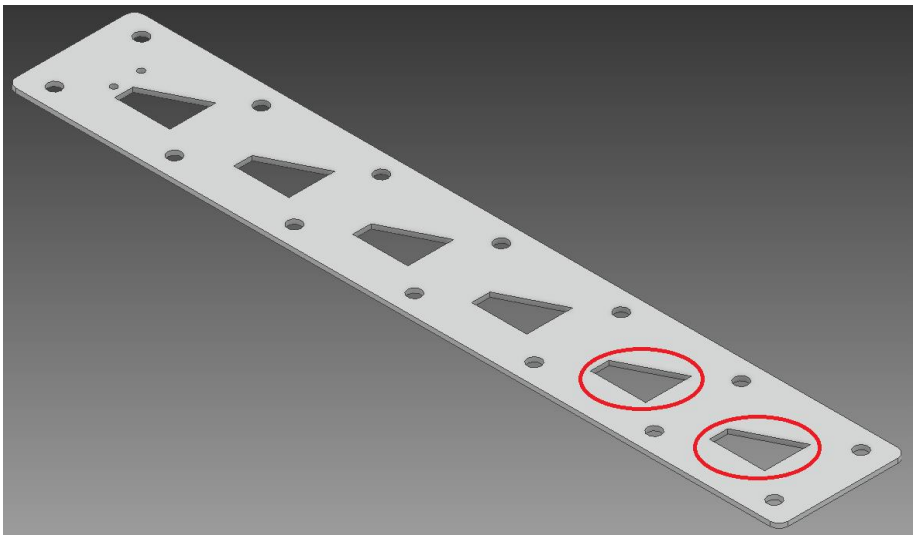

Figure 63: One of the 5 plates of the extended static mixer where the sample gets biaxial stretched

4.6.1 Test with the purple and white modeling clay mixtures

The design has been tested using the tensile machine with the purple and white modeling clay mixtures as test material. Because the static mixer is enlarged, more test material will be needed to completely fill the static mixer. Therefore, larger syringes are used during the test. The tensile machine pushed into the syringes with a speed of 1 mm/min instead of 10 mm/min.

Figure 64 and Figure 65 show the result of a test carried out with the extended lab scale static mixer. These figures show that the clay mixtures leave the static mixer along the side. Despite that the clay mixtures leave the static mixer along the side, the test still has been carried out further to obtain an output. This phenomenon is probably due to high viscosity. Because of the high viscosity, the pressure in the static mixer becomes too high even at small flow rates and the suspensions leave the static mixer the easiest way (the side of the static mixer). On the figures can also be seen that the purple clay mixture sticks at certain compartments during the flow (see red circles Figure 65).

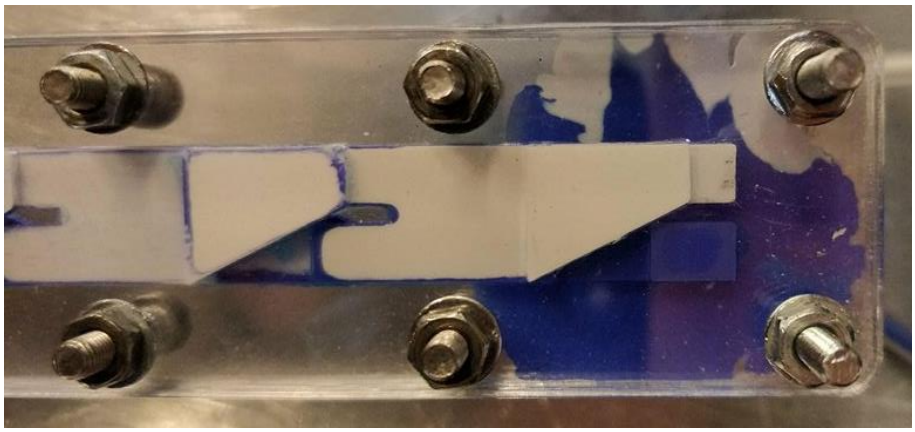

Figure 64: Result of a test carried out with the extended lab scale static mixer

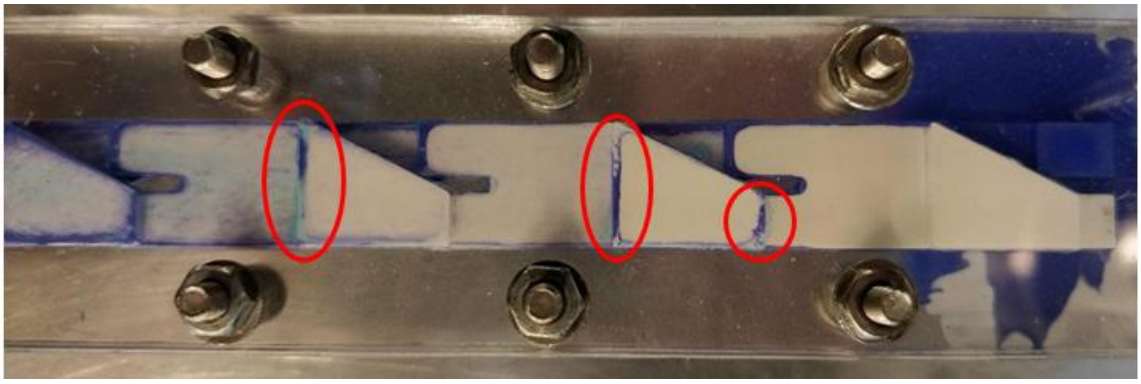

Figure 65: Result of a test carried out with the extended lab scale static mixer

Figure 66 and Figure 67 shows the inner structure of the clay output. These figures show that there are multilayers on one side of the output. These layers are not uniform as the shear rate with the static mixer is not constant. On the other side of the output no layers can be observed. A possible reason for this can be that the purple clay mixture sticks at certain compartments during the flow (see red circles Figure 65). Because the purple clay mixture will stick, this purple clay mixture shall form non or a few layers. Also can be occur that the white clay mixture contain purple clay particles (from the purple clay that sticks in the compartments) in its white layers. Due to this, the contrast between the white and the purple layers will fade and it will be difficult to observe layers in the inner structure.

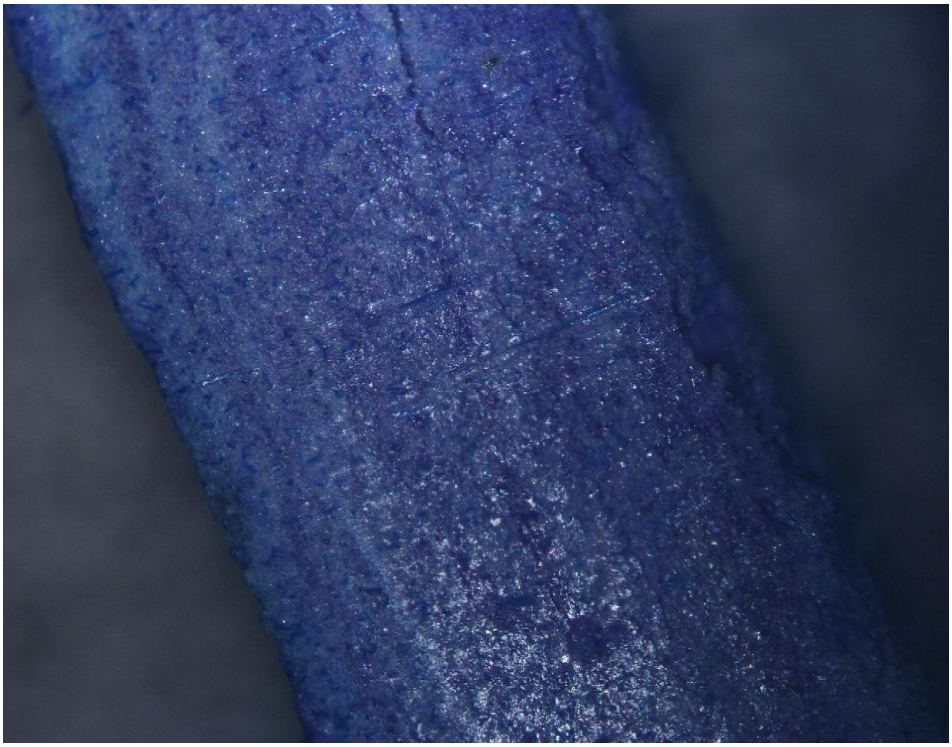

Figure 66: Microscopic view (with magnification of 5X) of the output created with the extended lab scale static mixer

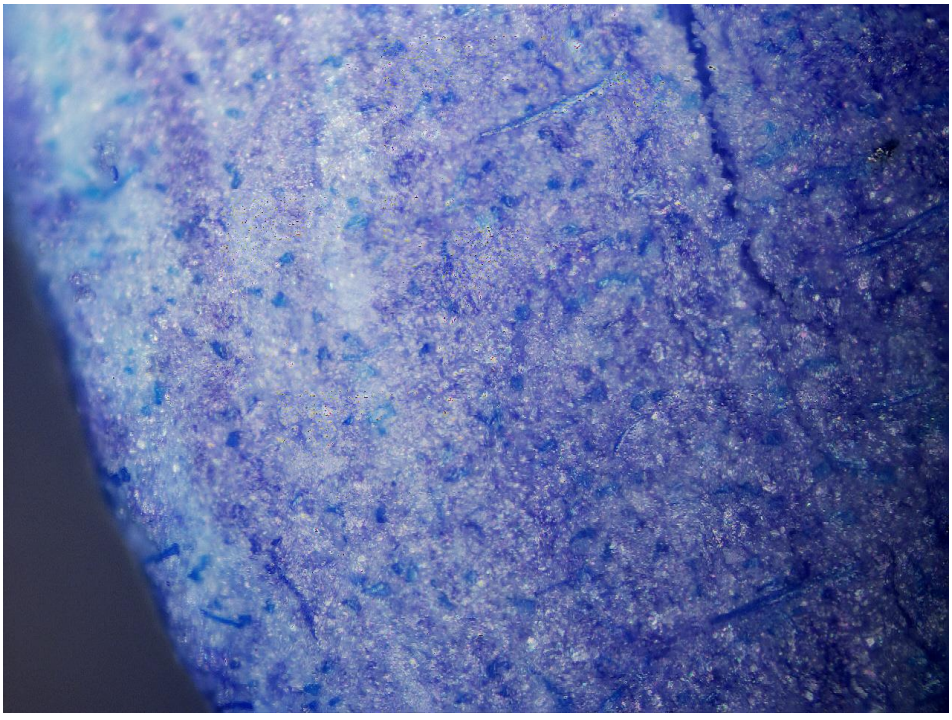

Figure 67: Microscopic view (with magnification of 10X) of the output created with modeling clay and the extended lab scale static mixer

4.6.2 Test with Epofix mixtures

A second test has been carried out using Epofix solutions as test materials. These solutions are made out of 5 ml Epofix resin and 0.5 ml Epofix hardener. In these solutions no particles are

added because the purpose of the test is to see 64 alternating layers. To see the contrast between the different Epofix layers, blue ink is added to 1 solution. The tensile machine pushed into the syringes with a speed of 1 mm/min. The cures sample are sanded with a p180 sanding belt to flatten the surface of the samples. A p180 sanding belt contains particles with an average diameter of 78 µm [29].

Figure 66 and Figure 67 shows the inner structure of the Epofix output. These figures show that there are multiple layers. It is not sure or these layers are obtained by the static mixer or by sanding the samples with sand belt. Theoretically, the output has to contain 64 layers. The thickness of the sample is 2 mm thus every layer has to have (theoretically) a thickness of:

$$\text{Thickness of 1 layer} = \frac{2\ mm}{64\ layers} = 0.03125 \text{ mm} = 31.25\ \mu\text{m}$$

On Figure 68 and Figure 69, the dimensions of a number of layers are indicated. The dimensions of these layers correspond to the theoretical thickness of 1 layer. Also big layers can be seen on the figures. These layers are probably made by the sanding belt since the average particles diameter of the sanding belt is 78 µm.

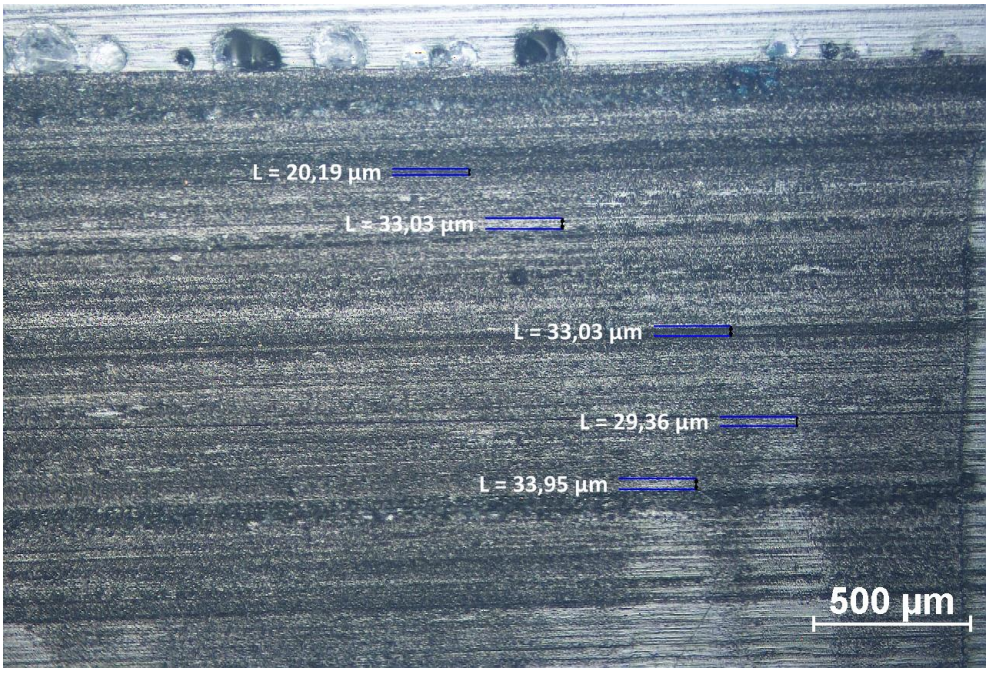

Figure 68: The microscopic view (with magnification 10X) of the output created with Epofix mixtures and the extended lab scale static mixer

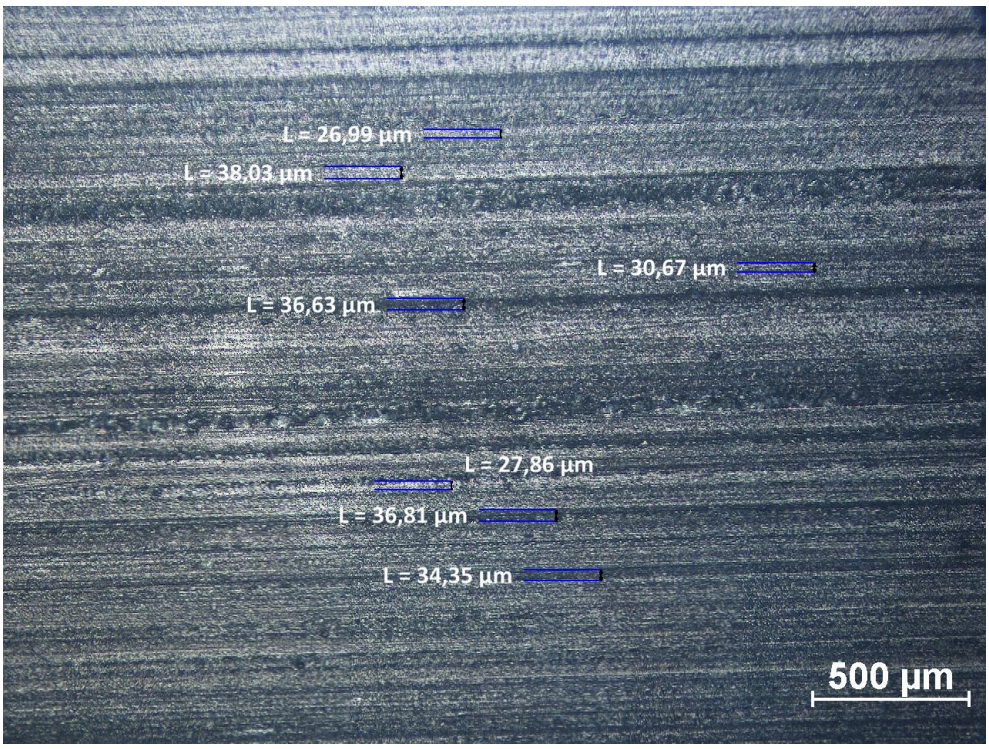

Figure 69: The microscopic view (with magnification 10X) of the output created with Epofix mixtures and the extended lab scale static mixer

5 Conclusion

This thesis has shown that multilayers can be produced with the help of static mixers. Viscosity is shown to have a large influence on the formation of uniform multilayers. When the viscosity was too low, the test materials were mixed. Because of this, no layers were formed or the obtained output sheet collapsed, so the layered structure could not be observed. A too high viscosity resulted in a high pressure in the components of the setup causing defects such as leaks and burst. In addition to viscosity, the shear resistance also has an influence on the formation of uniform multilayers. Because test materials move against the walls of the static mixer, shear resistance next to the wall will be highest. The variation in the speed between different layers in the static mixer results in non-uniform layer thickness. In future work one can try to avoid this by making the static mixer walls slippery to the flowing material. In this thesis it is shown that using a slippery material (children's modeling clay) a uniform multilayered structure could be produced.

For the first time it is shown that multilayered polymer composites can be produced using polymer colloids and clay platelets. Here the layers were not uniform due to the complex rheological properties of the composite material which changes significantly during flow. Additional effects such as no slip at the wall, high pressure required to push the rheologically complex material through the static mixer resulted in non-uniform layers. In spite of this difficulty it is shown that a particle based composite multilayer sheets can be produced using our static mixer.

Further research in this topic can take several directions for carrying out investigations concerning a wide range of applications which requires unique solutions. In future studies, it is recommended to look at other materials from which the static mixer can be made. Materials which show less shear resistance can be one option. Another option would be to apply a coating on the inner walls of static mixer so that the test materials move along the walls without encountering resistance (coatings that causes slip). In this project, tests were carried out using suspensions in which particles are stacked on top of each other. In subsequent studies, research can be done to obtain stacked layers that are apart from each other. Here one option could be to use another polymer in-between the particle filled stacked layers. This allows the barrier properties of outputs to be improved significantly

Bibliography

[1] J. Geys, "Nanopartikels in voeding," AFSCA, 2012.

[2] UHasselt, "Het VerpakkingsCentrum," 21 October 2017. [Online]. Available: https://www.uhasselt.be/UH/verpakkingscentrum/Het-VerpakkingsCentrum.html.

[3] Fostplus, "Wat is de functie van verpakkingen?," Fostplus, [Online]. Available: https://www.fostplus.be/nl/wat-de-functie-van-verpakkingen. [Accessed februari 2017].

[4] M. Stevens, "Permeation and its impact on packaging," MOCON, Minneapolis, MN 55428 USA, 2014.

[5] C. Abeykoon, A. L. Kelly, E. C. Brown, J. Vera-Sorroche, P. D. Coates, E. Harkin-Jones, K. B. Howell, J. Deng, K. Li and M. Price, "Investigation of the process energy demand in polymer extrusion: A brief review and an experimental study," Elsevier, Bradford, Belfast UK, 2014.

[6] V. Siracusa, "Food packaging permeability behaviour: A report," 2012.

[7] M. Stevens, "Permeation and its Impact on Packaging," MOCON, Minneapolis, MN 55428 USA , 2014.

[8] Y. K. S. R. K. B. v. H. D. Cui, "Gas barrier properties of polymer/clay nanocomposites," Royal Society of Chemistry, 2015.

[9] H. Sehaqui, J. Kochumalayil, A. Liu, T. Zimmermann and L. A. Berglund, "Multifunctional nanoclay hybrids of high toughness, thermal, and barrier performances," in *ACS Appl. Mater. Interfaces, vol. 5, no. 15*, 2013, pp. 7613-7620.

[10] R. K. Bharadwaj, "Modeling the barrier properties of polymer-layered silicate nanocomposites," 2001.

[11] A. Veldman and A. Velick´a, "Stromingsleer," Rijksuniversity Groningen, Netherland, Groningen, 2010-2011.

[12] R. K. THAKUR, C. VIAL, K. D. P. NIGAM, E. B. NAUMAN and G. DJELVEH, "STATIC MIXERS IN THE PROCESS INDUSTRIES - A REVIEW," Institution of Chemical Engineers, France, India, USA, 2003.

[13] J. v. d. Hoeven and R. W.-F. H. Meijer, "Homogeneity of multilayers produced with a Static Mixer," Philips Research Laboratories, Netherlands, Eindhoven.

[14] W. Reusch, "Visible and Ultraviolet Spectroscopy," International Organization for Chemical Sciences in Development, 5 May 2013. [Online]. Available: https://www2.chemistry.msu.edu/faculty/reusch/virttxtjml/spectrpy/uv-vis/spectrum.htm. [Accessed 13 May 2018].

[15] Kleishop, "Darwi Classic 1 Kilo," Kleishop, 2016. [Online]. Available: https://www.kleishop.nl/shop/luchtdrogende-klei/darwi-classic-1-kilo/. [Accessed 30 april 2018].

[16] Sigma-Aldrich, "Poly(ethylene glycol)," Sigma-Aldrich, 2018. [Online]. Available: https://www.sigmaaldrich.com/catalog/product/sial/p5413?lang=en&region=BE&gclid=CjwKCAjwi6TYBRAYEiwAOeH7Ge57wby7P4ni7oVs5cBkoguTxNti9C31NhMhdxmMZpcMeBeXGMtj2hoCna8QAvD_BwE. [Accessed 13 mei 2018].

[17] Q.-H. Nguyen and N.-D. Nguyen, "Incompressible Non-Newtonian Fluid Flows," intechopen, Vietnam, 2012.

[18] F. Duan, D. Kwek and A. Crivoi, "Viscosity affected by nanoparticle aggregation in Al2O3-water nanofluids," Nanoscale Research Letters, Singapore, 2011.

[19] Polymer Properties Database, "FLOW PROPERTIES OF POLYMERS," Polymer Properties Database, 2015. [Online]. Available: http://polymerdatabase.com/polymer%20physics/Viscosity2.html. [Accessed 10 mei 2018].

[20] N. Reddy, "Rheology," University og Hasselt, Belgium, Diepenbeek, 2018.

[21] S. Lower, "Liquids and their interfaces," Simon Fraser University, 23 November 2017. [Online]. Available: http://www.chem1.com/acad/webtext/states/liquids.html. [Accessed 13 May 2018].

[22] DataPhysics Instruments GmbH, "Solid surface energy data (SFE) for common polymers," [Online]. Available: http://www.dataphysics.de/fileadmin/user_upload/pdf/DataPhysics_Surface_Tension_Energy.pdf. [Accessed 13 mei 2018].

[23] L. Shartsis and A. W. Smock, "Surface Tensions of Some Optical Glasses," U. S. Department of Commerce, National Bureau of Standards , 1947.

[24] B. N. Pitta, "Is the method for measuring gas permeability significant in determining the result?," Universiteit Hasselt, Diepenbeek, België, 2014.

[25] Electron Mircroscopy Sciences, "Technical Data Sheet: Epofix cold-setting ambedding resin," Electron Mircroscopy Sciences, 2018. [Online]. Available: https://www.emsdiasum.com/microscopy/technical/datasheet/1232.aspx. [Accessed 13 mei 2018].

[26] Struers, "Safety data sheet: Epofix hardener," Struers , Australia, 2018.

[27] G. Tillman, "Use of cold setting resins," University of Wollongong , Australia.

[28] P. Geertsma, "Wat is polijsten en hoe wordt deze bewerking toegepast?," Technisch werken, 2014.

[29] A. Scott, "Sandpaper: the nitty-gritty," *American Woodturner,* p. 5, October 2010.

Appendices

Appendix A: Technical drawings of the existing static mixer

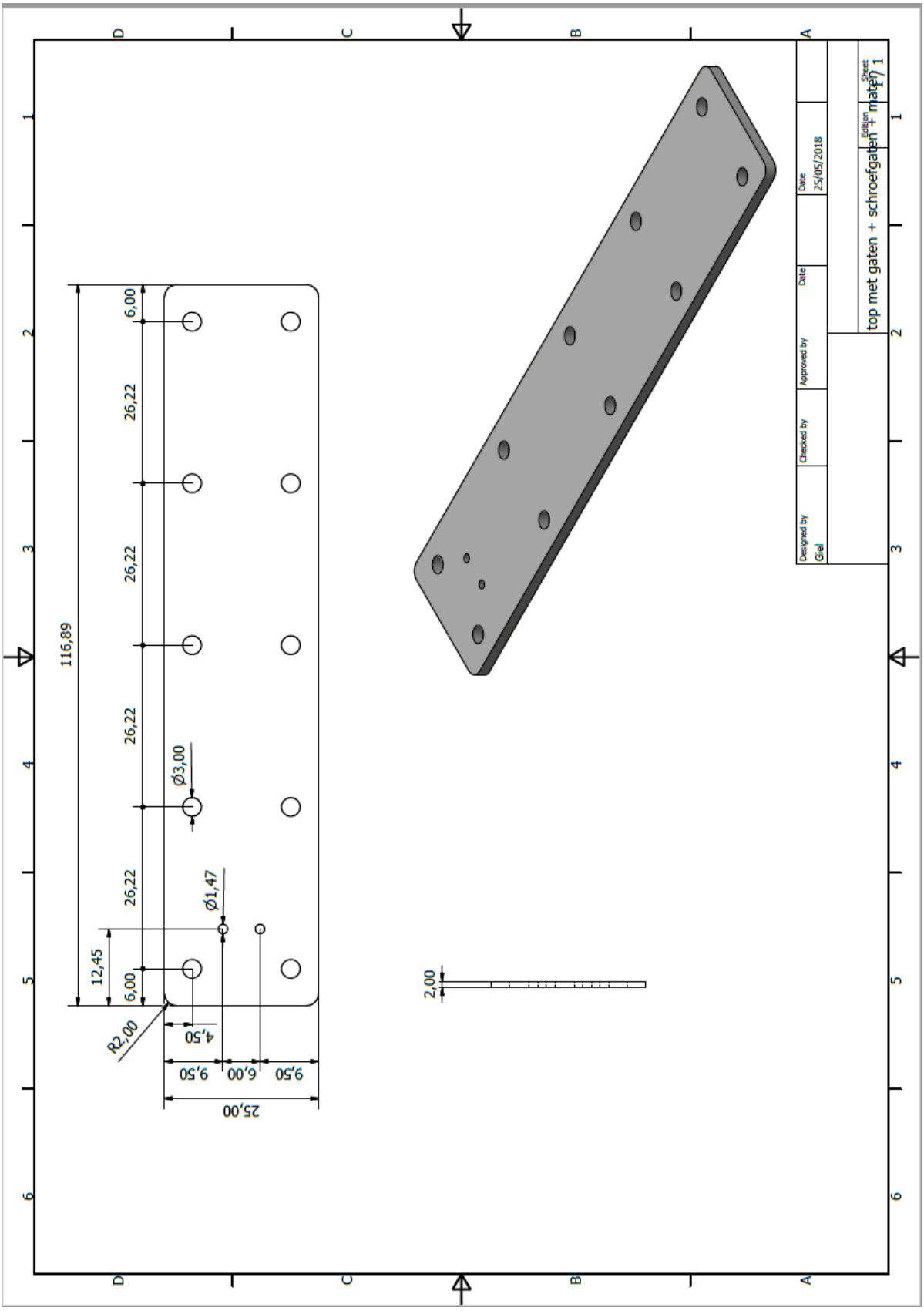

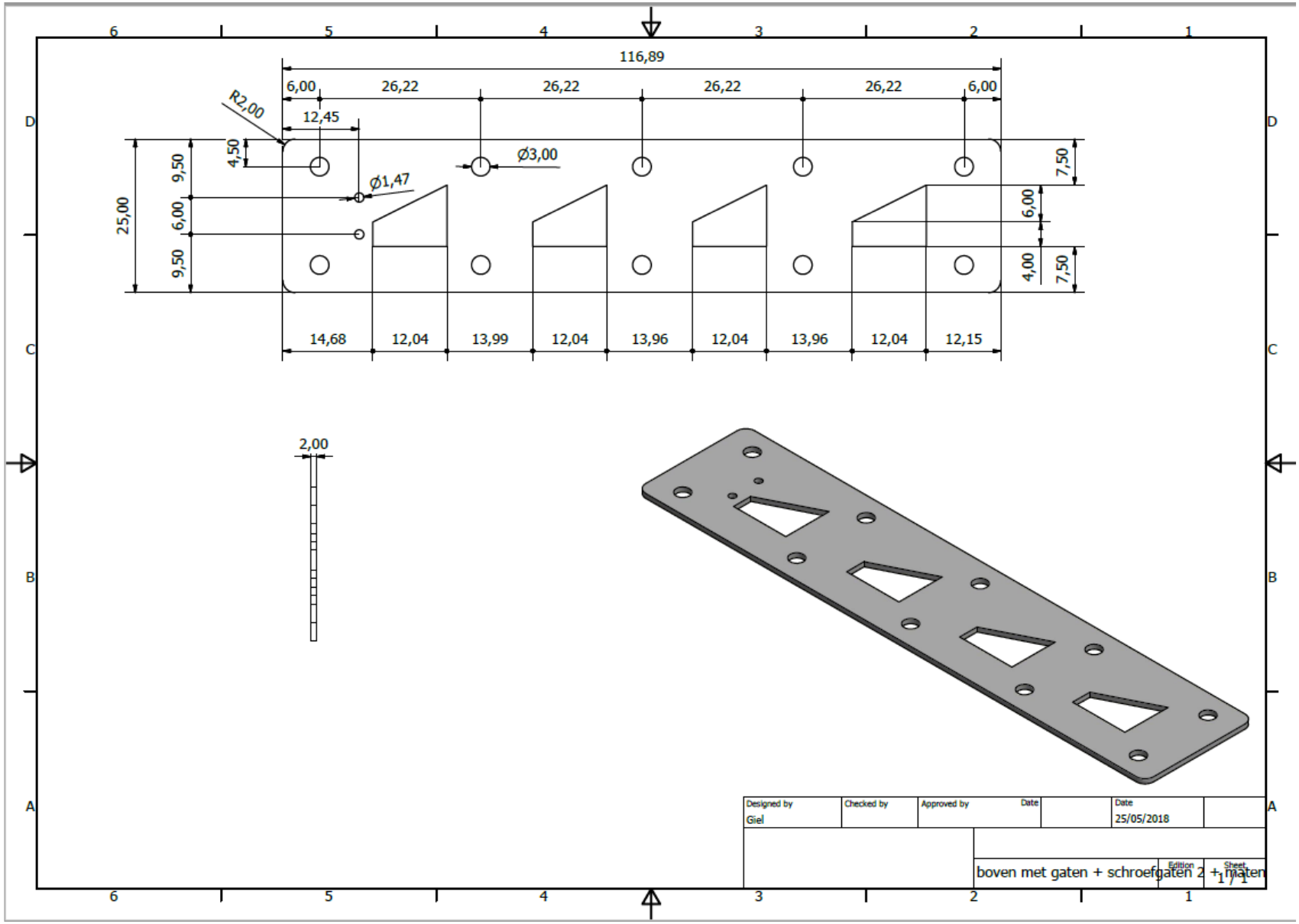
116,89
6,00
26,22
26,22
26,22
26,22
6,00
R2,00
12,45
4,50
Ø3,00
Ø1,47
25,00
9,50
6,00
9,50
7,50
6,00
4,00
7,50
14,68
12,04
13,99
12,04
13,96
12,04
13,96
12,04
12,15
2,00
Designed by
Giel
Checked by
Approved by
Date
Date
25/05/2018
boven met gaten + schroefgaten 2 + maten
Edition
Sheet
1/1

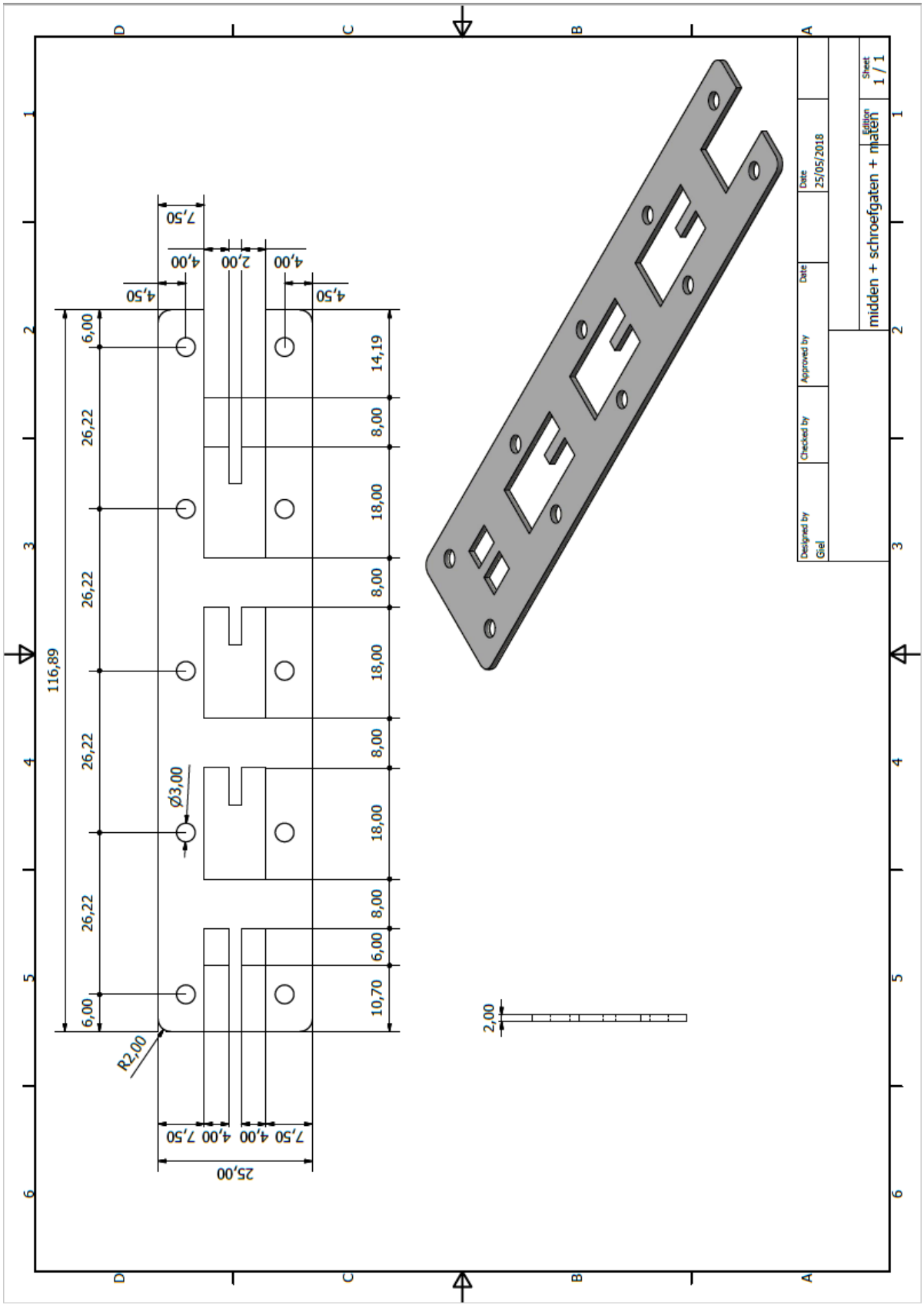
midden + schroefgaten + platen
Designed by Giel
Checked by
Approved by
Date
25/05/2018
Edition
Sheet 1 / 1
116,89
26,22
26,22
26,22
26,22
6,00
6,00
14,19
8,00
18,00
8,00
18,00
8,00
18,00
8,00
6,00
10,70
4,50
4,00
2,00
4,00
7,50
Ø3,00
R2,00
25,00
7,50 4,00 7,50
2,00

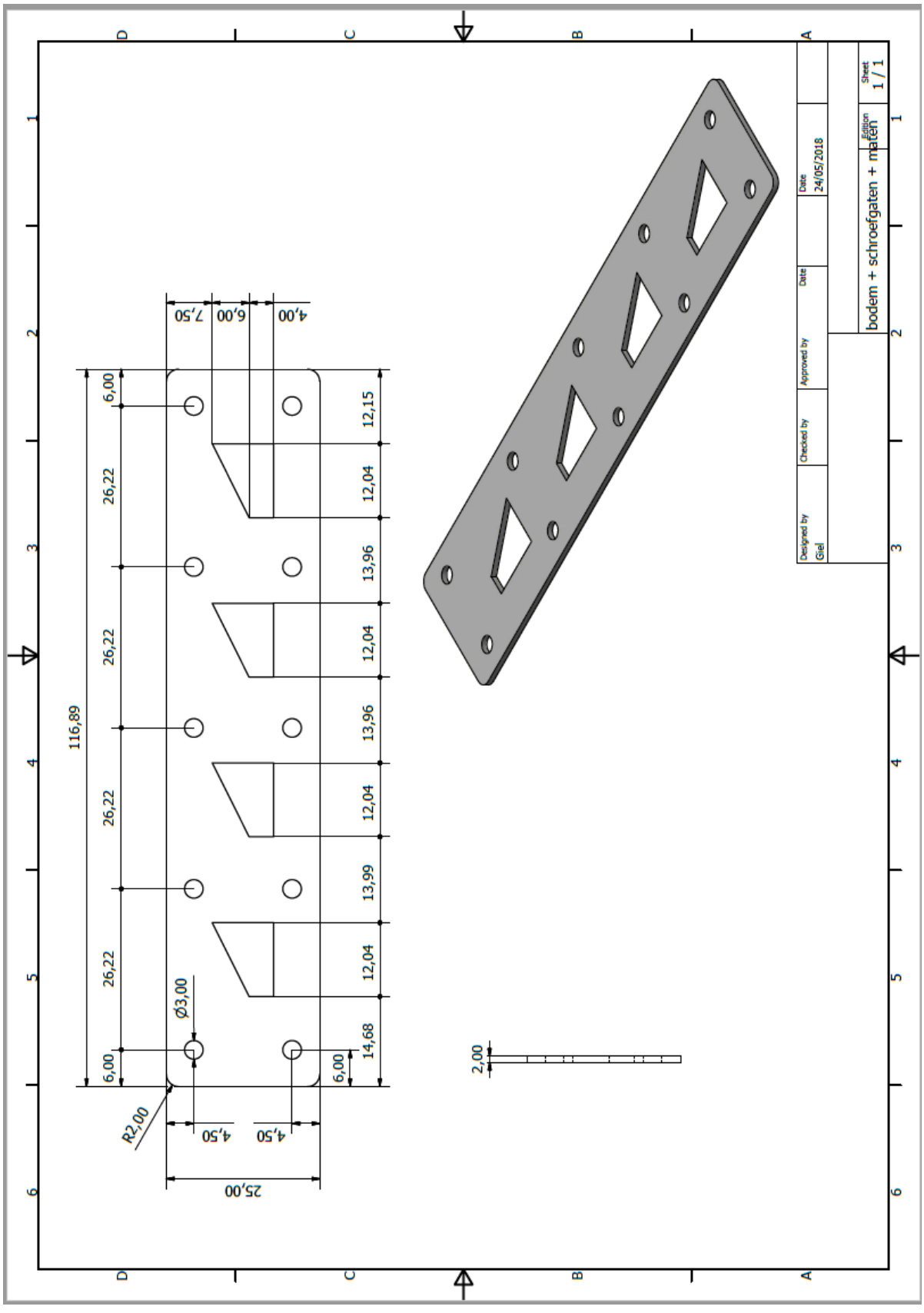
bodem + schroefgaten + maten
Designed by
Giel
Checked by
Approved by
Date
24/05/2018
Edition
Sheet
1 / 1
116,89
26,22
26,22
26,22
26,22
26,22
6,00
6,00
6,00
12,15
12,04
13,96
12,04
13,96
12,04
13,99
12,04
14,68
7,50
6,00
4,00
Ø3,00
R2,00
4,50
4,50
25,00
2,00

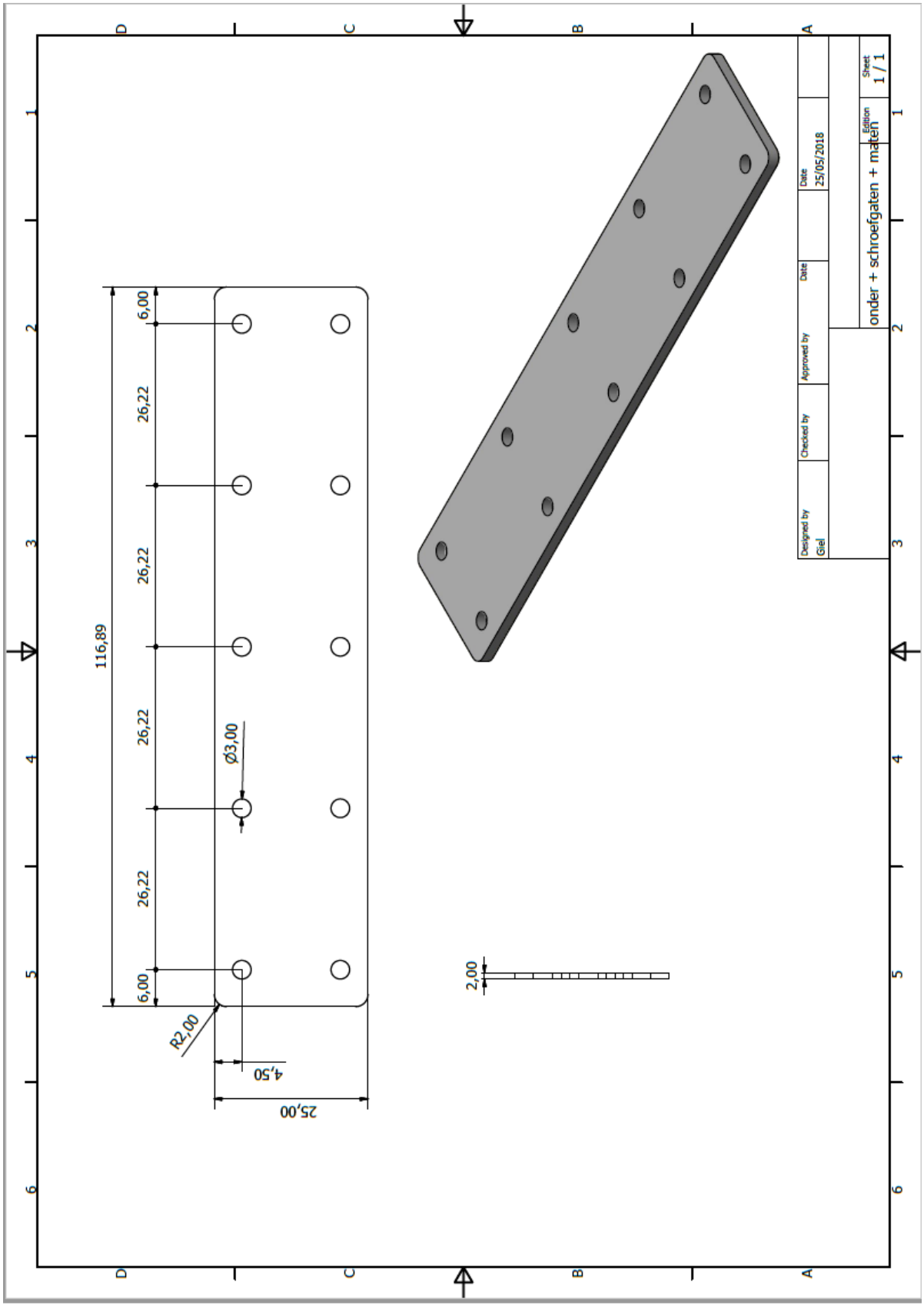
onder + schroefgaten + maten
Designed by Giel
Checked by
Approved by
Date
25/05/2018
Edition
Sheet 1 / 1
116,89
6,00
26,22
26,22
26,22
26,22
6,00
Ø3,00
R2,00
4,50
25,00
2,00

Appendix B: Technical drawings of the first version of the modified static mixer

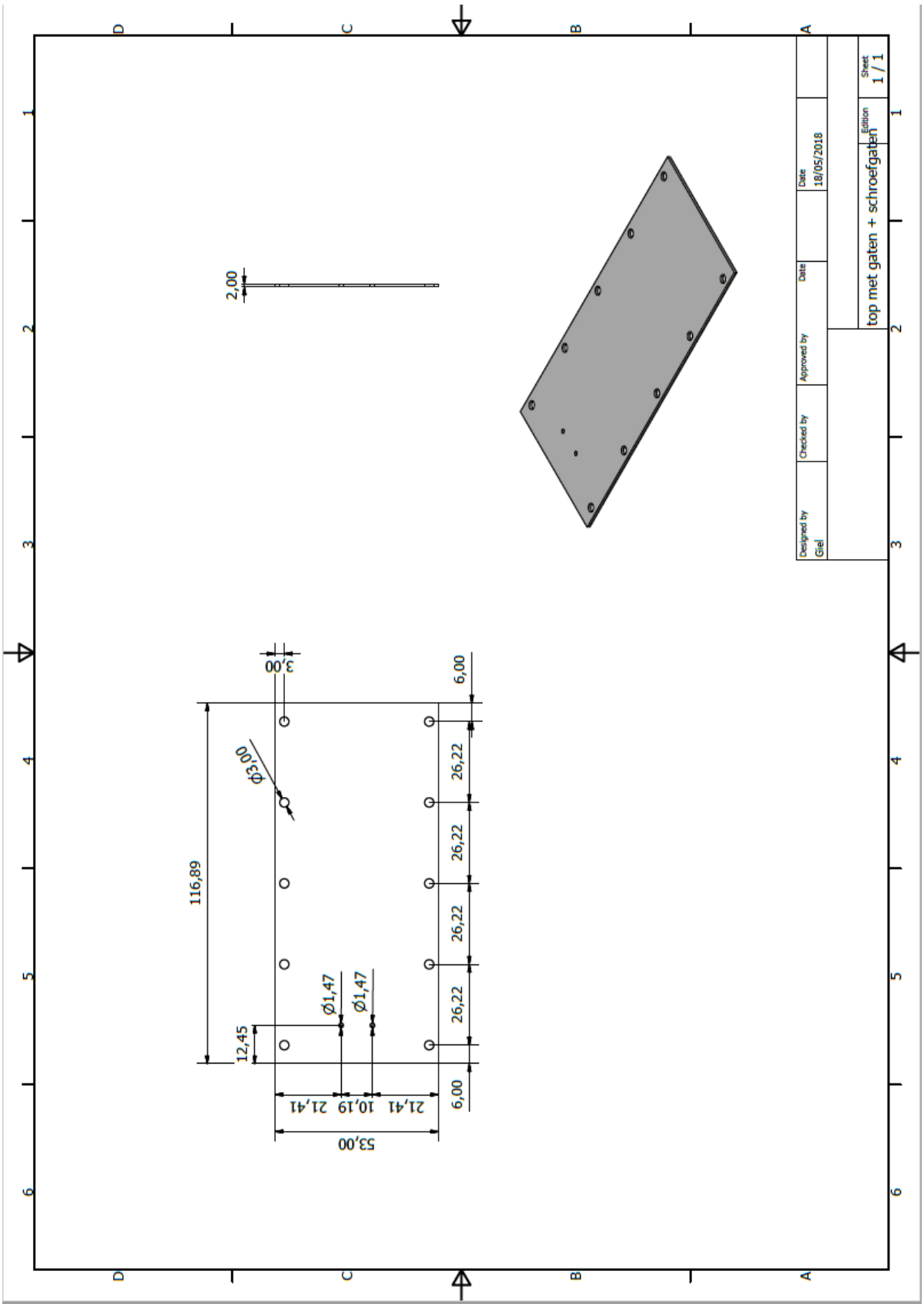

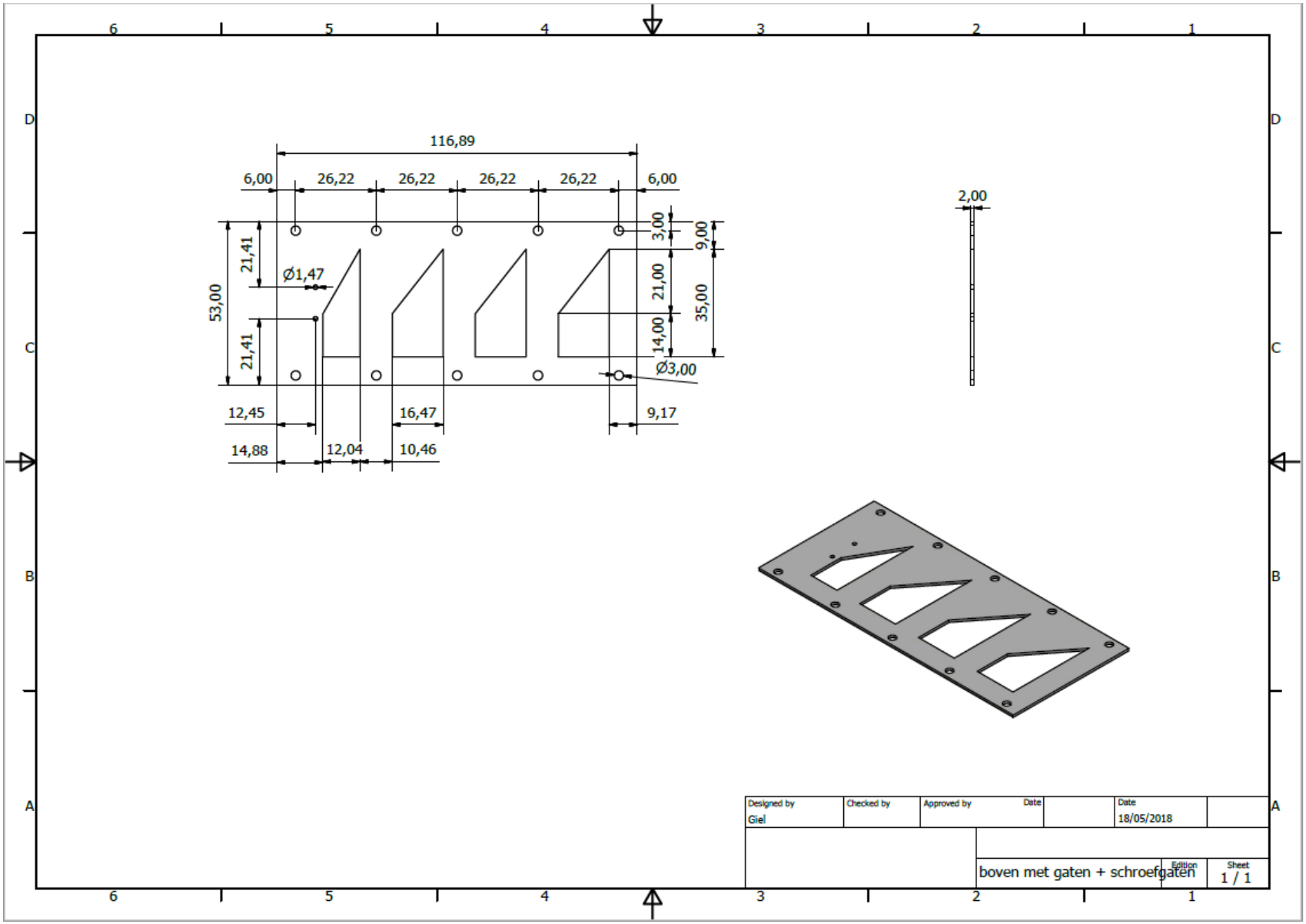
116,89
6,00
26,22
26,22
26,22
26,22
6,00
3,00
9,00
21,41
Ø1,47
53,00
21,00
35,00
21,41
14,00
Ø3,00
12,45
16,47
9,17
14,88
12,04
10,46
2,00
Designed by
Giel
Checked by
Approved by
Date
Date
18/05/2018
boven met gaten + schroefgaten
Edition
Sheet
1 / 1

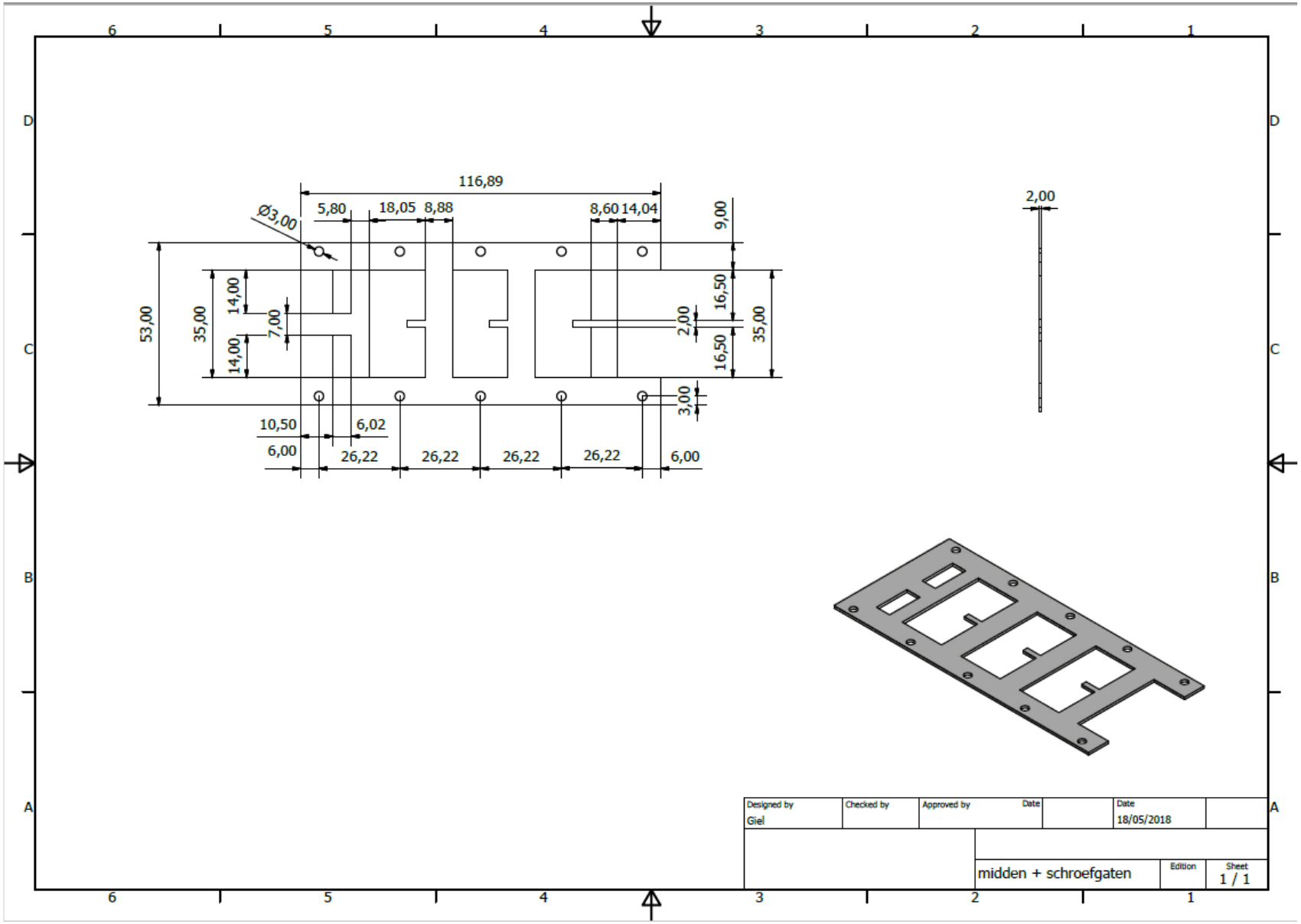
116,89
5,80
18,05
8,88
8,60
14,04
Ø3,00
9,00
53,00
35,00
14,00
7,00
14,00
16,50
2,00
16,50
35,00
3,00
10,50
6,02
6,00
26,22
26,22
26,22
26,22
6,00
2,00
Designed by
Giel
Checked by
Approved by
Date
Date
18/05/2018
midden + schroefgaten
Edition
Sheet
1 / 1

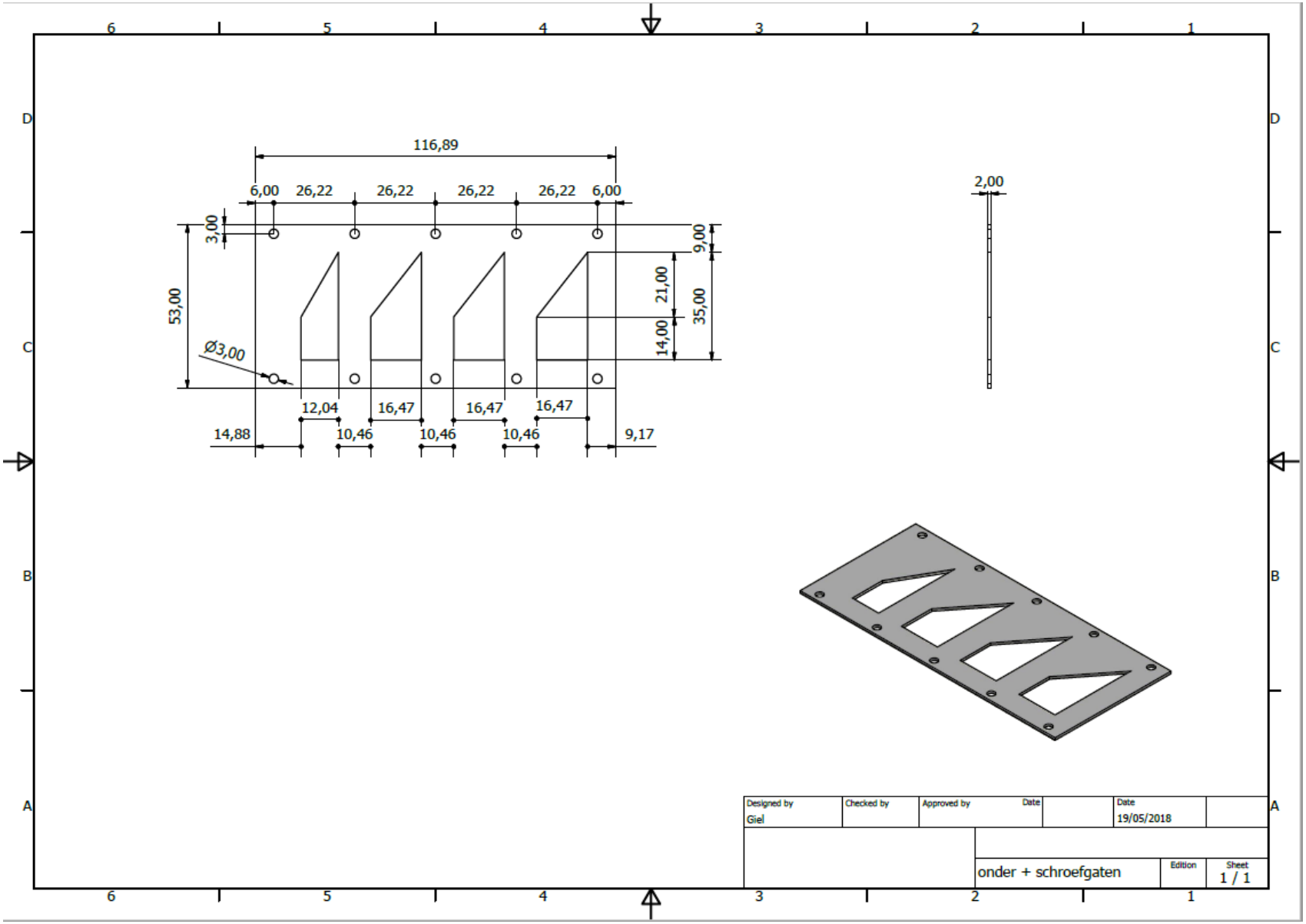
116,89
6,00
26,22
26,22
26,22
26,22
6,00
3,00
9,00
21,00
35,00
14,00
53,00
Ø3,00
12,04
16,47
16,47
16,47
14,88
10,46
10,46
10,46
9,17
2,00
Designed by
Giel
Checked by
Approved by
Date
Date
19/05/2018
onder + schroefgaten
Edition
Sheet
1 / 1

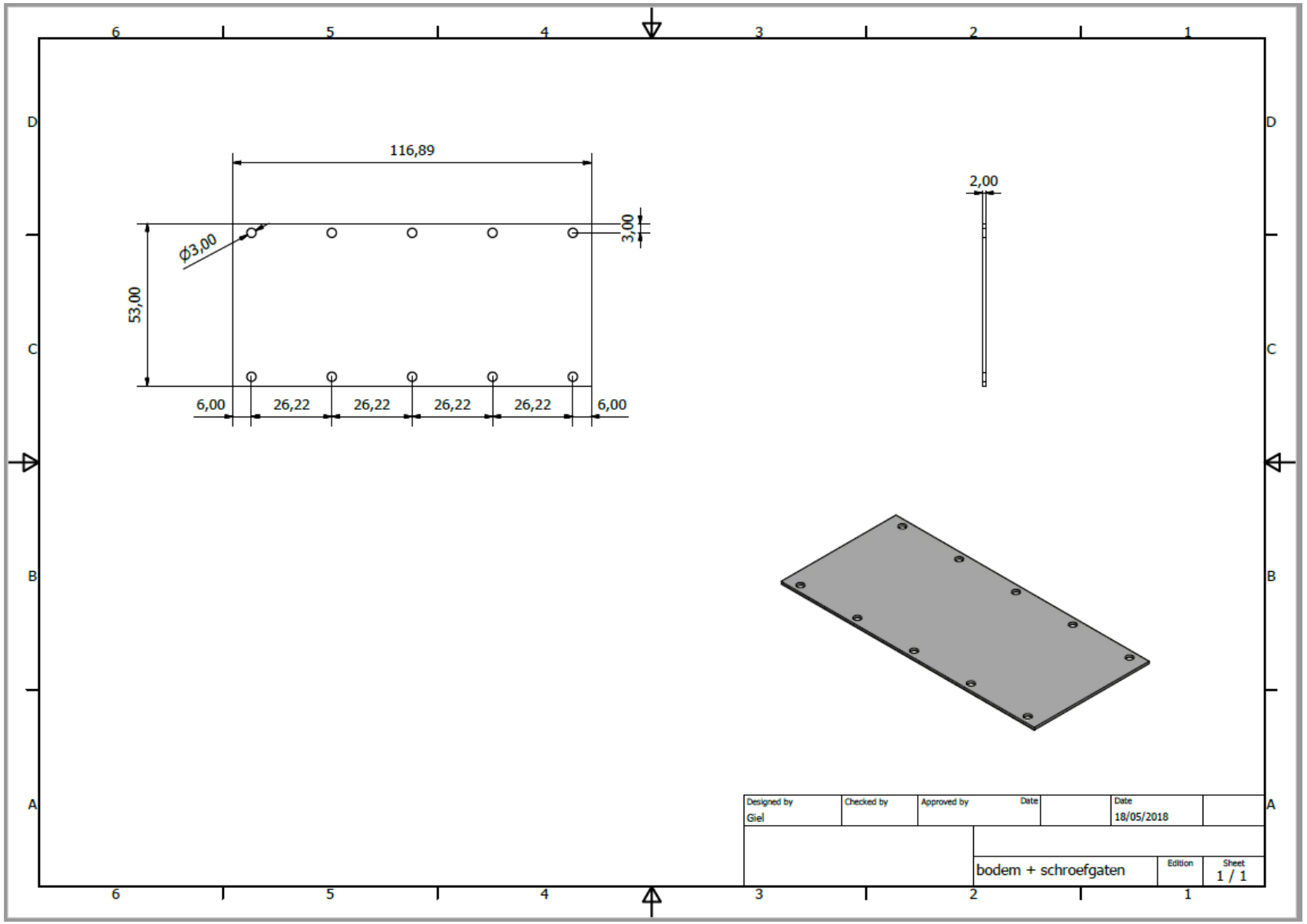
116,89
Ø3,00
3,00
53,00
6,00
26,22
26,22
26,22
26,22
6,00
2,00
Designed by
Giel
Checked by
Approved by
Date
Date
18/05/2018
bodem + schroefgaten
Edition
Sheet
1 / 1

Appendix C: Technical drawings of the second version of the modified static mixer

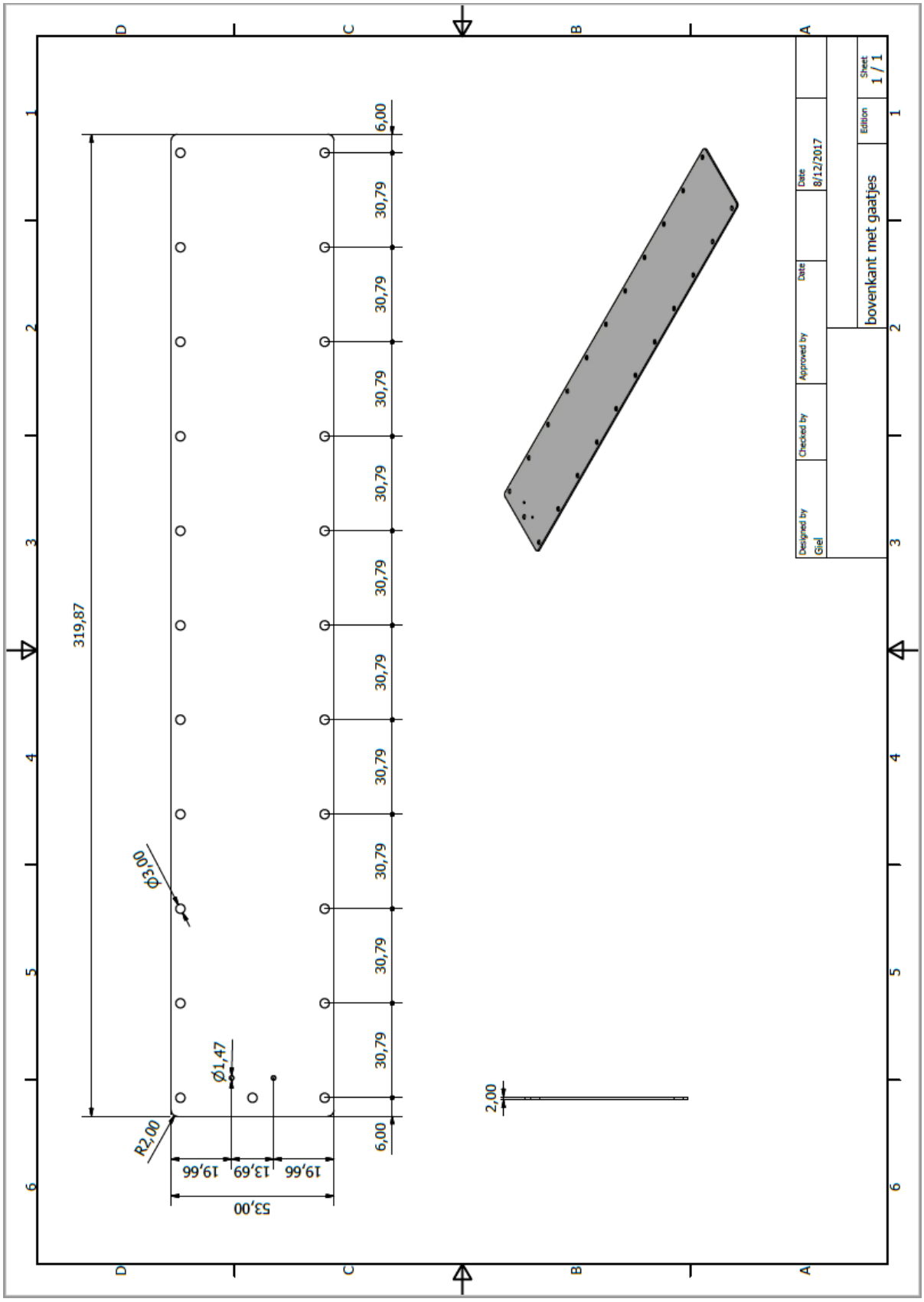

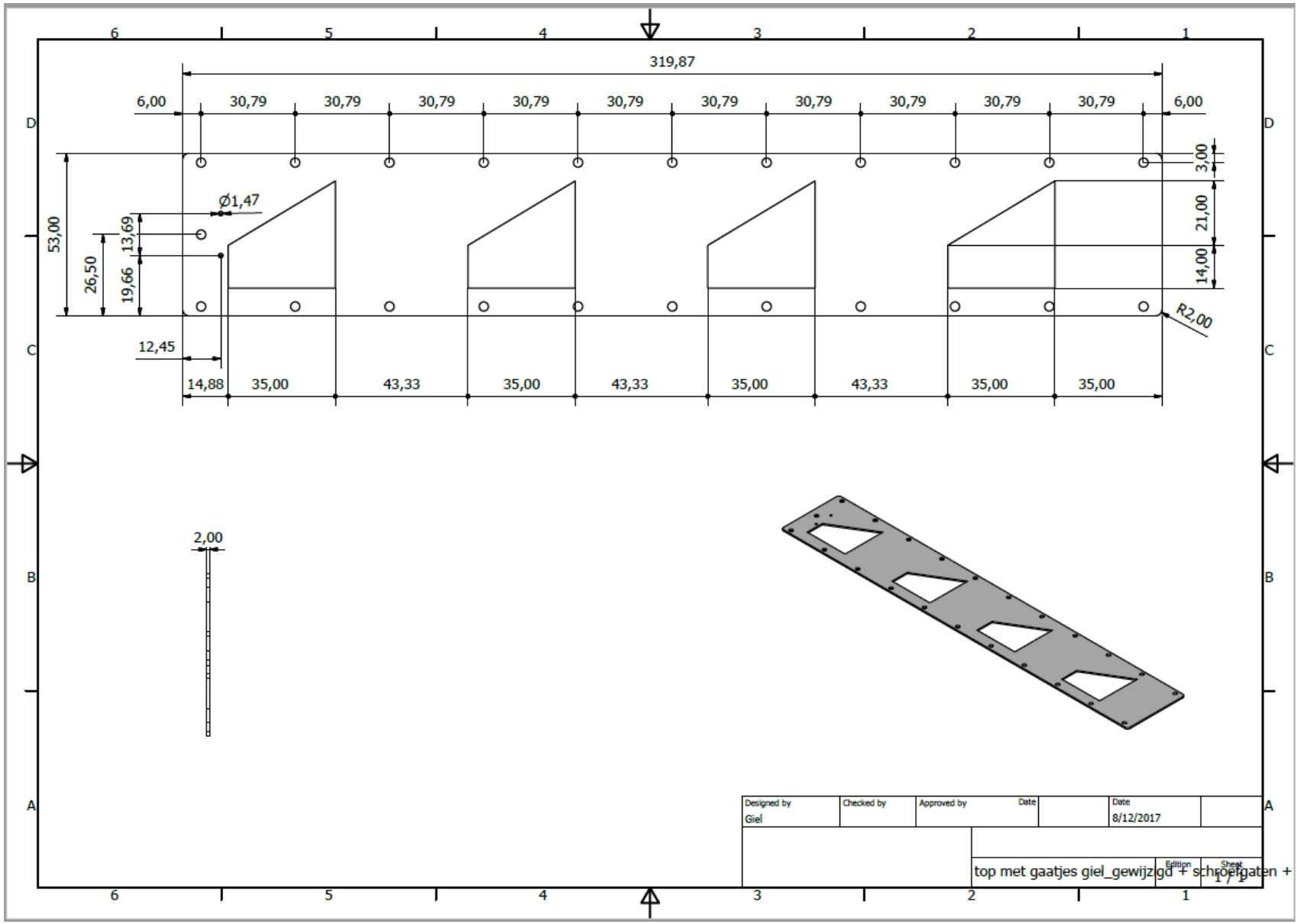
319,87
6,00
30,79
30,79
30,79
30,79
30,79
30,79
30,79
30,79
30,79
30,79
6,00
3,00
21,00
14,00
53,00
26,50
19,66
13,69
Ø1,47
R2,00
12,45
14,88
35,00
43,33
35,00
43,33
35,00
43,33
35,00
35,00
2,00
Designed by
Giel
Checked by
Approved by
Date
Date
8/12/2017
top met gaatjes giel_gewijzigd + schroefgaten +
Edition
Sheet
1 / 1

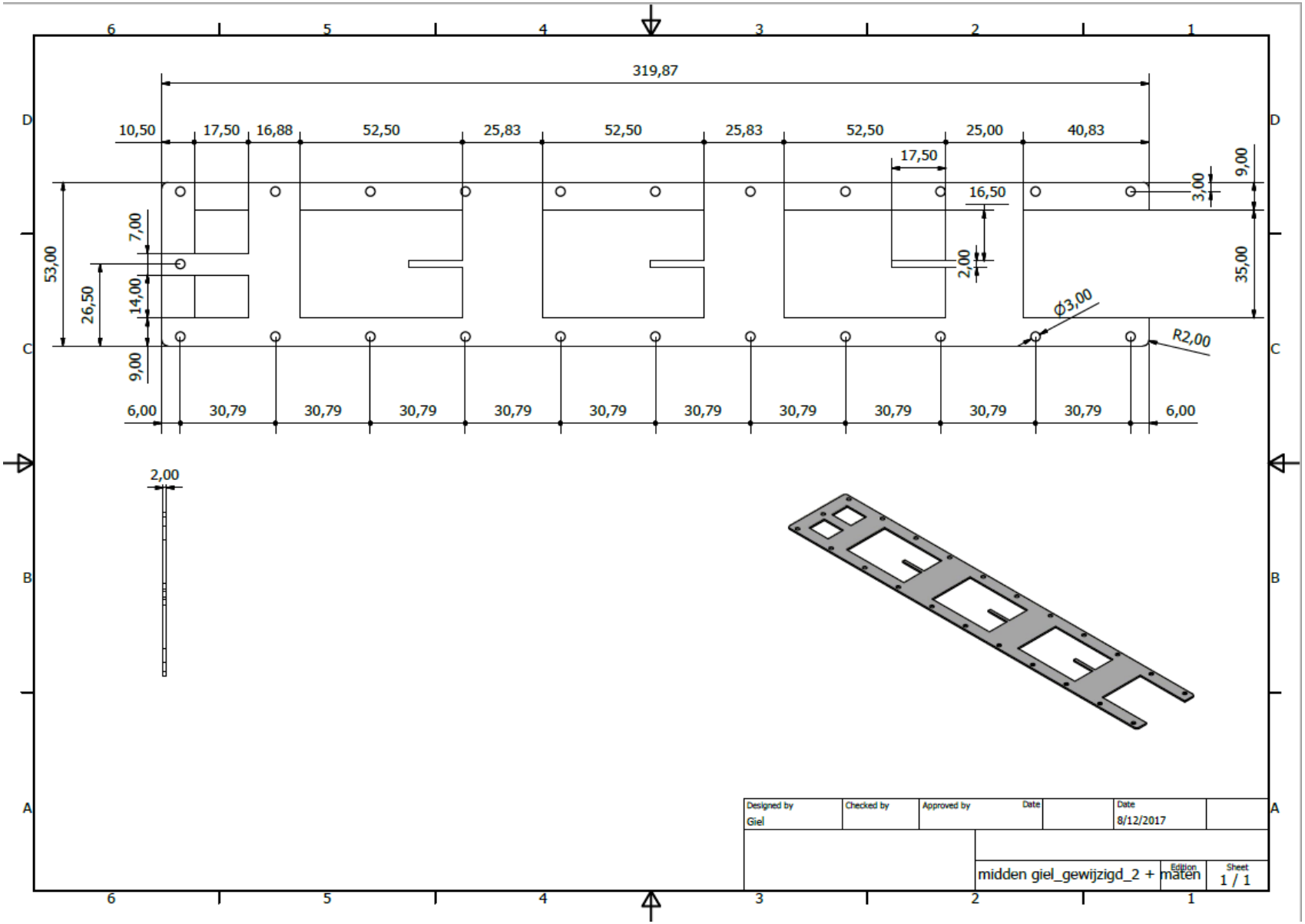
319,87
10,50
17,50
16,88
52,50
25,83
52,50
25,83
52,50
25,00
40,83
17,50
16,50
3,00
9,00
53,00
26,50
7,00
14,00
9,00
2,00
35,00
Ø3,00
R2,00
6,00
30,79
30,79
30,79
30,79
30,79
30,79
30,79
30,79
30,79
30,79
6,00
2,00
Designed by
Giel
Checked by
Approved by
Date
Date
8/12/2017
midden giel_gewijzigd_2 +
Edition
maten
Sheet
1 / 1

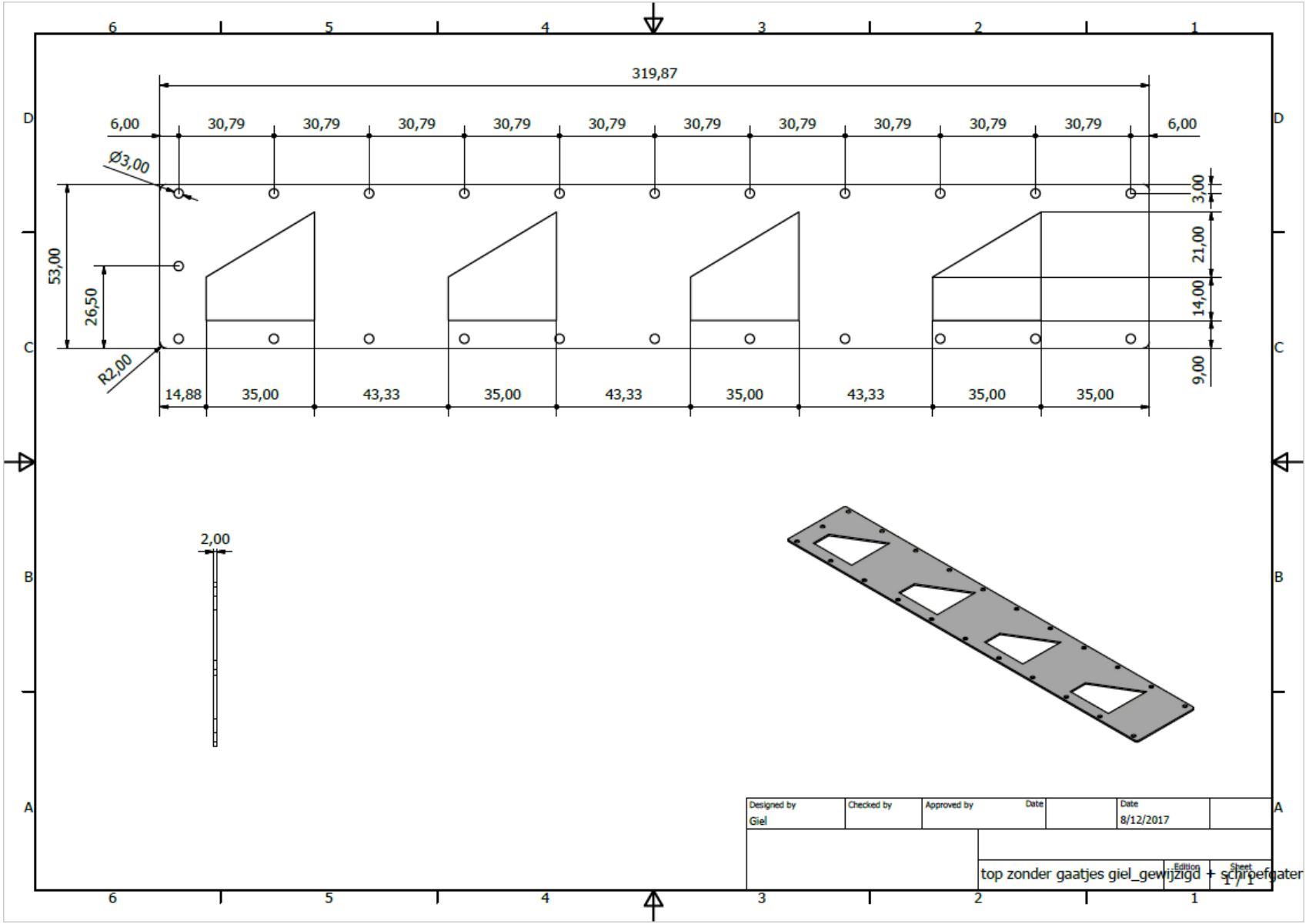
319,87
6,00
30,79
30,79
30,79
30,79
30,79
30,79
30,79
30,79
30,79
30,79
6,00
Ø3,00
53,00
26,50
R2,00
3,00
21,00
14,00
9,00
14,88
35,00
43,33
35,00
43,33
35,00
43,33
35,00
35,00
2,00
Designed by
Giel
Checked by
Approved by
Date
Date
8/12/2017
top zonder gaatjes giel_gewijzigd + schroefgater
Edition
Sheet
1/1

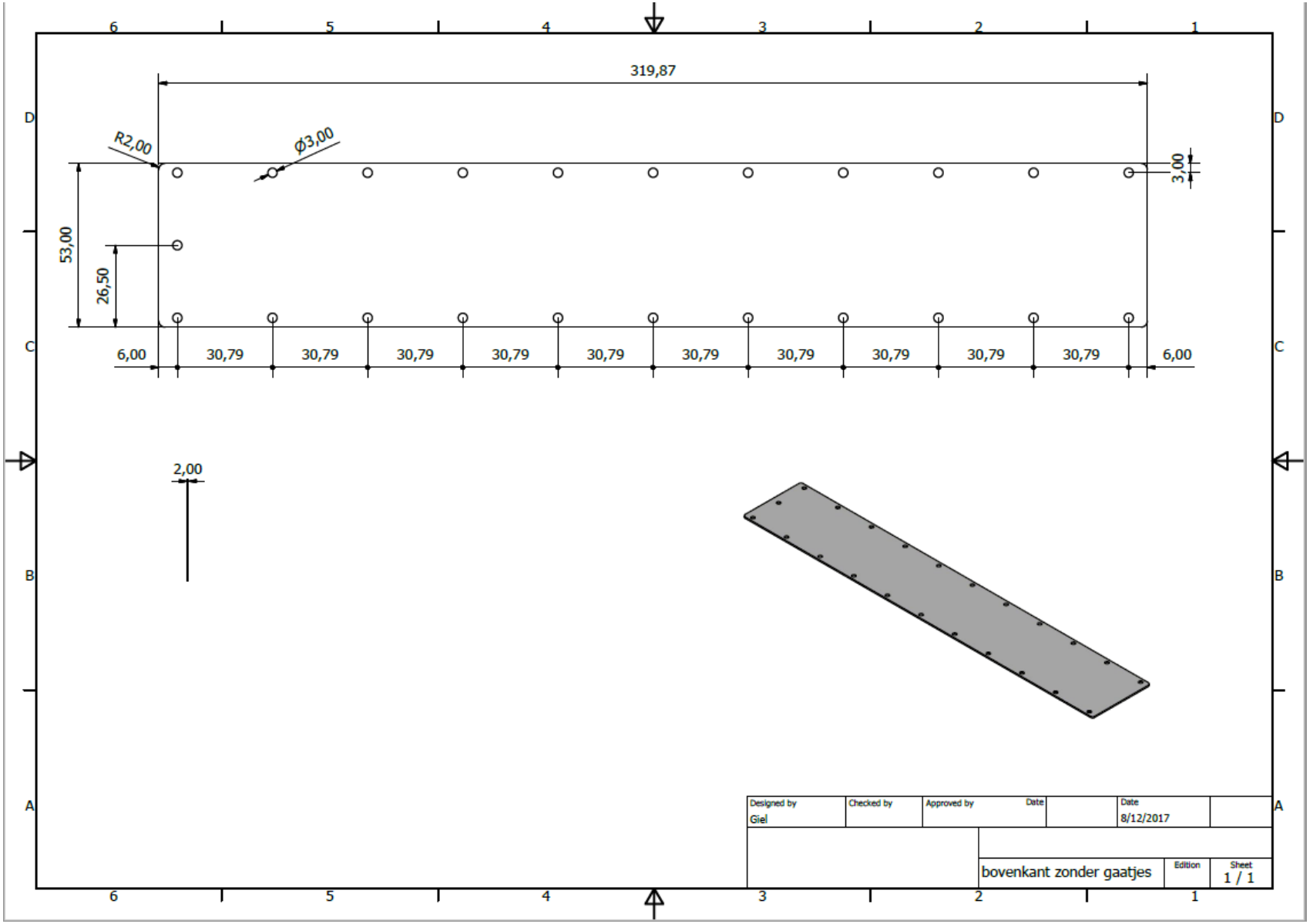
319,87
R2,00
Ø3,00
3,00
53,00
26,50
6,00
30,79
30,79
30,79
30,79
30,79
30,79
30,79
30,79
30,79
30,79
6,00
2,00
Designed by
Giel
Checked by
Approved by
Date
Date
8/12/2017
bovenkant zonder gaatjes
Edition
Sheet
1 / 1

Appendix D: Technical drawings of the static mixer that creates 64 layers

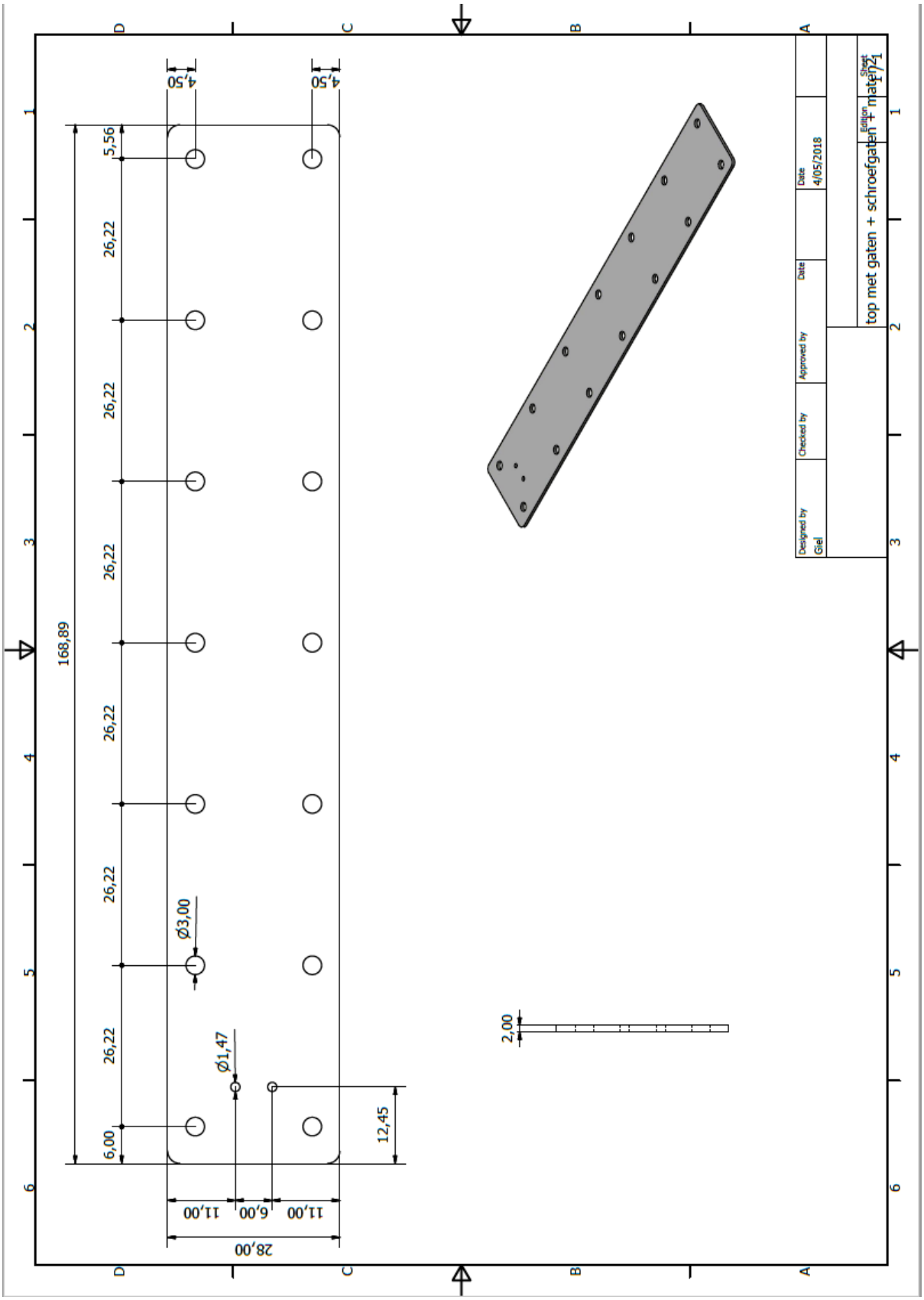

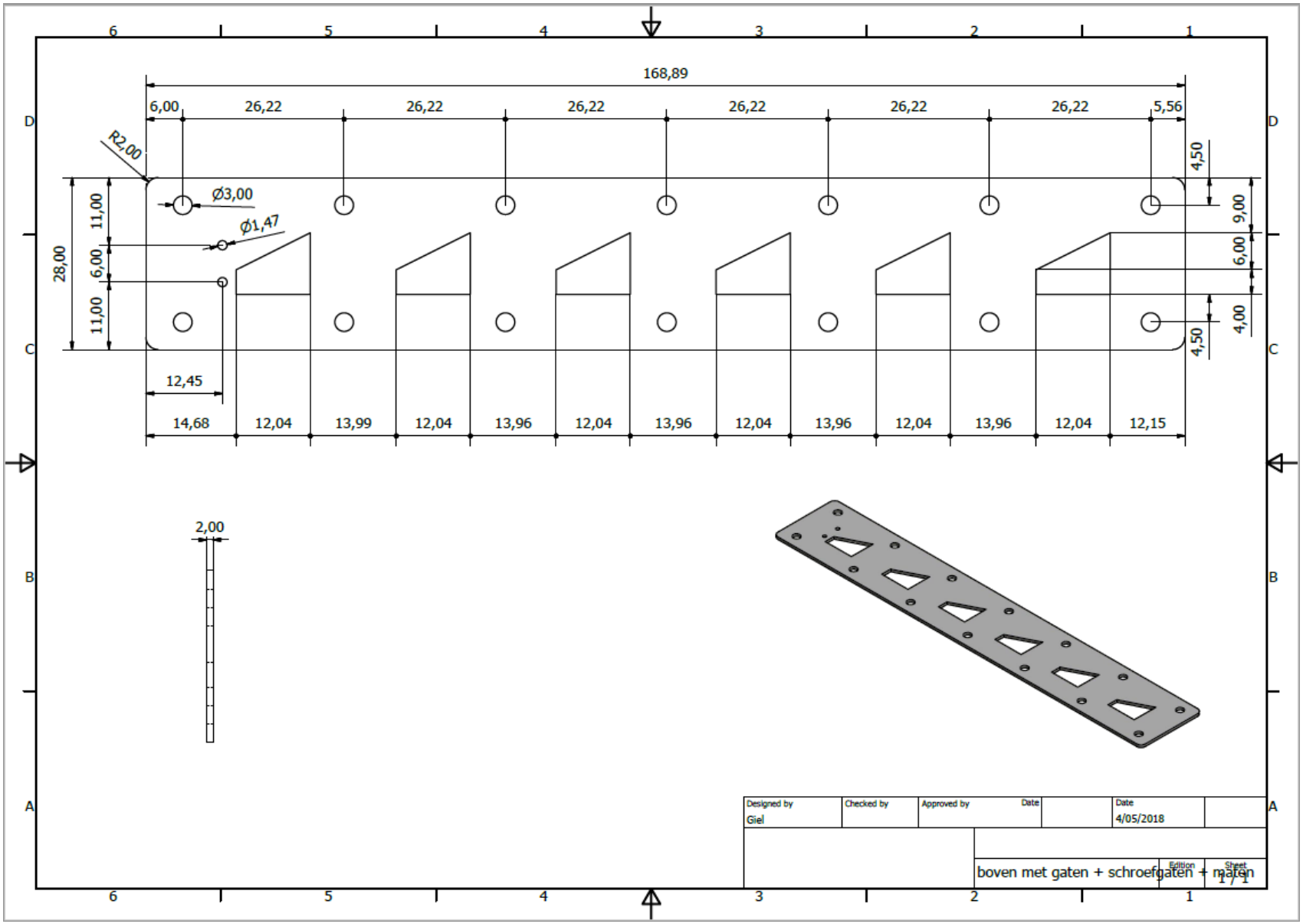
168,89
6,00
26,22
26,22
26,22
26,22
26,22
26,22
5,56
R2,00
Ø3,00
Ø1,47
28,00
11,00
6,00
11,00
4,50
9,00
6,00
4,00
4,50
12,45
14,68
12,04
13,99
12,04
13,96
12,04
13,96
12,04
13,96
12,04
13,96
12,04
12,15
2,00
Designed by
Giel
Checked by
Approved by
Date
Date
4/05/2018
boven met gaten + schroefgaten + maten
Edition
Sheet
1 / 1

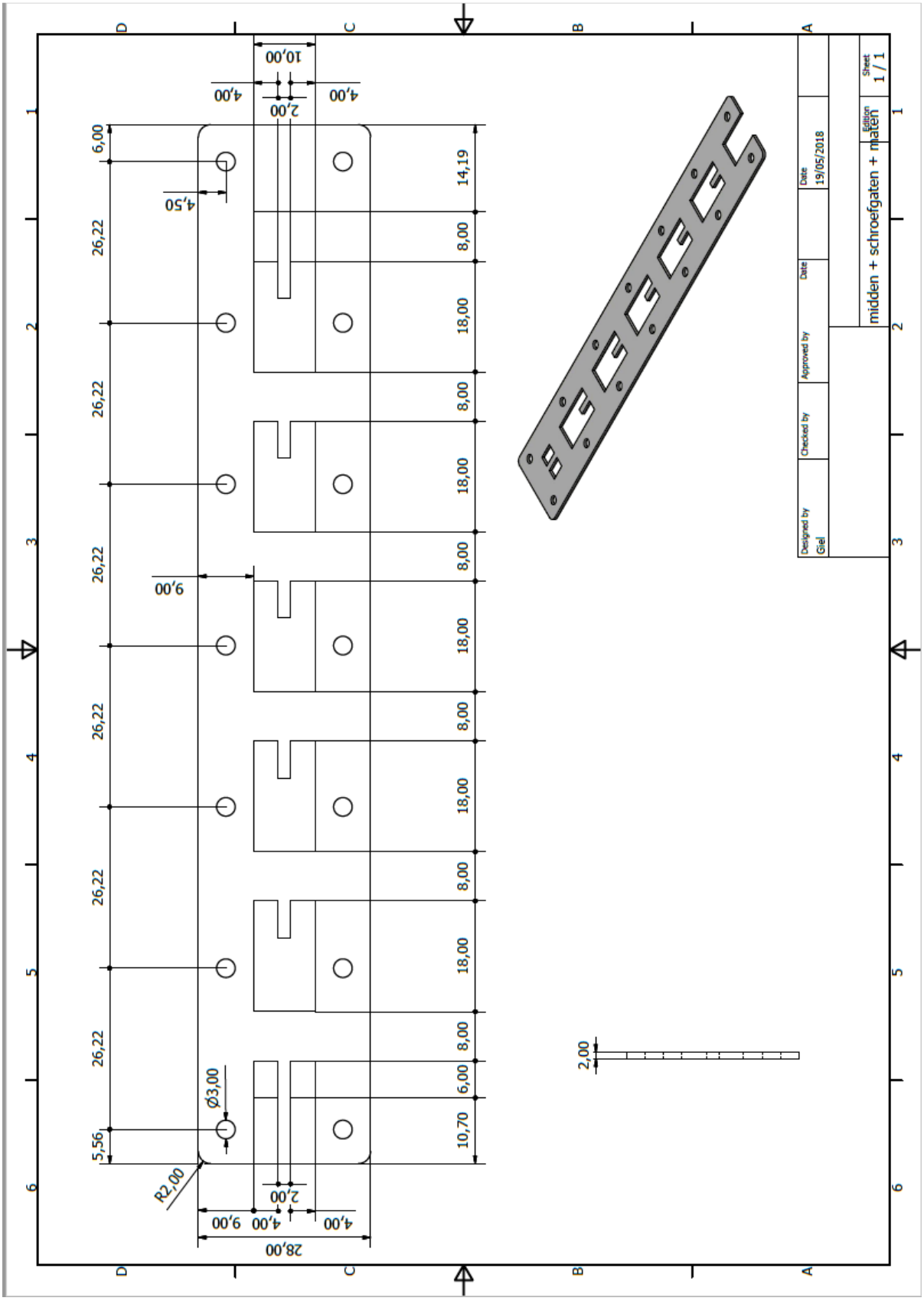
midden + schroefgaten + platen
Designed by Giel
Checked by
Approved by
Date 19/05/2018
Sheet 1 / 1
10,00
4,00
2,00
6,00
26,22
4,50
14,19
8,00
18,00
9,00
Ø3,00
5,56
10,70
R2,00
28,00
2,00

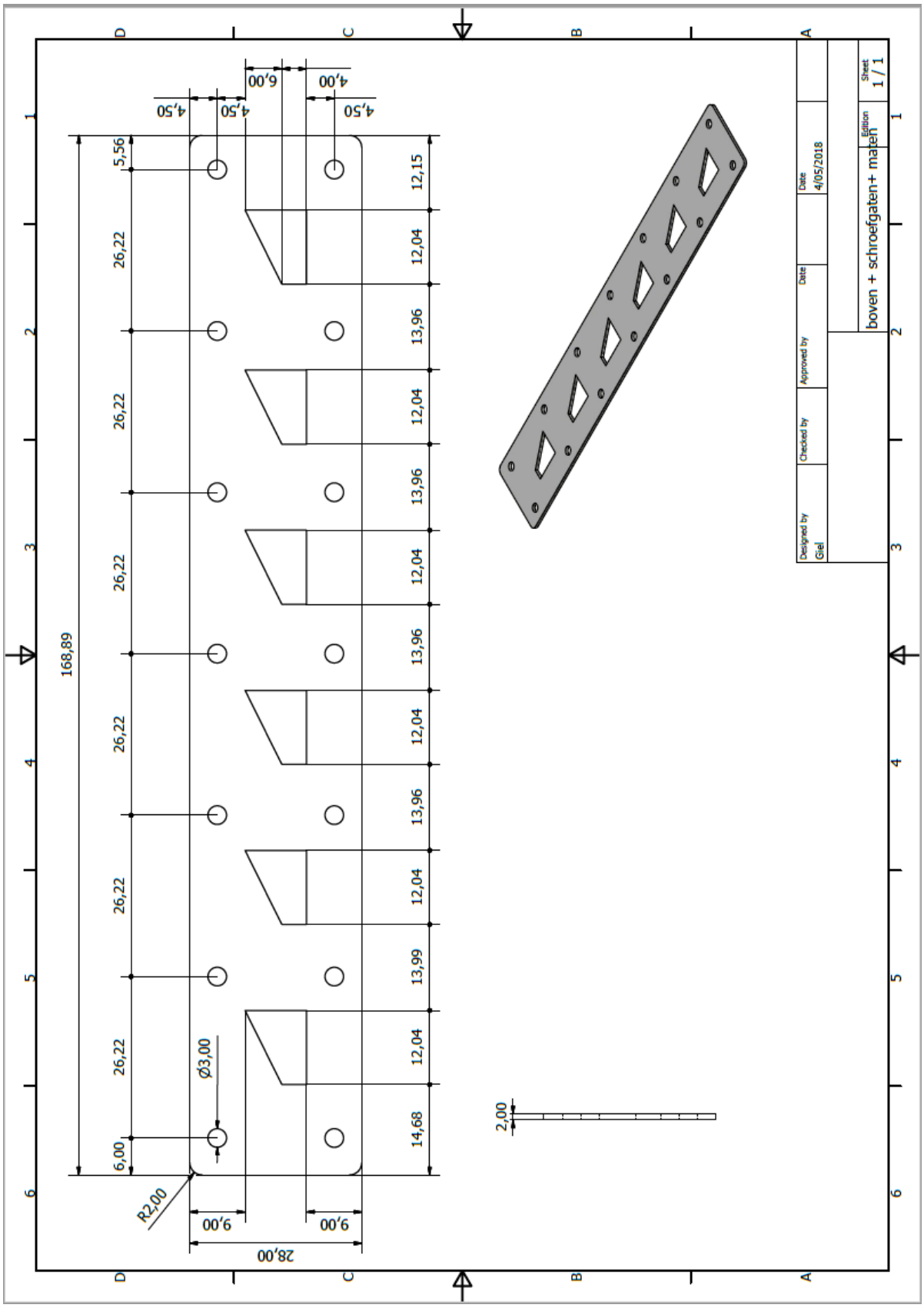
boven + schroefgaten+ maten
Designed by
Giel
Checked by
Approved by
Date
4/05/2018
Edition
Sheet
1 / 1
168,89
5,56
26,22
26,22
26,22
26,22
26,22
26,22
6,00
12,15
12,04
13,96
12,04
13,96
12,04
13,96
12,04
13,99
12,04
14,68
4,50
4,50
4,50
6,00
4,00
Ø3,00
R2,00
9,00
9,00
28,00
2,00

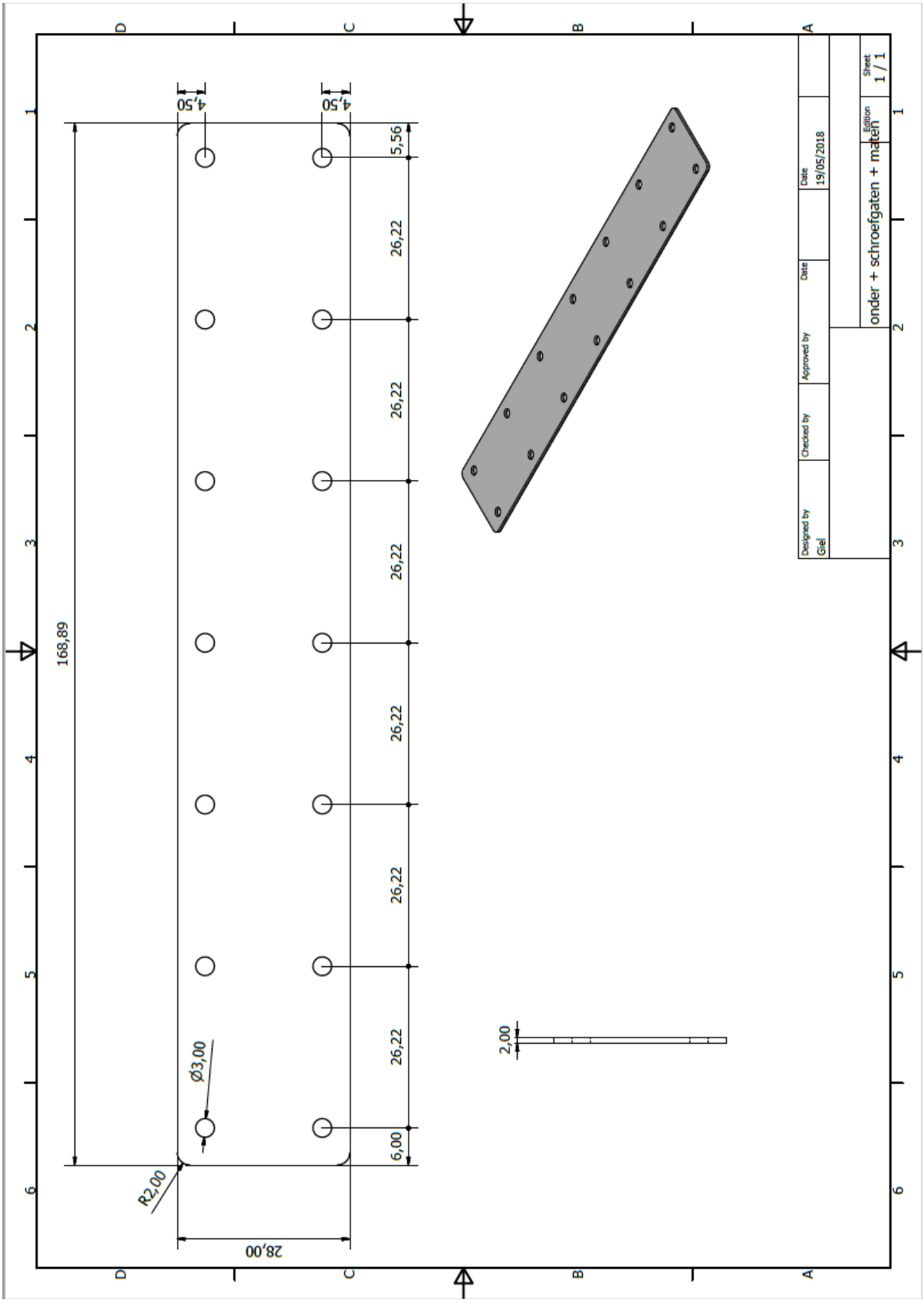
onder + schroefgaten + maten
Designed by Giel
Checked by
Approved by
Date
19/05/2018
Edition
Sheet 1 / 1
168,89
4,50
4,50
5,56
26,22
26,22
26,22
26,22
26,22
26,22
6,00
Ø3,00
R2,00
28,00
2,00

Appendix E: Technical drawings of the tripod for syringes of 10 ml

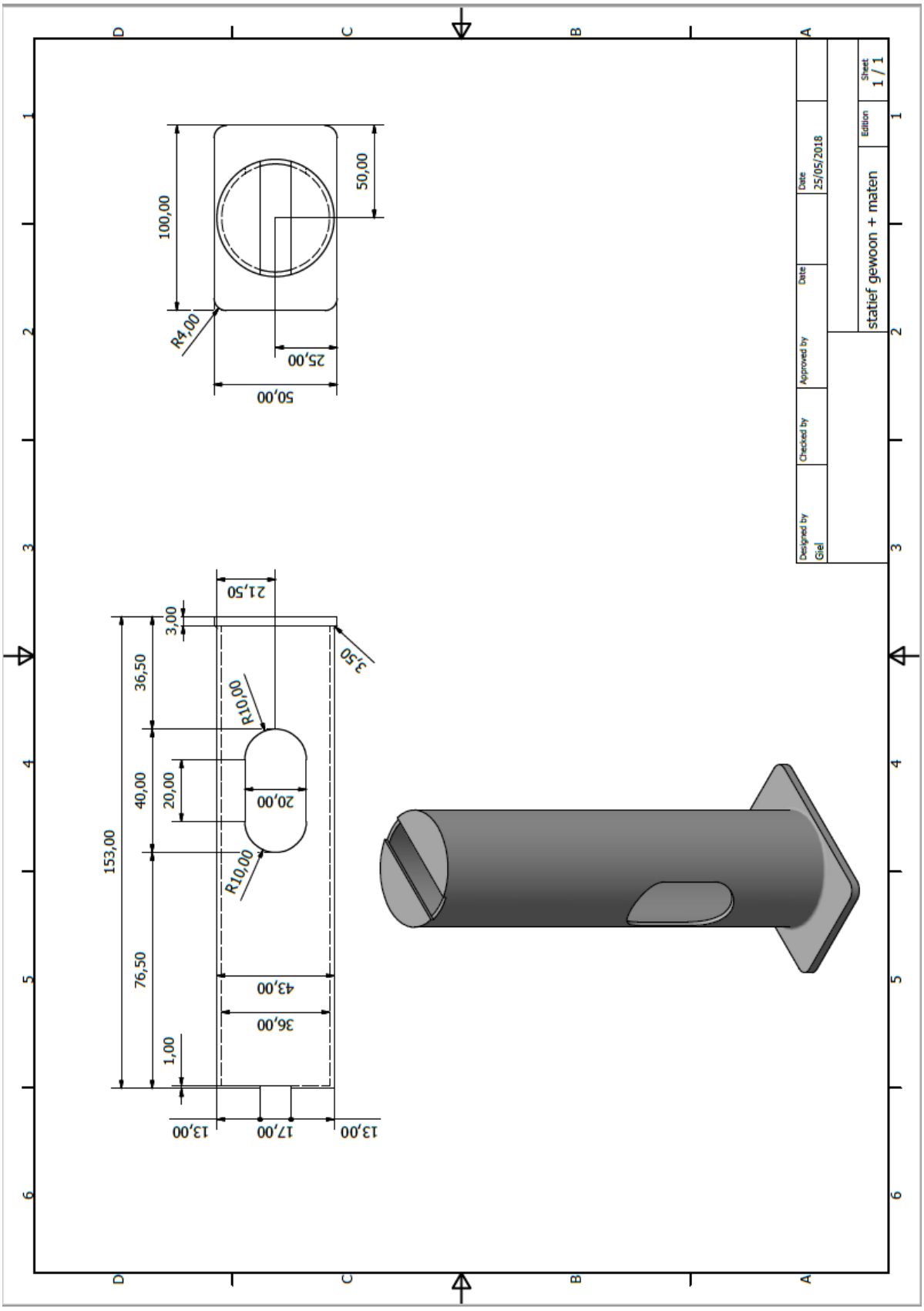

Appendix F: Technical drawings of the tripod for syringes of 20 ml

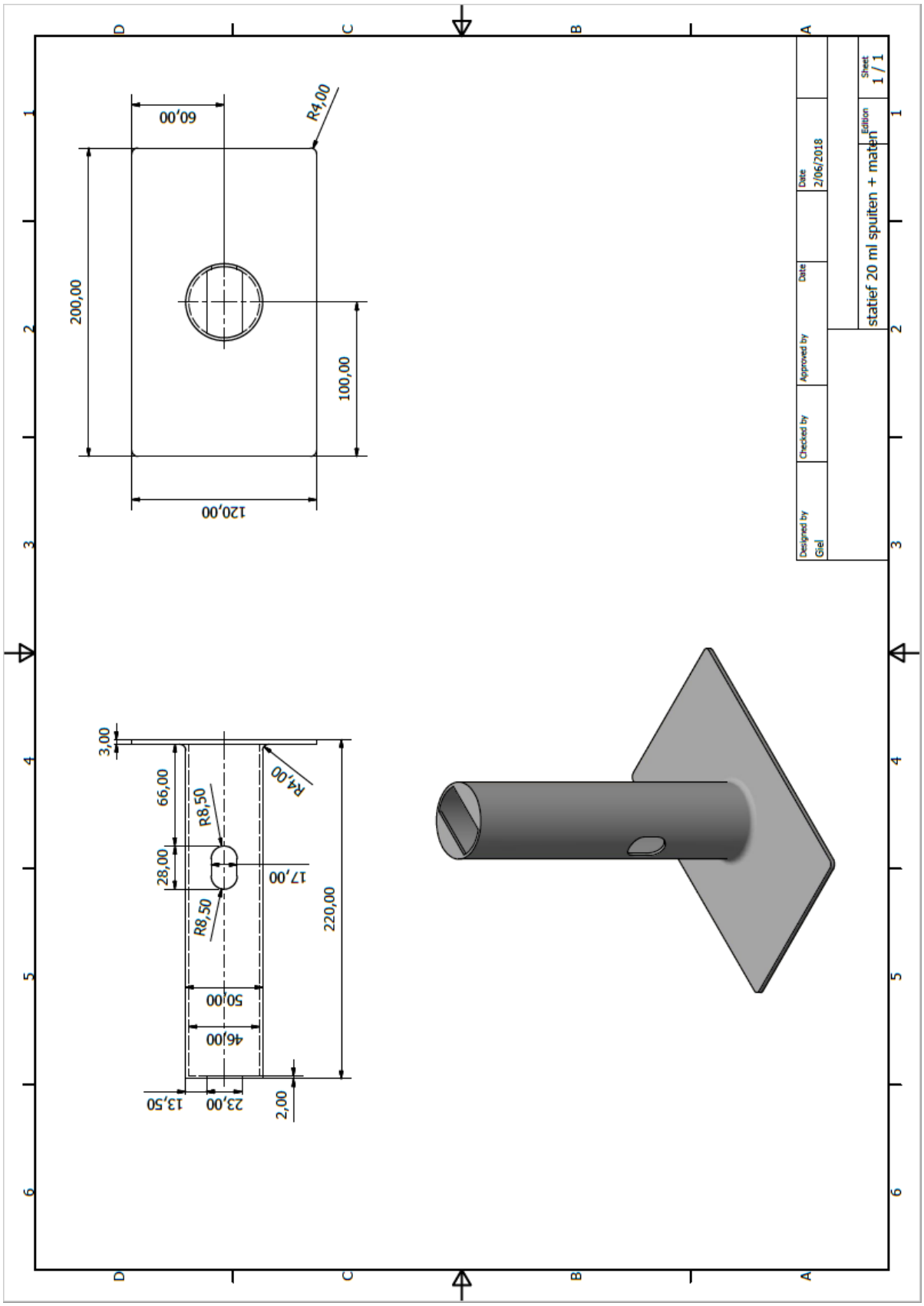

Auteursrechtelijke overeenkomst

Ik/wij verlenen het wereldwijde auteursrecht voor de ingediende eindverhandeling:
Creating multilayered polymer nanocomposites using a static mixer

Richting: **master in de industriële wetenschappen: verpakkingstechnologie**
Jaar: **2018**

in alle mogelijke mediaformaten, - bestaande en in de toekomst te ontwikkelen - , aan de Universiteit Hasselt.

Niet tegenstaand deze toekenning van het auteursrecht aan de Universiteit Hasselt behoud ik als auteur het recht om de eindverhandeling, - in zijn geheel of gedeeltelijk -, vrij te reproduceren, (her)publiceren of distribueren zonder de toelating te moeten verkrijgen van de Universiteit Hasselt.

Ik bevestig dat de eindverhandeling mijn origineel werk is, en dat ik het recht heb om de rechten te verlenen die in deze overeenkomst worden beschreven. Ik verklaar tevens dat de eindverhandeling, naar mijn weten, het auteursrecht van anderen niet overtreedt.

Ik verklaar tevens dat ik voor het materiaal in de eindverhandeling dat beschermd wordt door het auteursrecht, de nodige toelatingen heb verkregen zodat ik deze ook aan de Universiteit Hasselt kan overdragen en dat dit duidelijk in de tekst en inhoud van de eindverhandeling werd genotificeerd.

Universiteit Hasselt zal mij als auteur(s) van de eindverhandeling identificeren en zal geen wijzigingen aanbrengen aan de eindverhandeling, uitgezonderd deze toegelaten door deze overeenkomst.

Voor akkoord,

Jansen, Giel

Datum: **4/06/2018**